



Instituto de Ciencias del
Mar (CSIC)



Universidad de
Barcelona



Universidad Politécnica
de Cataluña

PROGRAMA DE DOCTORADO EN CIENCIAS DEL MAR

Shoreline and nearshore bar morphodynamics of beaches affected by artificial nourishment

Memoria presentada por

Elena Ojeda Casillas

Para optar al grado de Doctor por la
Universidad Politécnica de Cataluña

Director:

Jorge Guillén Aranda

Barcelona, Diciembre de 2008

Contents

Acknowledgements	vii
Summary	ix
Resumen	xiii
List of figures	xvii
List of tables	xxi
1. Introduction	1
1.1. The coastal system	1
1.2. Artificial nourishments	3
1.3. Video monitoring	5
1.3.1. Introduction	5
1.3.2. Previous works	7
1.4. Study sites	8
1.5. Objectives and thesis outline	9
2. Shoreline dynamics of embayed beaches	13
2.1. Introduction	13
2.2. The study area: Barcelona city beaches	15
2.3. Methodology	17
2.4. Results	21
2.4.1. Shoreline evolution	22
2.4.1.1. Megacusps	22
2.4.1.2. Beach mobility	25
2.4.1.3. Response to storms	26
2.4.2. Beach area	26
2.4.3. Beach orientation	28
2.5. Discussion	31
2.6. Conclusions	34

3. Dynamics of single-barred embayed beaches	37
3.1. Introduction	37
3.2. Field site	40
3.3. Methodology	41
3.3.1. Shoreline and barline extraction	41
3.3.2. Morphological descriptors	43
3.3.3. Wave data	44
3.4. Wave conditions	45
3.5. Alongshore-uniform behaviour	47
3.6. Alongshore non-uniform behaviour	50
3.6.1. Bar and shoreline evolution	51
3.6.1.1. La Barceloneta	51
3.6.1.2. Bogatell	55
3.6.2. Bar and shoreline orientations	57
3.7. Discussion	59
3.8. Conclusions	62
4. Morphodynamic response of embayed beaches to a beach nourishment	65
4.1. Introduction	65
4.2. Study area	66
4.3. Methodology	68
4.4. Results	69
4.4.1. Description of the nourishment	69
4.4.2. Beach evolution after the nourishment	71
4.4.2.1. Emerged beach	71
4.4.2.2. Submerged sandbars	73
4.5. Discussion	74
4.6. Conclusions	76
5. Morphodynamic response of a two-barred beach to a shoreface nourishment	79
5.1. Introduction	79
5.2. Field site description	81

5.3. Methodology	83
5.3.1. Video imagery	84
5.3.2. In situ surveys to obtain shoreline and bathymetric data	86
5.4. Results	87
5.4.1. Sandbars	87
5.4.1.1. Nourishment behaviour	87
5.4.1.2. Bar section in front of the nourishment	88
5.4.1.3. Bar sections on both sides of the nourishment	91
5.4.2. Shoreline response to the nourishment	96
5.5. Intersite comparison	97
5.6. Conclusions	100
6. Conclusions and future research	103
6.1. Methodological contributions	103
6.2. Morphodynamics of artificial embayed beaches	105
6.2.1. Seasonal and interannual beach morphodynamics	106
6.2.2. Beach morphodynamics related to storms	108
6.3. Morphodynamic impact of artificial nourishments	109
6.3.1. Beach nourishment	109
6.3.2. Shoreface nourishment	110
6.4. Future research	111
7. Bibliography	113

Acknowledgements

Agradecer a las personas que han estado cerca durante estos años no es nada sencillo. Son muchos y no me gustaría dejarme a nadie atrás.

A Jorge Guillén. Siempre se agradece al director de tesis y se dice que sin él la tesis no hubiese llegado a nacer. En este caso es totalmente cierto. Jorge me dio la opción de empezar a investigar sin fechas, con calma y esperando a que naciese el cariño entre las playas y yo, las ganas de empezar un doctorado. Gracias jefe por tener tiempo para discutir sobre el trabajo y para charlar, por trabajar con buen humor y dándole a las cosas su justa importancia. Y por enseñarme también eso de “un problema, una solución”.

A los compañeros del grupo. En especial a Oscar Chic, por su disponibilidad para prestarme ayuda en cualquier momento y a Raúl González por transformar algunas de mis rutinas de MatLab en herramientas entendibles para los demás, por la super-web de la Estación Litoral de Barcelona que me facilita la vida y por las fotos de la portada de la tesis. Y a mi gente de los muestreos mensuales de HABES-PUDEM.

También a quienes pasaron por aquí a hacer prácticas o estancias con nosotros. Simone Simeone, Francesca Malena o Niels van der Berg. Siempre hemos tenido muy buena suerte con los visitantes que iban llegando y muchos de ellos se convirtieron en buenos amigos. A Timothy Price y Gemma Ramaekers les agradezco especialmente por su ayuda con el análisis de parte de los datos del capítulo 3 de la tesis pero, sobre todo, por ser buenos amigos y unos de mis mejores compañeros de payasadas.

Cesca Ribas no sólo ha sido mi compañera de despacho, la encargada de conseguirme entradas para buenos conciertos o la compañera de viajes. Además, es una buena amiga con quien hablar de ciencia y de paciencia, alguien de quien coger parte de su cariño por las barras y con quien disfrutar de este mundillo costero.

During some four months in 2005 I had the privilege to work under the supervision of Gerben Ruessink during a stage at the Utrecht University. The work with Gerben matured to become a paper, chapter 5 of this thesis. Thank you Gerben and thanks also to everyone in the Physical Geography department for their warm welcome.

I am grateful to Ruud Spanhoff (Rijkswaterstaat) for providing the bathymetric surveys used in chapter 5. I also want to thank for chapter 5 data to Susanne Quartel (Utrecht University), for the dGPS surveys and for taking me, for the very first time (the one and only, actually), to Noordwijk aan Zee on a calm and sunny day.

Gracias a los buenos amigos de los comienzos por Barcelona (los tiempos de Tirma), los del doctorado, los de la comida, los más nuevos y los que siempre han estado. A mi nueva familia que he hecho en Barcelona durante estos años y, por supuesto, a los amigos de viajes y aventuras.

A mi familia. Tengo la suerte de tener una familia grande de esas en las que hay muchas cosas buenas y poquitas malas. Hace unos años, nombrar a cada uno de ellos en estos agradecimientos me hubiese llevado muchísimo tiempo y tinta; pero después de estos años en Barcelona, mi familia se ha multiplicado y ahora sí que resultaría totalmente imposible. Sí quiero tener un recuerdo muy especial por quienes se fueron en estos años, Facisco, Octavio y mi abuelo Felo. Y por los que llegaron o están a punto de llegar. Gracias Adriano por alegrarme los días con solo decir mi nombre.

La otra extensión de la familia llegó con Tona. Mi familia mexicana también es deliciosa (como la canaria) y grande. Gracias a Vicky y Ernesto por hacerme sentir tan querida y a Lyz, Becky y Daniel por convertirse en mis nuevas hermanas y hermano ¡y por hacerme tía!

A mis padres, que tantas veces me dieron el empujoncito necesario para lanzarme a hacer cosas (al fin y al cabo es a ellos a quienes les debo agradecer todo-todo), mis hermanas y mi hermano, que son quienes están ahí y de quienes nunca me olvido, a Sergio, Adrián y Lama. Y a mi abuela Isabel, que es el centro y la fuerza que me llama hacia mi tierra.

A Tonatiuh. Porque encontrarte en Barcelona hizo que parte de mi historia tuviese todo el sentido. Gracias por hacerme sentir cada día que la vida me sonríe.

Este estudio se ha realizado en el marco del proyecto PUDEM (REN2003-06637-C02-01/MAR) financiado por el Ministerio de Educación y Ciencia. También me gustaría agradecer al mismo ministerio por la beca de Formación de Personal Universitario (FPU) de la que disfruté entre 2004 y 2007.

Summary

This thesis aims to deepen the knowledge about the morphodynamics of anthropogenic impacted beaches focusing at a spatial scale of tens of metres to kilometres and time scales ranging from several hours (e.g. response to a storm event) to interannual (e.g. interannual migration pattern). With this purpose two stretches of coast subject to human interventions but with different characteristics have been monitored:

- Three of the beaches of the coast of Barcelona city: La Barceloneta, Nova Icaria and Bogatell (Mediterranean Sea, Spain), which are a series of artificial embayed beaches enclosed by perpendicular groins in the laterals and a promenade in their backside.
- Noordwijk beach (North Sea, the Netherlands), a sandy beach with a narrow dune field on its backside, which is part of the ~120 km long central Dutch coast.

The previous scientific knowledge of the morphodynamics of both regions prior to this study was quite different. While the dynamics of Barcelona city beaches was poorly known before this study, the nearshore dynamics of Noordwijk have been widely studied (e.g., Van Enckevort and Ruessink 2003a, 2003b; Quartel *et al.*, 2007, 2008). For this reason, the first two chapters of the thesis are dedicated to investigate the morphodynamics of Barcelona city beaches, and the following two chapters analyze the response of the nearshore after artificial nourishments at Barcelona and Noordwijk beaches. Both beaches are monitored through an Argus video system that comprises five video cameras pointing at the beaches. At Noordwijk the cameras are located at a height of approximately 60 m, in Barcelona at about 142 m.

Chapters 2 and 3 focus in the shoreline and sandbar dynamics of Barcelona city beaches respectively, investigating the nearshore response to storm events, the behaviour of the emerged beach area, the three-dimensional changes in the sandbar configuration and the beach rotation at different time-scales.

The beach of Nova Icaria is the most stable of the three beaches. Its dynamics during the study have shown a non-barred beach that is typically at the Reflective beach state. Occasionally the southern section of the beach is at the Low Tide Terrace beach state. This beach, the most protected one, is capable of self-recovery after erosive periods so it has not required beach nourishment after its creation. During certain storm events, there are rapid changes of the beach orientation, most of them related to the erosion of the southern section of the beach. After these abrupt modifications of the beach plan shape, the gradual recovery of the beach after those storm events imply episodes of beach rotation (change in the beach orientation without change in the total emerged beach area).

Bogatell is a barred beach often showing a terraced-bar. It switches among the different *Intermediate Beach* states. The sandbar dynamic depends on the wave conditions and is characterized by numerous changes from a shore-parallel to a crescentic bar. After the nourishment performed on summer 2002 this beach followed an erosive trend for approximately a year and a half, until it reached a stable beach area that remained almost constant in the following years. Episodes of beach rotation occur at this beach at two different timings: rapid episodes related to storm events or human interventions, and slow episodes related to the recovery of a certain beach shape.

The beach of La Barceloneta is also a barred beach that switches among the different *Intermediate Beach* states, with the difference that at this beach the complete reset of the bar configuration (i.e., the Longshore Bar and Trough state) is uncommon due to the almost-permanent presence of a crescentic shape (protuberance) at the southern limit. During the monitored years, La Barceloneta showed an erosive trend temporary alleviated with human interventions (artificial nourishment and sand relocation). Beach rotation episodes were less common than in Bogatell, but they also occurred with the described two timings. La Barceloneta and Bogatell beaches experienced periods of low wave energy that caused the arrest of the nearshore morphology. At those moments, the beach state was not in accordance with the prevailing wave conditions.

The dynamics of the shore-parallel submerged sandbars of La Barceloneta and Bogatell shows the alongshore-averaged cross-shore migration of the bars to have an overall onshore migration trend; while the interannual component of

this migration was observed to be coupled with the interannual wave climate. There was a relationship between the bar sinuosity and the sediment availability in the submerged profile, with crescentic shapes occurring in the bar after periods of shoreline retreat. At La Barceloneta and Bogatell the beach evolution is also influenced by the formation of long-lasting megacusps. In addition to this coupling of the three-dimensional configuration of the beach, the bar and the shoreline also show a coupling in their orientations at time scales ranging from seasons to years.

The morphodynamic response of the nearshore to the beach nourishment of Barcelona and the shoreface nourishment of Noordwijk is analyzed in Chapters 4 and 5 respectively.

Due to the high relevance of the beach nourishment on the dynamics of La Barceloneta and Bogatell beaches, Chapter 4 focuses on the period after the nourishment. La Barceloneta and Bogatell beaches were nourished between June and July 2002 with 110000 m³ of sand, after a very energetic period that produced widespread beach erosion. The nourishment at La Barceloneta beach produced an increase of the emerged area of 5000 m² with a mean advance of the shoreline of 14 m, whilst at Bogatell, the area increased by 12750 m² and the mean advance of the shoreline position was 20 m. The recorded storms did not significantly reduce the beach area overall. After the nourishment both beaches showed a reduction in their beach areas with mean losses, calculated for a year and a half later, of 23 m²/day at La Barceloneta and 18 m²/day at Bogatell.

Chapter 5 describes the response of the two-bar system at Noordwijk to a shoreface nourishment carried out from February to March 1998 with 1.7 Mm³ of sediment. The nourishment formed a 3 km alongshore bump seaward of the outer bar that migrated more than 300 m onshore in 4 years before losing its integrity. The nourishment did not influence the shoreline position as its trend did not undergo distinctive variations after 1998. However, it interrupted the autonomous seaward migration of the inner and the outer bar for the entire duration of the study period. Moreover, the nourishment also produced clear head effects on both flanks, with the bar becoming discontinuous and the flank section decaying or becoming attached to an offshore-located bar, while the section of bar landward of the nourishment became attached to a landward-located bar. This sequence of morphologies is known as bar switching. Each switching episode took almost one

year to complete and therefore could not be ascribed to individual wave events. We suspect that shoreface nourishments enhance the possibility of bar switching by creating alongshore variability in the position and depth of the outer bar and in its cross-shore migration rate and direction. Allaying earlier fears, the nourishment of Noordwijk did not intensify the three-dimensional patterns in the bars, such as the crescentic plan-shape and rip channels.

Resumen

El objetivo de esta tesis es profundizar en el conocimiento de la morfodinámica de playas afectadas por actividades humanas, considerando escalas espaciales de decenas de metros a kilómetros y escalas temporales que varían desde algunas horas (por ejemplo, la respuesta ante un temporal) hasta varios años (por ejemplo, los patrones de migración interanuales). El estudio se basa en la monitorización de dos áreas costeras con diferentes características. Por un lado, las playas del litoral de la ciudad de Barcelona, en la costa mediterránea del NE de la península ibérica. De las siete playas que forman el litoral de la ciudad de Barcelona, se estudian las playas de Nova Icaria, La Barceloneta y Bogatell. Se trata de playas artificiales, encajadas entre diques perpendiculares a la costa y limitadas en su parte interna por un paseo marítimo. Por otra parte, se estudió la playa de Noordwijk aan Zee, localizada en la costa central holandesa, en el Mar del Norte. En este caso se trata de una playa abierta y rectilínea, limitada en su parte interior por un cordón dunar.

Los estudios previos sobre la morfodinámica costera en ambas zonas de estudio ponen de manifiesto un grado de conocimiento desigual: la dinámica de las playas barcelonesas era poco conocida, mientras que la de Noordwijk había sido ampliamente estudiada (por ejemplo, Van Enckevort y Ruessink 2003a, b; Quartel *et al.*, 2007, 2008). Por este motivo, los dos primeros capítulos de la tesis se centran en el estudio de la morfodinámica de las playas de Barcelona y los dos siguientes analizan la respuesta de cada una de las zonas de estudio a sendas regeneraciones artificiales. La monitorización morfológica de las playas se ha llevado a cabo utilizando un sistema de video Argus, compuesto de cinco cámaras que apuntan a las playas. En Noordwijk las cámaras se encuentran a unos 60 m de altura y en Barcelona a 142 m.

Los capítulos 2 y 3 se centran en la dinámica de la línea de costa y de las barras de arena sumergidas de las playas de Barcelona, investigando la respuesta de la zona costera frente a temporales, la variación temporal del área de la playa emergida, los cambios en la forma en planta de las barras de arena y la rotación de las playas

a diferentes escalas temporales.

Nova Icaria es la más estable de estas tres playas. Se trata de la playa más protegida respecto al oleaje y es capaz de recuperar su configuración después de periodos erosivos, por lo que no ha sido necesario regenerarla artificialmente desde su creación. Su estado morfodinámico característico es el de *Reflective Beach* (playa Reflejante). Nova Icaria no tiene barra de arena sumergida aunque, en ocasiones, la sección sur de la playa se muestra en el estado *Low Tide Terrace*. La erosión de la zona sur de la playa durante determinados temporales ocasiona cambios de orientación, de los que se recupera gradualmente causando episodios de rotación (cambios en la orientación de la playa sin cambios en el área total emergida).

Bogatell es una playa con una barra de arena sumergida que, en ocasiones, carece de surco asociado y da lugar a una terraza (*terraced bar*). El estado morfodinámico de la playa varía entre los cuatro estados de *Intermediate beach*. La dinámica de la barra depende de las condiciones del oleaje y se caracteriza por los numerosos cambios entre una barra rectilínea y una barra con una configuración crescéntica. Después de la regeneración artificial de arena que se llevó a cabo en la playa en Junio-Julio de 2002, la playa de Bogatell mantuvo una tendencia erosiva durante un año y medio, hasta alcanzar un área de playa estable que se mantuvo prácticamente constante durante los años posteriores. Los episodios de rotación que tienen lugar en esta playa ocurren a dos escalas temporales diferentes: cambios rápidos asociados con temporales o con intervenciones humanas y cambios lentos debidos a la recuperación de la forma en planta de la playa.

La Barceloneta también tiene una barra de arena sumergida y su configuración morfológica varía entre los cuatro estados de *Intermediate beach*. A diferencia de Bogatell, el cambio desde una barra crescéntica a una rectilínea ocurre muy raramente. La singularidad de la playa de La Barceloneta radica en la presencia casi permanente de una protuberancia o saliente de la barra en la zona sur de la playa durante el periodo de estudio. Esta playa muestra una tendencia erosiva temporalmente aliviada por intervenciones humanas, es decir, por la regeneración artificial y el trasvase de arena de la zona sur a la zona norte de la playa. Los episodios de rotación son menos frecuentes que en Bogatell, pero también ocurren en las mismas escalas temporales (rápido, asociado a temporales, y lento, por la recuperación de la playa). En La Barceloneta y en Bogatell, se ha observado que, en periodos de baja energía del oleaje, la morfología de la playa corresponde a la de

un estado morfodinámico heredado de condiciones de mayor energía, pero que no es acorde con las condiciones del oleaje en ese momento.

La dinámica de las barras de arena sumergidas de La Barceloneta y Bogatell muestra una migración neta hacia la costa durante el período de estudio; y la componente interanual de esta migración parece estar ligada a la componente interanual de la energía del oleaje. Por otra parte, se pone de manifiesto que existe una relación entre la sinuosidad de la barra y la disponibilidad de sedimento en el perfil sumergido, con barras más crescénticas después de periodos de retroceso de la línea de costa. Además del acoplamiento de las morfologías durante determinados estados de la playa (barra crescéntica unida a megacúspides), en estas dos playas también hay un acoplamiento de la orientación de la línea de costa y las barras sumergidas a escalas temporales estacionales o anuales.

Los capítulos 4 y 5 de la Memoria analizan la respuesta morfodinámica de la zona costera a las aportaciones artificiales de arena. Las regeneraciones artificiales tuvieron lugar en la playa emergida y en la playa sumergida en Barcelona y Noordwijk aan Zee respectivamente.

La regeneración de las playas de La Barceloneta y Bogatell tuvo lugar entre junio y julio de 2002, después de un período con numerosos temporales que causaron una fuerte erosión de las playas. Se vertieron 39539 m³ de sedimento en La Barceloneta y 71282 m³ en Bogatell. La regeneración de La Barceloneta produjo un aumento del área de playa emergida de aproximadamente 5000 m², con un avance medio de la zona norte de la playa de unos 14 m. En Bogatell, el área de playa emergida aumentó unos 12750 m², mientras que el avance medio de la línea de costa fue de unos 20 m. Después de la regeneración, ambas playas mostraron una disminución de sus áreas con pérdidas medias (calculadas para un año y medio después de la intervención) de 23 m²/día en La Barceloneta y 18 m²/día en Bogatell. La erosión de las playas tras la regeneración no depende del contenido energético de los temporales sino del tiempo acontecido desde la regeneración. Un año y medio después de la regeneración, ambas playas mostraban valores de área de playa emergida muy similares a los anteriores a la regeneración; mientras que las barras sumergidas se hicieron más sinuosas. Los resultados sugieren que estas playas encajadas no son celdas totalmente aisladas ya que parece haber transporte longitudinal de sedimento sobrepasando los diques.

El Capítulo 5 describe la respuesta del litoral de Noordwijk a una regeneración del perfil de playa sumergido llevada a cabo entre febrero y marzo de 1998. Se vertieron 1.7 Mm³ de sedimento a una profundidad de entre 5 y 8 m, formando una barra artificial de unos 3 km de longitud paralela a la costa y localizada en la parte distal del perfil litoral. Después de su creación, la nueva barra migró unos 300 m hacia la costa en 4 años, antes de que el sedimento empezara a dispersarse y la barra a perder su identidad. La línea de costa no quedó afectada por la regeneración artificial; sin embargo, la regeneración sí tuvo efecto en la dinámica de las barras de arena sumergidas. La presencia de la nueva barra artificial detuvo la migración hacia la plataforma continental de las barras naturales localizadas frente a ella durante todo el período de estudio (es decir, casi 6 años después de la regeneración). Por otro lado, el tramo de las barras no afectado por la regeneración continuó su migración natural hacia la plataforma continental. Las diferencias entre la migración de las barras localizadas en la zona de sombra de la regeneración y las situadas a ambos lados de la regeneración provocan la fragmentación de la barra. La parte no afectada por la regeneración artificial continúa su migración alejándose de la costa, y se desvanece o se une a una barra más externa. Por otra parte, la sección de la barra localizada en la zona de sombra de la regeneración se une a otra barra más cercana a costa. Este patrón morfológico es conocido como sustitución de barras (*bar switching*). En el caso de Noordwijk, esta secuencia de morfologías ocurrió a ambos lados de la regeneración, y cada una tuvo una duración de aproximadamente un año. La influencia de la regeneración frenando la migración de las barras en la zona de sombra de la regeneración y, por tanto, aumentando la diferencia en la localización de la barra a lo largo de la costa, estimuló estos episodios de sustitución de barras.

List of figures

1.1.	Spatial and temporal scales in beach morphology.	2
1.2.	Example of the three types of images obtained from the Argus video system at Noordwijk station (6 February 2007): a) snap shot image, b) time-exposure image and c) variance image.	6
1.3.	Example of the panoramic and rectified plan view obtained from the Argus station of Barcelona city beaches (21 October, 2001). Five individual time-exposure images are used to compose these merged images.	7
2.1.	Parameters used to define beach rotation	14
2.2.	Significant wave heights off Barcelona during the study period	15
2.3.	Study area	16
2.4.	Argus plan view of the study area showing beach <i>control transects</i> . Distances are given in meters.	18
2.5.	Time-space diagrams of the deviations of the shoreline location referring to the <i>reference shorelines</i> . Warm colours are related to advances in the shoreline location and cold colours to retreats; colour bar values are given in meters. The x axis refers to the alongshore location and the y-axis to the time. Main storm events (A-Q) are indicated.	23
2.6.	Time series of shoreline position changes along <i>control transects</i> . From top to bottom: La Barceloneta, Bogatell and Nova Icaria. Y axis gives the variation along transects in meters. The grey lines indicate storms commented in the text and the rectangles, the nourishments.	24
2.7.	Beach mobility at the different alongshore locations in La Barceloneta, Bogatell and Nova Icaria beaches.	25
2.8.	Time series of emerged beach areas: a) La Barceloneta, b) Bogatell and c) Nova Icaria.	27
2.9.	Time series of the beach orientation: a) La Barceloneta, b) Bogatell and c) Nova Icaria.	28
2.10.	Change in beach orientation (squares) and mean S_{xy} (rhombus) for each storm event calculated for Bogatell beach. Mean S_{xy} during the event calculated for waves ≥ 1.5 m. The x-axis relates the name of the events; their dates are given in Table 2.2.	30
2.11.	Change in the shoreline position of Nova Icaria beach between the first and last day of the study period. The picture shows the last day (1st January 2005) with the first (black line) and the last (white) shorelines superimposed.	33

3.1.	Study area with the location of the Argus station. The white rectangle indicates the area visible with the video cameras.	39
3.2.	Plan view obtained after rectifying and merging the time-exposure images of the five video cameras from 17 April, 2004. The origin of the coordinates is at the video camera's position. The alongshore coordinate, y , increases northwards and the cross-shore coordinate, x , increases seawards. Dotted lines indicate the location of the bathymetric profiles presented in Figure 3.3.	40
3.3.	Representative bathymetric profiles of the four studied beaches. The solid line corresponds to the bathymetry on 4 October 2003 and the dotted line to that on 5 November 2003. See profile locations in Figure 3.2.	42
3.4.	a) Significant wave height (H_s), and b) mean wave direction with respect to north. Black dots represent the most significant storm events occurring during the study period (a further explanation can be found in the text), labelled using roman numerals. Given the high H_s values reached during Event ii, this figure and the following figures of this chapter with H_s will show a vertical scale with values ranging between 0 and 6, therefore excluding the 3 values of $H_s > 6$ m occurring during Event ii ($H_s = 6.8, 8.8, \text{ and } 8.7$ m).	45
3.5.	a) Wave energy content for the WANA data set, subsequently separated into b) interannual [$E_{ia}(t)$], c) seasonal [$E_s(t)$] and d) weekly [$E_w(t)$] component.	47
3.6.	Time evolution of significant wave height (a), and alongshore-averaged mean cross-shore location of the bar (b) and the shoreline (c) at La Barceloneta and the bar (d) and the shoreline (e) at Bogatell during the study period. Measurements in (b) and (d) correspond to bar measurements containing more than 80% of the data surveyed when H_s was lower than 1.90 at La Barceloneta and 1.70 in Bogatell.	48
3.7.	a) Alongshore-averaged cross-shore positions [$Xy(t)$] for the bar at La Barceloneta and Bogatell separated into b) yearly [$X_{ia}(t)$], c) seasonal [$X_s(t)$] and d) weekly [$X_w(t)$] components.	49
3.8.	Time-averaged barlines during the study period (dark line) and the most remote locations reached by the bars during the study period (lighter lines). Cross-shore distances are relative to the <i>reference shoreline</i> .	50
3.9.	Daily-averaged values of the sinuosity of the bar at La Barceloneta (a) and Bogatell (b).	51
3.10.	Time-space diagrams of the shoreline (left) and barline (centre) positions at La Barceloneta beach. The colour scales are given in metres and represent the distance from the <i>reference shoreline</i> . Cold colours represent the most shoreward locations and warm colours the most seaward locations. White horizontal bands in the bar plot represent moments when no data were available. Significant wave height (H_s) is given on the right.	52

3.11.	Examples of the different beach states attained at La Barceloneta: <i>Longshore Bar and Trough</i> (a), <i>Rhythmic Bar and Beach</i> (b), <i>Transverse Bar and Rip</i> (c and d), and <i>Low Tide Terrace</i> (e).	54
3.12.	Time-space diagrams of the shoreline (left) and barline (centre) positions at Bogatell beach. The colour scales are given in metres and represent the distance from the <i>reference shoreline</i> . Cold colours represent the most shoreward locations and warm colours the most seaward locations. White horizontal bands in the bar plot represent moments when no data were available. Significant wave height (H_s) is given on the right.	55
3.13.	Examples of the different beach states attained at Bogatell: a) <i>Longshore Bar and Trough</i> , b) <i>Rhythmic Bar and Beach</i> , c) and d) <i>Transverse Bar and Rip</i> , and e) <i>Low Tide Terrace</i> .	56
3.14.	Orientation of a) the shoreline at La Barceloneta, b) the barline at La Barceloneta, c) the shoreline at Bogatell and d) the barline at Bogatell, where the angles are measured with respect to north.	58
4.1.	Location of the study area.	67
4.2.	Significant wave height measured near Barcelona city during the study period.	69
4.3.	Plan views of the beaches in summer 2002. Top: 1st June, before the start of the nourishment works. Center: 19th June, nourishment taking place in Bogatell beach with the ship discharging sand. Bottom: 13th July, nourishment taking place in La Barceloneta beach with presence of the ship in its northernmost section.	70
4.4.	Shoreline evolution of La Barceloneta beach. Upper illustration: significant wave height. Lower illustration: time series of shoreline position changes along <i>control transects</i> in La Barceloneta (Y axis gives the variation along the transect in meters).	71
4.5.	Shoreline evolution of Bogatell beach. Upper illustration: significant wave height. Lower illustration: time series of shoreline position changes along <i>control transects</i> in Bogatell (Y axis gives the variation along the transect in meters).	72
4.6.	Emerged beach area evolution of La Barceloneta and Bogatell beaches. a) significant wave height, b) time series of La Barceloneta emerged beach areas, and c) time series of Bogatell emerged beach areas.	73
4.7.	Planview of Bogatell beach on 17 October 2003.	76
5.1.	Study region with the location of the Argus station. Beach poles indicate distance in kilometres from a regional zero. Beach pole 82 corresponds to $y = 0$.	81
5.2.	Example of bar switch. The image corresponds to the area around beach pole 84 ($y = 2000$ in local coordinates) on 6th November, 1996 (Adapted from Van Enckevort, 2001).	82

5.3.	a) First Argus image with the bumped region corresponding to the nourishment; b) Noordwijk bathymetry of the study area on 9th June 2000, the first one showing the bumped region formed by the nourishment, and c) 5th April 2002 bathymetry. Notice the differences in the bar configuration between b and c (decrease of bar trough depth). Alongshore distance, in local coordinates, corresponds to beach poles 79 (-3000) to 85 (3000).	83
5.4.	Cross-shore profile of the bathymetric survey performed on 9 June 2000. Alongshore location $y = 0$.	84
5.5.	Alongshore-averaged cross-shore location for the nourishment and for the inner and outer bar in the central section. Grey: pre-nourishment data.	88
5.6.	a) Inner and outer bar alongshore averaged cross-shore positions [$Xy(t)$] after the nourishment separated into b) yearly [$Xia(t)$], c) seasonal [$Xs(t)$] and d) weekly [$Xw(t)$] component.	89
5.7.	Sinuosity of the a) inner and b) outer bar at the 3-km central section for the pre-nourishment (grey line) and the post-nourishment (black line) situations. Note the different scales on the y-axis.	91
5.8.	Inner and outer bar timestacks. Colours represents the cross-shore location (in metres) of the bar for each alongshore location and time. Blanks represent time gaps equal or longer than 30 days.	92
5.9.	Time series of a) Hrms (m), and the cross-shore location of the inner (grey) and outer (black) bar on the b) northern, c) central and d) southern sections.	93
5.10.	Bar switching episode northward of the study region. a) Situation before the bar became discontinuous, b) outer bar separated, c) forked shape formed between the inner and the intertidal bar, d) forked shape formed between the inner and the outer bar, e) outer bar joins the landward section of inner bar and inner bar become discontinuous, f) forked shape formed between the inner and the intertidal bar, g) inner bar switching.	94
5.11.	Bar switching episode southward of the study region. a) Initial morphology before the formation of the discontinuous outer bar, b) offshore migration of the outer bar, c) offshore migration of the inner bar, d) forked shape and, e) and f) new arrangement of the bar system.	95
5.12.	Shoreline locations alongshore-averaged for the 6 km study region except for the dGPS surveys, which represent only a 1.5 km section in front of the nourishment area.	96
5.13.	Location of the nearshore nourishments in a) Terschelling, b) Noordwijk and, c) Egmond. Notice that this sketch does not represent the real bathymetry at each site.	97

List of tables

2.1.	Mean and standard deviation of the alongshore differences between dGPS-surveyed and Argus-derived shorelines (values given in meters).	19
2.2.	Storms with H_s reaching 2.5 m.	20
2.3.	Statistical values for the area measurements during the study period.	27
2.4.	Changes produced by storm events in the beach orientation and at the beach area at each side of the pivotal point (northern and southern sections).	29
2.5.	R-squared values resultant from the comparison between the beach area change (considering the northern and southern sections of each beach independently) and the change in beach orientation due to storm events. Values printed in cursive are those significant at the 95% confidence level; bold are highly significant.	32
3.1.	Morphological characteristics of the four studied beaches.	41
3.2.	Characteristics of the storms most mentioned in the text.	46
4.1.	Main features of the study beaches.	67
5.1.	Cross-shore migration rates for the pre-nourishment (grey background) and post-nourishment situations.	90
5.2.	Characteristics of the three discussed shoreface nourishments. The D_{50} value refers to the nourished sand.	97

1 Introduction

1.1. THE COASTAL SYSTEM

The coastal system is in incessant change, subject to the constant action of waves and tides (in addition to the wind action) that shape its morphology. The mutual interaction and adjustment of the seafloor topography and the fluid dynamics involving the motion of sediment is known as *coastal morphodynamics* (Voigt, 1998). This interrelation can be explained as follows: in the nearshore region the water motion is influenced by the seafloor topography and is responsible of sediment transport. Gradients in the sediment transport produce morphological changes in the seafloor. The loop is complete as hydrodynamic processes respond to the modified bathymetry.

The morphology of sandy beaches changes over a large range of scales in time and space (Figure 1.1.). For instance, we can observe wave ripples with wave lengths of tens of centimetres, which can form or change within minutes (Becker *et al.*, 2007); and individual storm events that can alter the nearshore in hours, flattening the beach profile and causing offshore sandbar migration (Shepard, 1950). But we can also observe seasonal variations in the beach profile (Komar, 1998); shoreline sand waves with spatial scales of several kilometres and time scales of the order of several years (Verhagen, 1989); or inter-annual changes in the submerged sandbar morphology like the so-called Net Offshore Migration pattern which imply cyclic offshore migration of up to 15 years (e.g., Ruessink and Kroon, 1994). Since the study of the nearshore is concerned with a large range of scales, this must be contemplated when approaching a certain problem at the coastal system. An ideal measurement campaign requires some previous knowledge of the scales in order

to define the spatial and temporal resolution of the survey and its duration. At a certain scale of interest, the effect of the higher scales will be described as *boundary conditions* and the effect of lower scales will be considered *noise*.

This variability in beach dynamics has originated numerous studies from different standpoints, objectives and processes. In the nearshore region of sandy beaches, the shoreline and the nearshore sandbars are two of the main features that have been studied from daily to decadal time scales and concerning spatial scales ranging from tens of meters to kilometres. These two elements are of valuable importance; they represent the buffering region of the beach (where the waves liberate their energy) and they are subject to frequent changes. From a coastal management perspective, the shoreline delineates the beach available for users and the bars represent a sand supply to and a protection of the emerged beach.

The shoreline is the limit between the water and the exposed beach (Komar, 1998). It is widely used as a proxy for the volume of sand in the beach (Farris and List, 2007) and, for this reason it has been investigated in a number of settings. Shoreline studies are directed to understand a variety of components of the beach dynamics; for instance, shoreline mobility (e.g., Dolan *et al.*, 1978), long-term erosion or accretion patterns (e.g., Guillén *et al.*, 1999), beach rotation (e.g., Short and Masselink, 1999), plane shape of the beach (mainly in the case of embayed beaches) (e.g., Silvester, 1960), changes due to human interventions (e.g., Grunnet

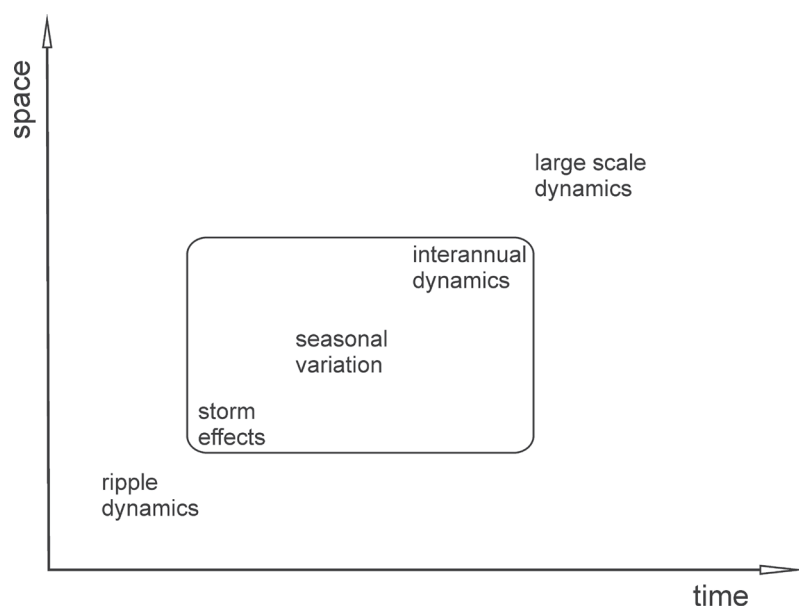


Figure 1.1. Spatial and temporal scales in beach morphology.

and Ruessink, 2005), or shoreline sand-waves (e.g., Stewart and Davidson-Arnott, 1988).

Nearshore sandbars are elongated shoals typically located parallel to the shoreline and accompanied by a depression in their landward side, the trough. Occasionally the trough is not present; we will refer to those sandbars as *terraced bar*. Depending on their location nearshore sandbars can be *intertidal* (the ones found in the area between the mean low- and high-water level) (Masselink *et al.*, 2006) or *subtidal* (those below low-water level). In this thesis we will focus on subtidal sandbars. Subtidal sandbars can be present individually (in single-barred beaches) or up to four bars (in multi-barred beaches). They are highly dynamic formations that present changes in their cross-shore profile and also in the plan shape. In the cross-shore section they tend to migrate offshore during storm wave conditions and onshore during conditions dominated by smaller waves and swell (e.g. Elgar *et al.*, 2001). Their simplest plan-shape form is shore parallel (*alongshore uniform* or *shore-parallel bars*), but they can also show crescentic shapes (*alongshore rhythmic bars*). When a section of the bar attaches to the shoreline, the latter acquires an undulated shape called *megacusp*.

Sandy beaches, particularly those in the European continent, are subject to important anthropogenic pressure. The effects of this anthropogenic influence must be considered in order to attain a complete understanding of the morphodynamic processes acting on a beach. This thesis involves two different study areas that have been affected by artificial nourishments: a series of urban beaches bounded by perpendicular groins and an open beach.

1.2. ARTIFICIAL NOURISHMENTS

Beach erosion occurs when the losses of beach sediment exceed the gains. The associated beach retreat joint to the presence of populations or structures in the back of the beach (an ever-increasing situation) creates the necessity of protection in order to reduce the erosion hazard. The artificial nourishment of the coast is one of the most used techniques of beach protection.

Artificial nourishments imply the addition of sediment from an external source (the borrow area) to the shore. They are widely carried out as a response to coastal erosion problems. Actually, in the last decades the implementation of these *soft engineering solutions* has taking the place of *hard engineering solutions* (e.g.

construction of shore-protection structures) since artificial nourishments represent less environmental and visual impact in the adjacent area and preserve the beach resource while hard engineering solutions often create damage to other parts of the coast (Hanson *et al.*, 2002).

Artificial nourishments are mainly carried out for safety or recreational reasons. The safety reasons include, for instance, attaining an improvement of the coastal stability, protecting onshore locations against flooding by storm surges, mitigating the effect of the shoreline retreat, or protecting structures placed close to the beach. While the recreational reasons aim for an increase of the beach width, maintaining a tourist resource, or creating new beaches.

Nowadays, these interventions are placed in a variety of locations of the beach profile: the first dune row, the dune face, the emerged beach, the surf zone or the shoreface (Hamm *et al.*, 2002). They can be broadly divided in:

- Backshore nourishment: the nourished sand is placed on the backshore or at the foot of the dunes. In this way, the dunes are reinforced against erosion and breaching during extreme events, protecting onshore locations against flooding. The purpose of this type of nourishments is to protect the region behind the beach, as they do not imply an augmentation of the natural value of the beach and neither an increase of the recreational use of the beach.
- Beach nourishment: the sand is placed on the emerged beach. In this case, the borrow sand must be similar to or coarser than the native sand to adjust to the natural profile. This type of nourishment is performed in order to maintain or increase the recreational use of the beach, to protect the beach or to protect the region behind the beach.
- Shoreface nourishment: the sand is placed in the submerged profile. The shoreface nourishment is expected to cause wave breaking over it (as it acts as a submerged sandbar) and, therefore, to decrease the energy of the waves reaching the coast, increasing coastal safety.

Shoreface and beach nourishments have been carried out simultaneously in order to reinforce the entire beach profile. Examples of the combined nourishment of the emerged and the submerged beach profile are those carried out in Perdido Key, U.S.A. (Browder and Dean, 2000) and Egmond, the Netherlands (van Duin *et al.*, 2004).

Once a nourishment has been carried out, it is important to monitor its effects on the beach dynamics and the durability of these effects as, although the nourishment mitigates coastal erosion, the nourished beach will continue having the erosive trend (as the sediment transport pattern has not changed because of the fill in).

Spain and the Netherlands are the biggest nourishing countries in Europe (Hanson *et al.*, 2002), but the motivation of the nourishments as well as its execution and the posterior monitoring differ in both countries. In Spain, artificial nourishments are mostly directed to increase the recreational value of the beach (to attain a certain beach width). While the primary concern behind artificial nourishment in the Netherlands is to prevent flooding, as an important part of the country is below mean sea level (polders). These different motivations imply (i) differences in the nourishing strategy: Spain lacked of a long-term coastal management strategy regarding nourishments (i.e., they are typically implemented as a remedial measure) while in the Netherlands the decision of nourishing is legislated by the policy of Dynamic Preservation (i.e., nourishments are typically implemented as a preventive measure); (ii) difference in the location of the incoming sand: in Spain the nourishments are typically implemented at the emerged beach, which implies an immediate increase in the beach surface, while in the Netherlands backshore and shoreface nourishments are also implemented.

In Spain the monitoring of the nourishments has been only accomplished in a few important projects (Hanson *et al.*, 2002). While in the Netherlands nourishments are traditionally evaluated with a sampling frequency of 2 to 3 times per year over several years. However, this scheme is not sufficient to accurately evaluate the nourishment performance (Kroon *et al.*, 2007).

1.3. VIDEO MONITORING

1.3.1. INTRODUCTION

Long-term data sets with high temporal and spatial resolution are scarce. Two of the most studied long-term data sets are the JARKUS data set which consists of yearly bathymetric surveys along the Dutch coast (e.g. Wijnberg and Terwindt, 1995) and the surveys undertaken in Duck (U.S.A.) (e.g. Birkemeier and Holland, 2001). At present, video monitoring stations like Argus and other new video monitoring systems (e.g., camEra, Sirena, Horus, or KOSTA System) represent a new source of knowledge. They have the capability to obtain inexpensive long-term data series and are a good alternative (and complement) to traditional field

surveys, providing high temporal and spatial resolution together with large spatial coverage (typically 3 to 6 km).

Video monitoring techniques give the possibility to study a range of spatial and temporal scales, from specific cross-shore profiles to several kilometres of coast and with sampling intervals depending on the required measurement. Moreover, this technique is not as conditioned by weather and wave state as traditional surveys. Standard cameras can sample every daylight hour, although during certain weather conditions (e.g., fog or heavy rain) the images may be not usable. However, video monitoring allows the collection of large quantities of images, and the acquisition of a series of hydrodynamic and topographic parameters.

The Argus program was started in 1992 by the Coastal Imaging Lab at Oregon State University. An extensive description of the system and its history can be found in Holman and Stanley (2007). A typical Argus station is composed of a number of video cameras placed at a certain height above sea level and pointing towards the coast. The cameras are connected to a host computer that controls the capture, storage, pre-processing and transfer of images to the database and to the Internet.

The primary sampling technique is directed to obtain time-exposure images. This sampling is done every daylight hour during a ten-minute period (1 image per second). From the 600 images obtained, the system keeps three types of images (Figure 1.2): a snap shot, a time-exposure image (which contains the ten-minute average of the image intensity) and a variance image (which contains the standard deviation of the image intensity). In order to obtain real-world coordinates from these oblique video images each camera must be calibrated, to remove the radial lens distortion, and the image must go through some geometrical transformation



Figure 1.2. Example of the three types of images obtained from the Argus video system at Noordwijk station (6 February 2007): a) snap shot image, b) time-exposure image and c) variance image.

to find the relation between the image coordinates and the real-world locations. The process is described with detail in Holland *et al.* (1997). Once the images of the different cameras are rectified, they can be merged to obtain a plan view of the area (Figure 1.3).

1.3.2. PREVIOUS WORKS

Since the first times of the Argus system, a number of PhD theses related with the coastal system have covered a variety of subjects. A number of these theses aimed to develop new techniques and others were based on video monitoring to study the system. Some of the most relevant works are chronologically mentioned here. For instance, the work on edge waves developed by Lippmann (1992), the work on swash motion carried out by Holland (1995), the development of the first tool to map the shoreline location and the study of interannual shoreline and sandbar behaviour carried out by Plant (1998). Van Enckevort (2001) used video images to study the nearshore bar behaviour of Noordwijk (the Netherlands) at time scales ranging from days to years; and Siegle (2003) used video monitoring (combined with numerical modelling) to study the morphodynamics of an estuary mouth (Teignmouth, United Kingdom). Kingston (2003) used Artificial Neural Network and Evolutionary Computation techniques to study the coastal system, and to develop specific tools to extract data from video images (specifically, to produce morphological maps of the intertidal region and correct video estimations of sandbar location). Aarninkhof (2003) also developed specific tools to extract inter- and subtidal bathymetry from video images, and evaluated the possible utility of video techniques for coastal research and management purposes. Osorio (2005) proposed a new methodology to map the intertidal beach and also developed a



Figure 1.3. Example of the panoramic and rectified plan view obtained from the Argus station of Barcelona city beaches (21 October, 2001). Five individual time-exposure images are used to compose these merged images.

tool to determine the distribution of beach users. These two methods were applied to El Puntal beach (Spain). Quartel (2007) developed a new methodology to extract the morphology of the intertidal bar system (during low tide) and used this method to evaluate the role of daily morphologic changes in seasonal beach evolution. Chickadel (2007) used video images to measure nearshore waves and currents and study their dynamics over complex bathymetry.

Additionally to these PhD theses, a number of relevant papers covering a range of applications useful in coastal morphodynamic studies have appeared in the last decades. For instance, the estimation of hydrodynamic parameters have been improved thanks to methods to estimate longshore currents (Chickadel *et al.*, 2003), or wave parameters (Stockdon and Holman, 2000). Other measurements have taken place in the swash zone, like wave run-up (Holman and Guza, 1984) or swash maximum (Holland and Holman, 1993); and at the intertidal beach profile (Holman *et al.*, 1991; Madsen and Plant, 2001; Plant and Holman, 1997). Video techniques have also improved the monitoring of other morphologic features such as beach cusps (Holland and Holman, 1996; Holland, 1998, Almar *et al.*, 2008), rips (Holman *et al.*, 2006; Turner *et al.*, 2007), inlets (Morris *et al.*, 2001) or sandbars (Kingston *et al.*, 2000; Lippmann and Holman, 1989, 1990, 1993; Van Enckevort and Ruessink, 2003a, 2003b; Konicki and Holman, 2000); and the evaluation of specific processes such as nourishment evolution (Elko *et al.*, 2005).

These different methods and measurements have also reveal new applications suitable to coastal managers as the management of dynamic navigational channels (Medina *et al.*, 2007), the quantification of beach users (Guillén *et al.*, 2008), or the monitoring of river flumes (Morichon *et al.*, 2008). In fact, one of the most important projects related to the use of video monitoring on the coastal area at a European level was dedicated to develop video-derived products for coastal managers. It was the CoastView project (see Coastal Engineering Special Issue vol. 54, Issues 6-7 for more information). Besides, other projects have made use of Argus as a tool to achieve their objectives; for instance, the HUMOR and the Coast3D projects related to coastal morphodynamics, or the HABES project related to harmful algal blooms.

1.4. STUDY SITES

This thesis involves two stretches of coast of several kilometres alongshore and around 1 km across-shore: the artificial embayed beaches of Barcelona city

(NW Mediterranean, Spain) and the open beach of Noordwijk (North Sea, the Netherlands). Both study areas are subject to human interventions and attract high number of visitors; but they differ in their morphologies, and hydrodynamics.

The coast of Barcelona city contains a series of artificial embayed beaches enclosed by perpendicular groins in the laterals and a promenade in their backside. They were created as part of the recuperation plan that took place in the region for the 1992 Olympic Games and, only a few studies have been accomplished since their creation (MOPU, 1994; Sànchez, 2006). We will focus our study in three of the seven beaches in the city coast: La Barceloneta, Nova Icaria and Bogatell. These embayed beaches have lengths ranging between 400 and 1100 m. In October 2001 an Argus II video system was installed in the Mapfre building (142-m high) as part of the Coastal Monitoring Station of Barcelona (<http://elb.cmima.csic.es>). The system comprises five colour video cameras pointing obliquely towards the beaches and the Olympic Harbour.

Noordwijk beach is part of the ~120 km long central Dutch coast. The analyzed area comprises a region of 6.00 x 1.25 km. Noordwijk is a sandy beach with a single dune ridge on its backside. The nearshore region is characterized by an intertidal and two subtidal sandbars. Nearshore dynamics in Noordwijk have been widely studied (e.g., Van Enckevort and Ruessink 2003a, 2003b; Quartel *et al.*, 2007, 2008). In March 1995 an Argus video system was installed on the roof of *Huis ter Duin* Hotel, in Noordwijk aan Zee, the Netherlands at about 60 m height. This was an initial video system composed of two black and white video cameras looking approximately southward and northward. The system was updated in September 1998 with five colour cameras pointing at the beach and offering a 180° view of the coast.

1.5. OBJECTIVES AND THESIS OUTLINE

An ever increasing number of beaches are man-made or, at least, subject to frequent human interventions. However, only a limited number of studies on nearshore morphodynamics focus on these “artificialized beaches”. The majority of the studies aim to evaluate the performance of a certain intervention but they generally lack of sufficient temporal and spatial resolution.

The general objective of this thesis is *to deepen our knowledge about the morphodynamics of anthropogenic-impacted beaches focusing at a spatial scale of tens of metres to kilometres and time scales ranging from several hours (e.g. response to a storm event) to interannual (e.g. Net-Offshore-Migration pattern).*

The main tool used in the analysis is video imagery and the specific objectives are:

1. Characterize the shoreline dynamics of artificial embayed beaches, determining their natural trends and the elements responsible of their variability.
2. Characterize the dynamics of the submerged sandbars in artificial embayed beaches focusing on their cross-shore migration and their three-dimensional morphologies.
3. Study the coupling between sandbar and shoreline at different time scales.
4. Evaluate the morphological evolution of two types of artificial nourishments (beach and shoreface nourishments) and their impact on beach morphodynamics.

To achieve this purpose the two study sites (the artificial embayed beaches of Barcelona city and the open beach of Noordwijk) have been monitored using video techniques. The previous scientific knowledge of the morphodynamics of both regions was quite different. Whereas the nearshore morphodynamics of Noordwijk have been previously studied, the morphodynamics of Barcelona city beaches were poorly understood. For this reason the first two chapters of the thesis are dedicated to investigate the morphodynamics of Barcelona city beaches, and the following two chapters analyze the response of the nearshore after different types of nourishments at Barcelona and Noordwijk beaches.

The thesis is organized in chapters that are edited versions of scientific publications, including the obtained results and their interpretation. This structure means that some concepts may be repeated in different chapters. Chapter 2 focuses in the shoreline dynamics of the artificial embayed beaches in Barcelona city during a three-year period examining the behaviour of the emerged beach in order to assess the main factors affecting the shoreline, and to analyze the processes causing beach rotation at different time-scales. Chapter 3 characterizes the dynamics of the shore-parallel submerged sandbars of two of the artificial embayed beaches in Barcelona city (La Barceloneta and Bogatell) during a 4.3-year study period, and

the coupling between the bars and the shoreline. Chapters 4 and 5 are related to artificial nourishment, one describing the beach nourishment carried out in two of Barcelona city beaches (La Barceloneta and Bogatell) based on a 1.5-year period of video data, and one describing the response of the two-bar system at Noordwijk to a shoreface nourishment, based on daily time-exposure video images collected during about 6 years and complemented with topographic and bathymetric surveys. Chapter 6 summarizes the most relevant conclusions attained in the thesis, and includes open questions for future research.

2 Shoreline dynamics of embayed beaches

Edited version of E. Ojeda and J. Guillén, 2008. Shoreline dynamics and beach rotation of artificial embayed beaches. *Marine Geology* 253, 51–62.

2.1. INTRODUCTION

Rocky coastal zones represent approximately 80% of the world's coast (Trenhaile, 1987). Within these zones sandy beaches bounded by rock outcrops or headlands where the shoreline takes on some form of curvature are a common occurrence. Beaches of this type are known as curved, hooked, pocket, embayed or headland-bay beaches, and have been the subject of a variety of attempts to model their equilibrium plan forms (e.g. Silvester, 1960; González and Medina, 2001). Embayed beaches differ from long sandy beaches in the limited alongshore sediment transport, which varies according to the beach boundaries.

Artificial embayed beaches have been suggested as a means of stabilizing eroding shorelines (Klein *et al.*, 2003). Furthermore, the number of sandy beaches enclosed by artificial structures has increased in the last few decades due to the construction of harbours and other structures aimed at stabilizing coastlines threatened with erosion. However, little research has been conducted on these non-natural systems (González and Medina, 2001; Muller *et al.*, 2006). The study of embayed beaches is usually based on the concept of some static or equilibrium configuration of the shoreline; three main models are used to fit this equilibrium shape: logarithmic-spiral (Silvester, 1960), parabolic (Hsu *et al.*, 1989) and hyperbolic tangent (Moreno and Kraus, 1999). Beaches with two headlands are best described by the logarithmic-spiral model (Martino *et al.*, 2003). These equilibrium models are applied to fit the shoreline configuration with the mean shoreline position associated with some specific wave climate, they consider a perfect adjustment of the shoreline to the

incoming wave direction, in a simplification of the real morphology of the beaches. However, detailed observations of beach mobility are scarce and basic processes in embayed beaches such as beach rotation are still poorly documented.

Embayed beaches are typically affected by headland bypassing, when the sand moves subaqueously around its boundaries (Short, 2002), by the formation of rips (Holman *et al.* 2006), and by beach rotation, i.e. lateral movement of sand along the beach in response to a modification in the incident wave direction (Short and Masselink, 1999). Beach rotation causes localized retreat or advance of the shoreline along the beach, although it does not lead to a long-term loss or gain of sediment because the beach often returns to the initial location in response to a new shift in the wave direction (Klein *et al.*, 2002). It has been described at monthly to decadal time scales as being caused by variations in the wave direction related to the El Niño Southern Oscillation, alterations in the sediment supplied from nearby rivers, and seasonal changes in the wave climate (Anthony *et al.*, 2002; Klein *et al.*, 2002; Ranashinge *et al.*, 2004).

Beach rotation is schematized in Figure 2.1; the change in the shoreline from t_0 to t_1 implies an advance (retreat) of the left (right) section of the beach. One of the parameters involved in the determination of beach rotation events is this advance/retreat of the shoreline which is maxima near the limits of the beach and minima or zero at the central section represented by the pivotal point. Beach rotation can also be determined by the change in the orientation of the shoreline; however, these changes in orientation can be also related to other alterations of the shoreline such as differential erosion or accretion alongshore or beach nourishment.

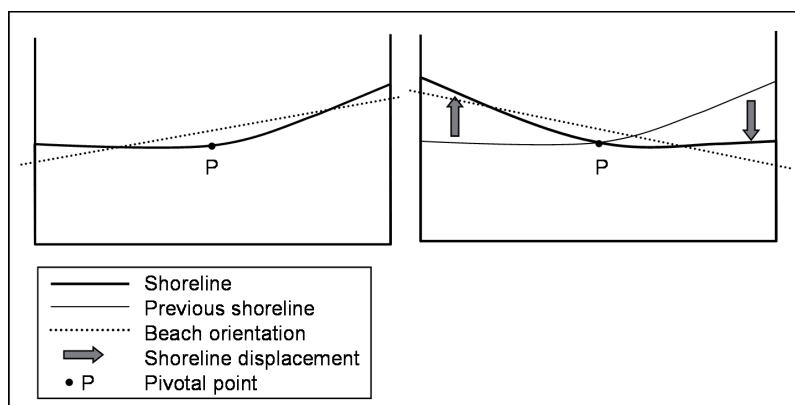


Figure 2.1. Parameters used to define beach rotation.

The general objective of this chapter was to achieve a better understanding of artificial embayed beach morphodynamics using shoreline position and beach area data from three beaches in Barcelona city during a three-year period. It analyzes the impact of natural processes and human interventions on the shoreline, focusing on mechanisms that cause beach rotation and the recovery of the former beach orientation. We first examine the dynamics of the shoreline of the three beaches and their changes in the emerged beach area. Secondly we compare the temporal evolution of the beach area with the temporal evolution of the beach orientation to establish which changes in beach orientation are related to episodes of beach rotation. Finally, we examine the response of the beaches to storm events and try to find a relationship between the alongshore component of the radiation stress and changes in the beach orientation.

2.2. THE STUDY AREA: BARCELONA CITY BEACHES

The Catalan coast is a micro-tidal zone (range <20 cm) in which waves are the main stirring mechanism controlling coastal evolution. The most energetic storms approach from the east, have a typical duration of a few days, and are often associated with the cyclonic activity in the western Mediterranean. Statistical analysis of wave conditions in the region from 1984 to 2004 shows mean significant wave height values (H_s) of 0.70 m, with H_s maxima of 4.61 and maximum wave heights of 7.80 m (Gómez *et al.*, 2005).

Significant wave height during the study period displayed a cyclic behaviour, with storm periods (October-April) separated by periods of low storm activity (May-October) (Figure 2.2). The most energetic period affecting Barcelona city beaches was from October 2001 to May 2002, with a major storm from the NE direction in

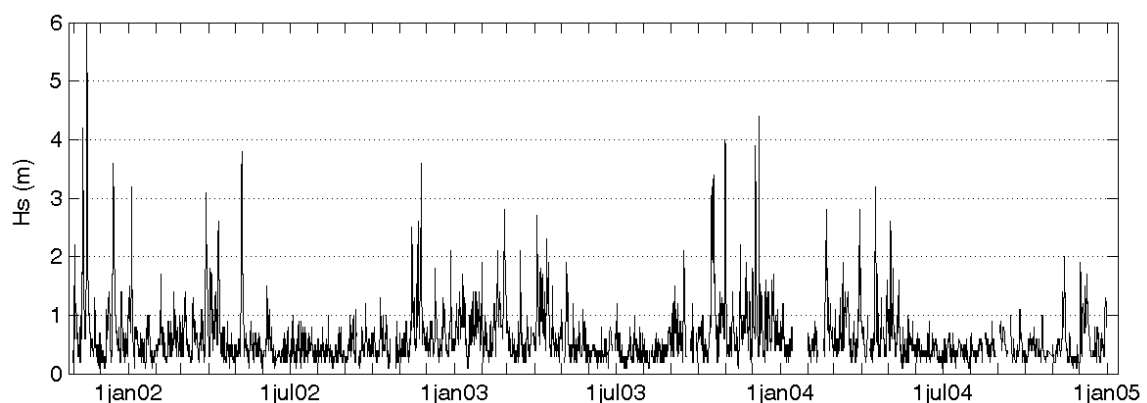


Figure 2.2. Significant wave heights off Barcelona during the study period.

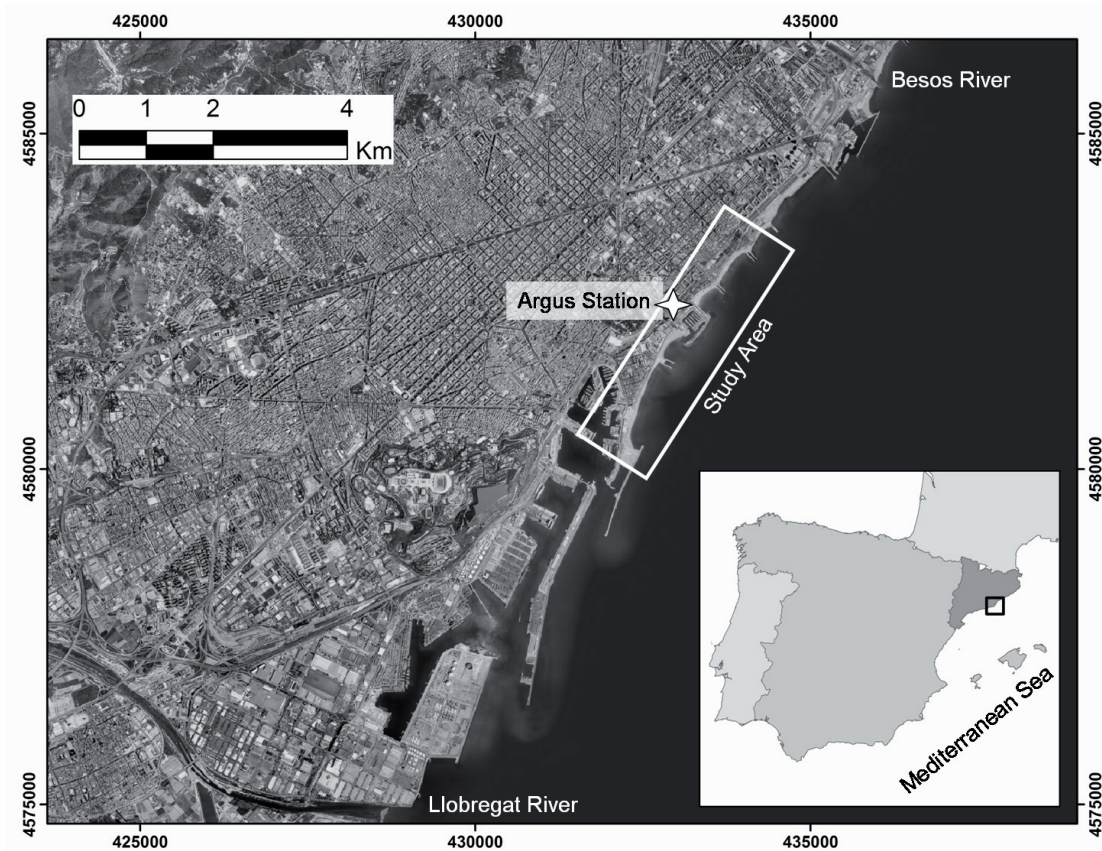


Figure 2.3. Study area.

November 2001 involving two consecutive intensity peaks separated by a short time lapse.

The city of Barcelona is located in the north-western Mediterranean, flanked by two rivers, the Besos in the north and the Llobregat in the south (Figure 2.3). It has approximately 13 km of coastline containing the city harbour in the southernmost part of the city, three marinas and more than three kilometres of beaches. These beaches are one of the city attractions and are occupied during most of the year by local inhabitants and tourists (Guillén *et al.*, 2008). The northern area of the city beach had almost disappeared by the 1980s due to the invasion of urban and industrial areas and the decrease in the input of sediment to the coastal zone. Only a section of approximately 1.5 km remained in the southern part, supported by the Barcelona Harbour dike. The beaches were created as part of the renewal plan that took place in the zone for the 1992 Olympic Games, when small industries, garages and industrial warehouses were eliminated to create the Olympic Village (now transformed into a residential district), and new beaches were built on both sides of the Olympic Marina. The beaches have now become a symbol of the city's revitalized waterfront.

This study focuses on three beaches (Figure 2.3 and 2.4): a) La Barceloneta, a barred beach bounded by Barcelona Harbour in the south and the Somorrostro dike in the north; b) Nova Icaria, a non-barred beach located on the north side of the Olympic Marina, separated from Bogatell beach by a double dike and also protected by two submerged breakwaters, the longest of which extends from the tip of the dike; and c) Bogatell, a barred beach at the northern limit of the study area, enclosed by two double dikes.

Barcelona's beaches are continuously affected by human activity such as sand cleaning before the summer season and small-scale sand redistribution along the beaches after storms. Two major beach interventions were carried out during the study period, a nourishment of Bogatell and La Barceloneta in summer 2002, and a sand relocation at La Barceloneta in summer 2004.

The nourishment was a rapid solution to the erosion caused by the highly energetic period from October 2001 to May 2002. The works commenced at Bogatell beach, which received around 70 000 m³ of sand in 22 days (between 13th June and 5th July), and continued at La Barceloneta beach, which received around 40 000 m³ of sand between 5th and 17th July 2002. The median grain size of the sand ranged between 0.45 and 0.9 mm, and it was pumped to the emerged beach from a ship.

The second human intervention was carried out at La Barceloneta beach in June 2004, with the transfer of about 30 000 m³ of sand from the southernmost region of the beach to the northern end. The relocation was performed with trucks, and the sand was flattened with caterpillar tractors days after the placing of the sand, leaving a steep beach profile for several days.

The sediment grain size is the result of the mixing of the original nourishments for the creation of the beaches (1988-1992) and the nourishment carried out in 2002. The beach sediment is composed of sands with some proportion of gravels. The median grain size shows high spatial and temporal variability and the average median grain size (D_{50}) ranges between 0.43 mm at Nova Icaria and 0.68 mm at La Barceloneta and Bogatell.

2.3. METHODOLOGY

The shoreline position of the beaches was obtained from November 2001 to December 2004 by means of an Argus video system (Holman and Stanley, 2007)

located atop a building close to the Olympic Marina at a height of around 142 m (Figure 2.3). The Argus station is composed of five cameras pointing at the beaches and offering a 180° view of the coast (Figure 2.4). An image processor controls the capture, storage, pre-processing and transfer of images to the database and to the Internet, where they are available at <http://elb.cmima.csic.es>. The images are in the visible range of light and the sampling is done every daylight hour during a ten-minute period (1 picture per second).

To obtain quantitative data from the images, a coordinate conversion must be used to transform the 2D image coordinates to real coordinates. This transformation is included in the Argus software and has been described in Holland *et al.* (1997). It requires measurements of control points and camera location and also the removal of radial lens distortion. Image resolution is better than 1.5 m in the cross-shore direction, whilst in the alongshore direction it is better than 11 and 19 m in the distant sections of Bogatell and La Barceloneta, respectively.

Due to the large amount of images available, video animations were generated to identify the most significant events. Shorelines were measured with a time gap between images varying from one to fifteen days, depending on the changes occurring at the coastline.

The shoreline position was obtained from the 10-minute time exposure images using the Intertidal Beach Mapper software (Aarninkhof *et al.*, 2003). Some problems were found when this program was used on Barcelona's beaches, mainly due to the lack of contrast between sand and water, particularly in summer, when low wave energy conditions (i.e. wave breaking does not occur or is too slight to be observed in the images) and large numbers of people hinder shoreline extraction using Intertidal Beach Mapper. Shoreline positions on these poor-contrast days were manually mapped from the images. In order to minimize errors due to sea level variations and the process of analysis, more than one shoreline per day was

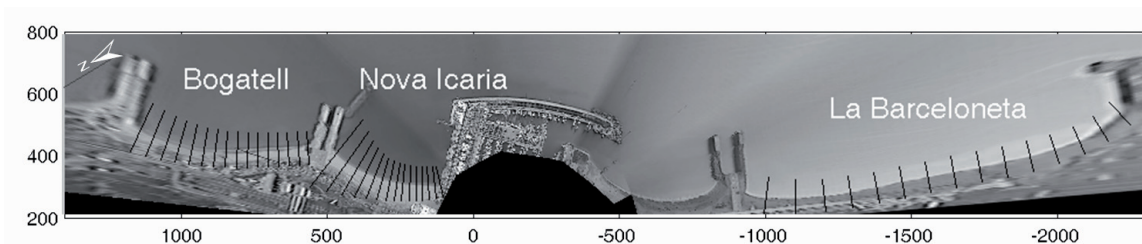


Figure 2.4. Argus plan view of the study area showing beach *control transects*. Distances are given in meters.

Table 2.1. Mean and standard deviation of the alongshore differences between dGPS-surveyed and Argus-derived shorelines (values given in meters).

	La Barceloneta	Bogatell	Nova Icaria
$mean_{abs}$	4.70	2.88	1.05
Standard deviation	2.98	2.73	1.22

mapped for most cases, and the average of these images was used instead of a single shoreline position.

Video-derived shorelines were compared with the ones obtained from differential Global Positioning System (dGPS) surveys performed at each of the beaches (one at Nova Icaria, two at Bogatell and three at La Barceloneta). Differences were evaluated on a grid with 2 m spacing in the y-direction and results are given in Table 2.1, where $mean_{abs}$ represents the average of the differences found for each point along the beach for all the dGPS surveys performed at the beach, without regarding the sign of the difference. For every comparison the Argus-derived shoreline was seaward of the dGPS-surveyed shorelines.

A *reference shoreline* was defined for each beach as the result of the averaged position from all available shorelines fitted to a polynomial curve. The shoreline dynamics was studied using lines perpendicular to this *reference shoreline* in order to avoid the error induced by the beach curvature. Although a larger number of transects was used for the analysis (actually, a transect every 4 metres at La Barceloneta and one every 2 metres at Bogatell and Nova Icaria), for visual reasons only 15 *control transects* will be shown for each beach in some figures of the results section (see the *control transects* marked in Figure 2.4).

Beach mobility was defined for each alongshore location as the standard deviation of the shoreline position throughout the study period. In order to calculate beach mobility, the entire time series of shoreline position were interpolated using a 1 day step assuming that when no data is available is because the shoreline does not experience any change.

The emerged beach area is defined as the area bounded by the shoreline and the hard structures in the rear and lateral part of the beaches. It was estimated using a routine that reduced the daily values of the shoreline to a mean, elongated the shoreline limit by linear fitting (when the extremities of the beaches were not clearly visible), and calculated beach area values. Time series of the emerged beach

area give an initial estimation of the trends of each beach during the study period as well as an initial view of its response to natural processes and human actions. Beach orientation during the study period was defined through linear regression as the best-fit line for each shoreline.

Wave data were characterized using information from the WANA model data set (node WANA2066051), computed by the Spanish National Institute of Meteorology using the HIRLAM and WAM numerical models (see Spanish Port Authority, <http://www.puertos.es>).

Significant storms affecting the Barcelona coast were subjectively defined by a H_s higher than 2.5 m during the peak of the storm, a threshold H_s of 1.5 m for estimating the storm duration and a minimum duration of 12 hours. Wave height can be below the threshold for 6 hours and waves with directions coming from land are not considered since they have no effect on the coast. Table 2.2 displays the characteristics of these storm events, excluding two episodes in March 2002 and February 2004 when gaps in the wave data prevented the calculations.

Mean values of the alongshore component of the radiation stress (S_{xy}) were computed for these storm events. The alongshore component of the radiation

Table 2.2. Storms with H_s reaching 2.5 m.

Event	Initial date	Mean H_s (m)	Mean wave direction relative to north	Duration (hours)
A	10-Nov-2001	3.2	73°	99
B	14-Dec-2001	2.4	68°	69
C	4-Jan-2002	2.3	105°	21
D	11-Apr-2002	2.0	89°	33
E	7-May-2002	2.6	93°	48
F	14-Nov-2002	1.9	193°	33
G	21-Nov-2002	2.1	200°	15
H	25-Feb-2003	2.0	118°	66
J	3-Apr-2003	2.1	59°	21
K	15-Oct-2003	2.5	80°	90
L	31-Oct-2003	2.8	200°	33
M	4-Dec-2003	2.6	95°	21
N	8-Dec-2003	3.0	83°	18
O	29-Mar-2004	1.9	89°	33
P	16-Apr-2004	2.2	104°	33
Q	3-May-2004	2.2	75°	24

stress was calculated as:

$$S_{xy} = -E c_g / c \sin\theta \cos\theta = -\rho g / 16 H_s^2 \sin\theta \cos\theta \text{ (Komar, 1998) ;}$$

where E is the wave-energy density, c_g is the group velocity, c is the phase velocity, θ is the wave angle with respect to the shore-normal direction, ρ is the water density and g is the gravity. Deep-water wave parameters were used because, when bottom friction is negligible, the radiation stress remains constant from deep water to the breaking point (Komar, 1998). The calculation was made for the time lapse between two Argus images: prior to and posterior to the storm event. S_{xy} values were first calculated for the entire WANA data set, and then the mean radiation stress for each studied episode was obtained for the time lapse between the two Argus-derived shorelines using only S_{xy} values corresponding to moments when H_s was greater than or equal to 1.5 m and wave direction (related to each beach orientation) was between -90 and 90 degrees.

The northern and southern sections of the beaches were analyzed independently and separated by a pivotal point, as defined by Short *et al.* (2000), around which the beach rotates. The division of the beach was accomplished using the point of the shoreline with minimum variability during the study period, which was interpreted as the representative pivotal point. Klein *et al.* (2002) found, instead of a pivotal point, a transitional zone located around the central region of the beach but varying from one storm event to another. This also appears to be the case on Barcelona's beaches and, obviously, shifts of the pivotal point would result in a different estimation of the emerged area for different episodes. However, it was found that these differences were of small magnitude and that the representative pivotal point gives a good estimation of the changes occurring at the Barcelona beaches.

2.4. RESULTS

Barcelona city beaches display a curved plane-form shape characteristic of embayed beaches (Figure 2.4). La Barceloneta is oriented approximately 20° from the north, with a length of 1100 m and an average emerged area during the study period of 70 x10³ m². Nova Icària is oriented 47° from the north, with a length of 400 m and an averaged emerged area of some 22 x10³ m². Finally, Bogatell is oriented 38° from the north, with a length of 600 m and an emerged area of 21 x10³ m².

This section describes the general evolution of the three beaches during the study period through the shoreline data, the beach area and the beach orientation.

2.4.1. SHORELINE EVOLUTION

La Barceloneta and Bogatell shorelines were characterized by a succession of distinctive configurations over time (Figure 2.5). The initial configuration was changed in November 2001 due to extreme wave conditions that caused an advance of the shoreline on the southern side and a retreat on the northern side. This configuration was artificially altered by the summer 2002 nourishment in the 350-m-long northern section of the beach at La Barceloneta and along the entire beach at Bogatell. At La Barceloneta the nourishment caused a mean advance of the shoreline of 14 m in the nourished section and lasted more than seven months (around February-March 2003). After this period the sediment eroded from the nourished area was partially transported alongshore towards the south. At Bogatell, the mean advance of the shoreline was of around 20 m; the sand was redistributed during the first weeks after the nourishment, leading to some retreat in the southern section of the beach and an advance in the northern section. The final configuration of the shoreline at both beaches was characterized by the presence of megacusps (Figure 2.5).

Nova Icaria beach showed the most stable configuration of all three beaches. The retreats and advances occurred in the southern region of the beach; they were abrupt, although in general the changes were minor in comparison with those of the other two beaches, and the protection structures meant that the beach was capable of self-recovery after energetic wave conditions.

2.4.1.1. *Megacusps*

Megacusps of approximately 10 m of horizontal amplitude or larger were observed during the study period at La Barceloneta and Bogatell beaches but not at Nova Icaria. They were formed after storms that transformed the submerged bars into crescentic bars and caused them to become attached to the beach during periods of high sediment availability (see Chapter 3 for a more detailed description). At Nova Icaria, the formation of submerged bars was not observed. This lack of bar, which prevents the formation of megacusps, is due to the higher degree of protection of this beach. La Barceloneta showed the largest and longest-lasting megacusps observed during the study period. The beach configuration was characterized by

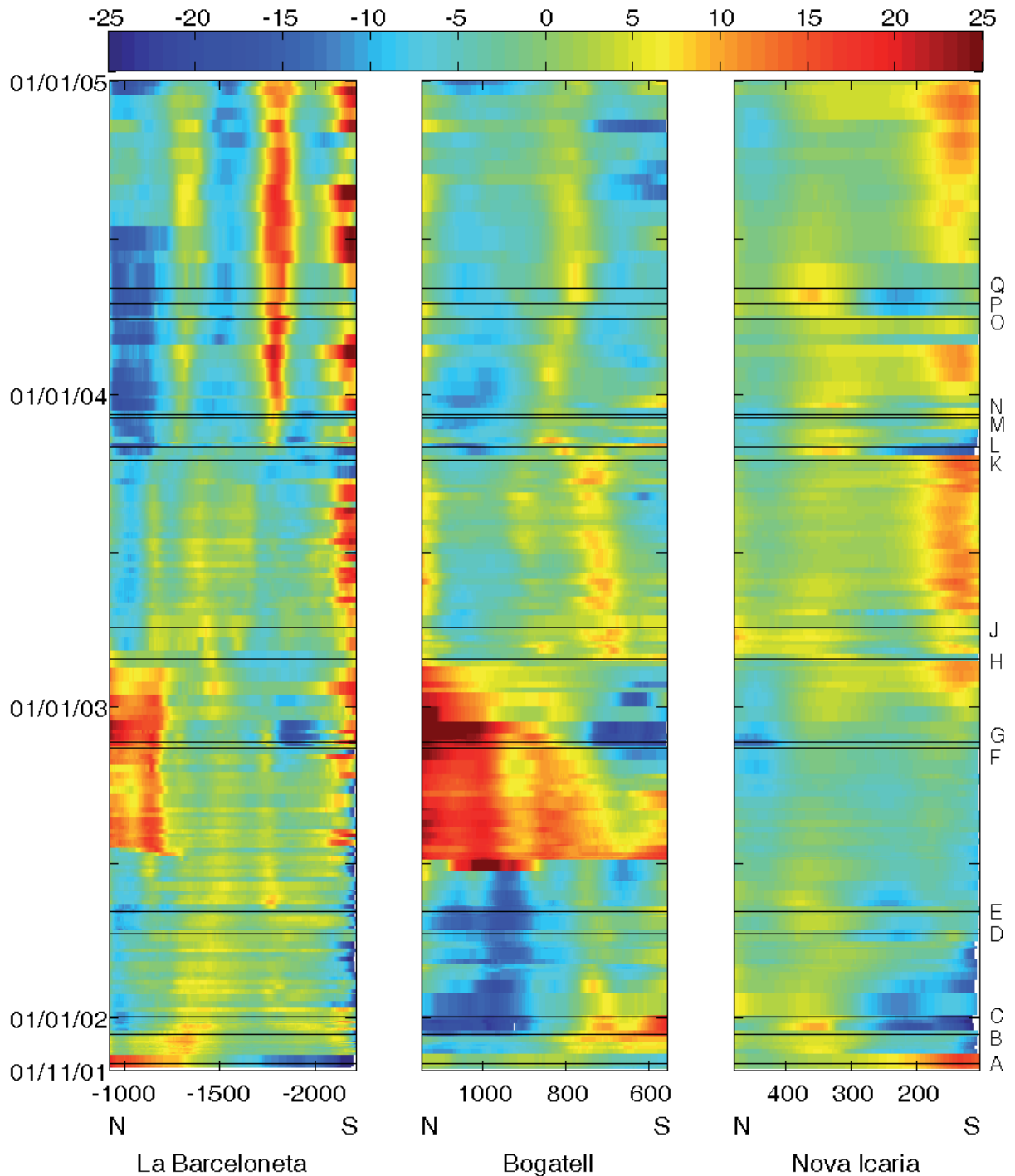


Figure 2.5. Time-space diagrams of the deviations of the shoreline location referring to the *reference shorelines*. Warm colours are related to advances in the shoreline location and cold colours to retreats; colour bar values are given in meters. The x axis refers to the alongshore location and the y-axis to the time. Main storm events (A-Q) are indicated.

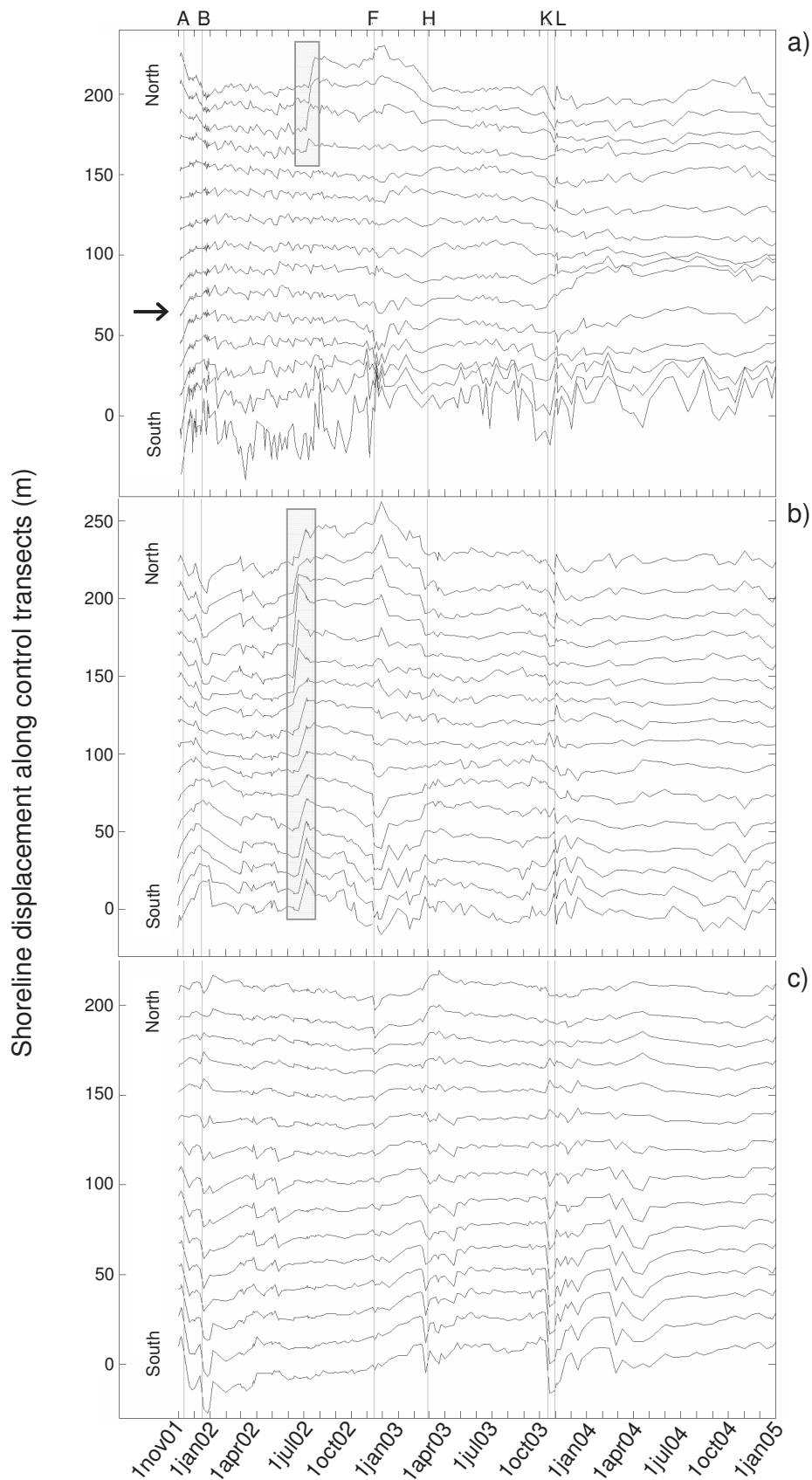


Figure 2.6. Time series of shoreline position changes along *control transects*. From top to bottom: La Barceloneta, Bogatell and Nova Icaria. Y axis gives the variation along transects in meters. The grey lines indicate storms commented in the text; the rectangles, the nourishments; and the horizontal arrow, the *control transect* that matches the location of the southern megacusps at La Barceloneta.

the development of two stable megacusps with eroded regions on their flanks in October 2003, after Event L, which lasted for more than a year. The southernmost megacusp matched the location of one of the *control transects* shown in Figure 2.6a (marked with an arrow in southern La Barceloneta) and produced a 20-m advance in the shoreline position.

Megacusps were dynamic morphological features at both beaches. They showed alongshore displacements of up to 50-70 m and their persistence varied from a few days to more than a year. However, the processes of megacusps development and migration remain unclarified in this study. For instance, a relationship between wave direction and formation of megacusps was not evident at the Barcelona beaches.

2.4.1.2. Beach mobility

The largest beach mobility values were found at the two ends of La Barceloneta, the northern end of Bogatell and the southern end of Nova Icaria (Figure 2.7). Maximum beach mobility at La Barceloneta was associated with changes in the beach orientation while the local maxima in the central section are related to the location of megacusps. The differences at Bogatell beach were caused by the faster erosion of the southern sector after the nourishment and by the fact that in the same sector the shoreline retreat was occasionally interrupted by a solid limit: the beach promenade. Finally, the lower beach mobility at the northern end of Nova Icaria was related to the higher protection caused by the defence structures on that side of the beach.

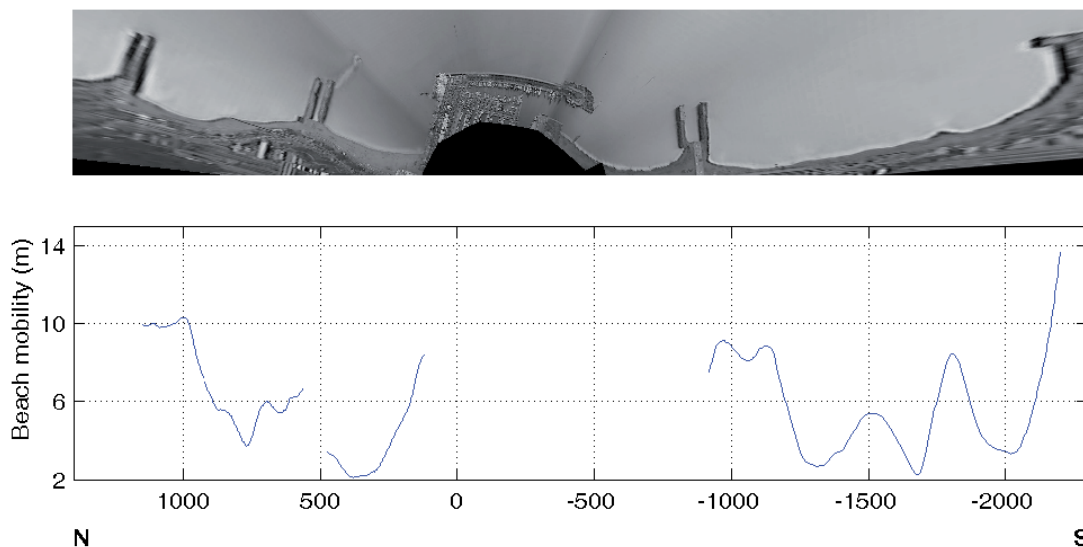


Figure 2.7. Beach mobility at the different alongshore locations in La Barceloneta, Bogatell and Nova Icaria beaches.

2.4.1.3. *Response to storms*

La Barceloneta and Bogatell beaches displayed similar responses to storm events (Figures 2.5 and 2.6). Shoreline displacements associated with storms varied between -18 and +34 m at La Barceloneta and -20 m and +15 m at Bogatell. Storms also played an important role in the evolution of the nourished sand. Major retreats of the beaches were associated with a sequence of storms from the east direction that took place in mid-February 2003 (Figure 2.2). Nova Icaria behaved differently to the others. Only waves coming from a narrow range of angles (68- 80°) caused a significant retreat in the shoreline. Events A and K produced mean retreats in the southern section of more than 15 m with maximum values at the southernmost points of almost 30 m, and Event B produced a mean retreat in the southern section of 10 m with maximum values of almost 20 m.

Alongshore averaging the shoreline displacements due to storm events resulted in values ranging from -3.2 and +5.4 m at La Barceloneta and from -3.8 to +1.0 m at Bogatell. These low values are explained by the fact that one of the most important responses of these beaches is erosion and accretion occurring simultaneously (beach rotation).

2.4.2. BEACH AREA

Figure 2.8 shows the temporal evolution of the emerged beach area at all three beaches. An initial distinction can be made between La Barceloneta and Bogatell that showed emerged beach area trends during the study period of -3.2 and -1.5 m²/day, respectively, and Nova Icaria that showed an accretionary trend of +1.9 m²/day (Table 2.3).

The nourishment carried out at La Barceloneta beach in summer 2002 caused an increase of 5 000 m² in the beach area and was followed by a progressive loss of beach area with a trend of -23 m²/day (calculated for the period 1st August 2002 to 31st December 2003), until values lower than the ones before its implementation were reached. The negative trend continued for almost a year, reaching an almost stable emerged beach area (with fluctuations) before the sand relocation performed in June 2004. This relocation left a steep beach profile for several days and led to a new increase in the beach area in July 2004, but with a confined effect in time and space that lasted for less than six months, as by the end of 2004 erosion was again visible on that side of the beach.

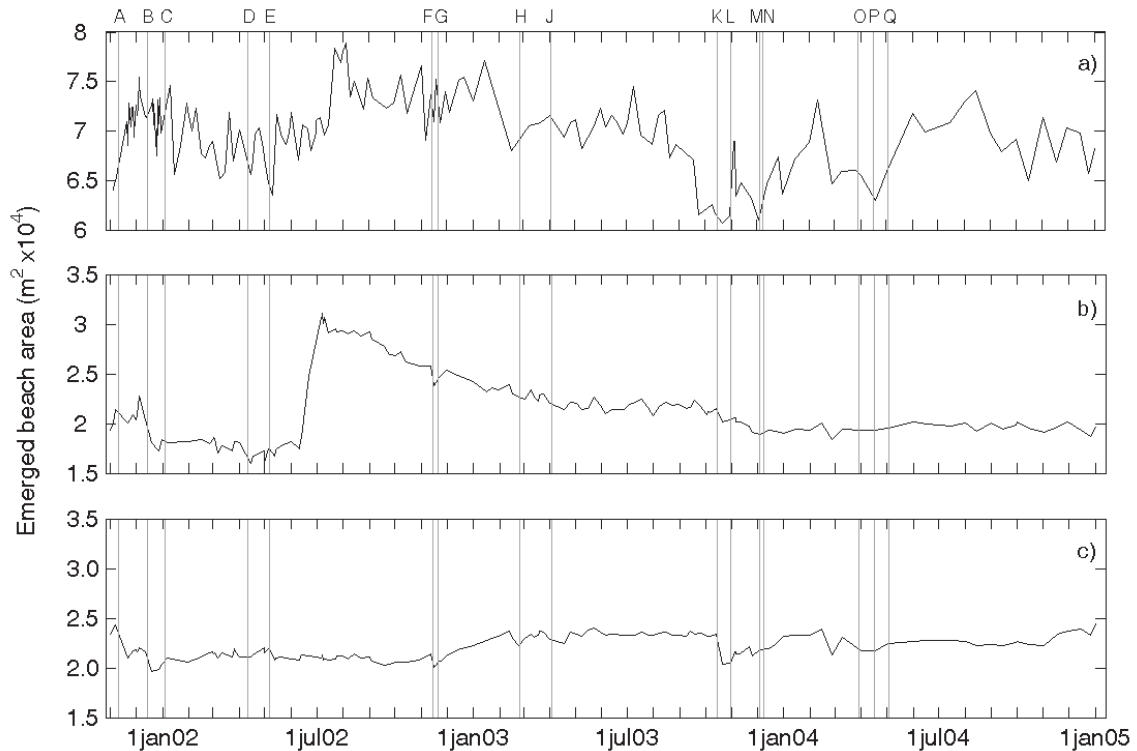


Figure 2.8. Time series of emerged beach areas: a) La Barceloneta, b) Bogatell and c) Nova Icaria.

The beach area at Bogatell and Nova Icaria beaches not varied as much as at La Barceloneta (Figure 2.8). However, the largest coefficient of variation was found at Bogatell due to the effect of the nourishment, which led to an increase in beach area of about 12 000 m², with a mean advance of the shoreline of around 20 m. Significant losses in beach area started some two months after the nourishment; the emerged beach area decreased at a rate of -17 m²/day (calculated for the period 1st August 2002 to 31st December 2003) and reached stable conditions by the end of 2003 (Figure 2.8).

Nova Icaria beach experienced two major erosive periods with emerged area recovery between them. These erosive periods took place in late 2001 and late

Table 2.3. Statistical values for the area measurements during the study period.

Beaches	Mean area(m ²)	Standard deviation	Coefficient of variation	Min. area(m ²)	Max. area(m ²)	Trend ^a (m ² /day)	Trend ^b (m ² /day)
Barceloneta	69542	3459	5.0 %	60668	78905	-23	-3.2
Nova Icaria	22190	1052	4.7 %	19640	24387	3.7	1.9
Bogatell	21253	3135	14.75 %	16014	31100	-17	-1.5

^a Values calculated after the nourishment (1st Aug. 2002 – 31st Dec. 2003).

^b Values for the whole study period.

2003 and were related to major peaks in significant wave height. The beach area recovered naturally from these erosive periods but with different timings: while the first area increase took place almost a year after the erosion, the second one appears to have been due to the natural recovery of the beach after the storm.

2.4.3 BEACH ORIENTATION

The temporal evolution of the beach orientation is shown in Figure 2.9 for the three beaches. In general, it was observed that abrupt changes in the orientation of the beach (due to nourishments or storm events) were normally followed by gradual recoveries towards a stable beach orientation. The range of variation in the beach orientation during the study period was 3.5° at La Barceloneta beach, 10.5° at Bogatell beach and 7.9° at Nova Icaria beach.

During certain periods, gradual changes in the beach orientation are related to variations in the beach area; for instance, at Bogatell beach, since September 2002 the beach area decreased and the angle of the beach orientation decreased due to higher erosion in the southern section. At Nova Icaria, since December 2002, the opposite pattern occurred with an increase in the beach area and a decrease

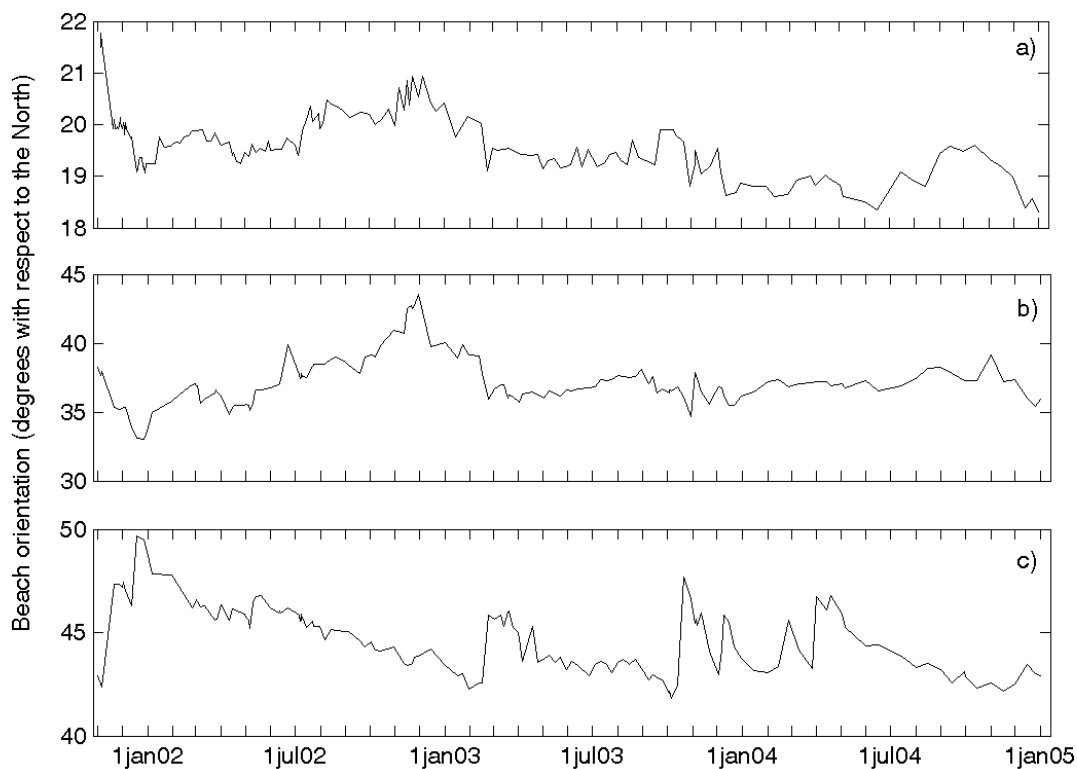


Figure 2.9. Time series of the beach orientation: a) La Barceloneta, b) Bogatell and c) Nova Icaria.

Table 2.4. Changes produced by storm events in the beach orientation and at the beach area at each side of the pivotal point (northern and southern sections).

Event	La Barceloneta			Bogatell			Nova Icaria		
	Orientation	Area N	Area S	Orientation	Area N	Area S	Orientation	Area N	Area S
A	1.65	-3026	9174	2.61	-3087	1782	-4.97	140	-3475
B	0.68	-1676	2774	0.84	-2052	-201	-3.41	229	-2250
C	0.00	2526	2321	-1.34	1003	-1352	1.07	240	394
D	0.26	1015	2680	-0.55	451	-275	-0.55	4	-137
E	-0.23	-10	-1301	-0.51	-1046	-1108	-1.25	-116	-1514
F	-0.57	376	-3102	-1.79	361	-2300	0.12	-808	-564
G	-0.36	1081	-1602	0.18	397	279	-0.04	230	241
H	-0.44	2694	-1613	-0.76	384	-620	0.19	482	299
J	0.02	-1766	-1391	-0.56	287	-107	1.08	19	860
K	0.15	-1143	166	0.81	-1289	-36	-5.26	203	-3296
L	-0.35	4939	2639	-3.24	2565	-2405	1.20	119	1021
M	0.46	2019	4737	0.06	-355	146	-1.25	140	-669
N	0.08	-2411	-1843	0.51	-514	325	-1.62	-103	-1256
O	0.18	-1090	573	-0.02	-505	-163	-3.46	-90	-2885
P	0.06	-1457	-1011	0.33	-767	190	-0.65	252	-942
Q	0.21	-3539	-865	0.34	-1240	-474	0.60	-488	-471

in the angle of the beach orientation due to larger accumulation in the southern side of the beach (Figures 2.8 and 2.9). On the other hand, some gradual changes in beach orientation at Bogatell and Nova Icaria are associated to almost constant emerged beach area, i.e., beach rotation is occurring (Figures 2.8 and 2.9). Clear periods of rotation are identified for these two beaches. At Bogatell these periods followed the nourishment (July to early September 2002) and also occurred after certain stormy periods (January - end of February 2002, April - September 2003, and December 2003 - end of January 2004). At Nova Icaria beach rotation occurred following storm events (March - October 2002, May - September 2003 or May - November 2004), after these storms the beach shifted towards certain equilibrium orientation.

Abrupt changes in beach orientation are mainly caused by storms. Table 2.4 presents the change in beach orientation for each storm event and the corresponding change in the beach area at each side of the pivotal point. Changes in the beach orientation during storm events ranged 2.2, 5.8 and 6.5° at La Barceloneta, Bogatell, and Nova Icaria beach respectively (Table 2.4). Abrupt changes can also occur with changes in the total emerged beach area or maintaining an almost constant total

beach area. As beach rotation is caused by alongshore sediment transport, it is expected that large (positive or negative) values of the alongshore component of the radiation stress (S_{xy}) will be related to episodes of beach rotation, which will imply changes in the beach orientation, while low values of S_{xy} during storms will imply predominance of cross-shore sediment transport and therefore no changes in the beach orientation. Figure 2.10 shows changes in beach orientation due to storm events and the corresponding S_{xy} at Bogatell beach. The results showed a significant correlation between the change in the beach orientation at Nova Icaria beach and the S_{xy} value (r^2 of 0.27), and highly significant correlations at La Barceloneta and Bogatell beaches ($r^2 = 0.71$ and 0.60 , respectively). As expected, S_{xy} improved the results obtained using the mean wave direction and the mean significant wave height studied independently, as for these cases r^2 ranged from 0.16 at Nova Icaria to 0.38 at La Barceloneta and Bogatell for the wave direction and from 0.08 at Bogatell to 0.21 at La Barceloneta for H_s .

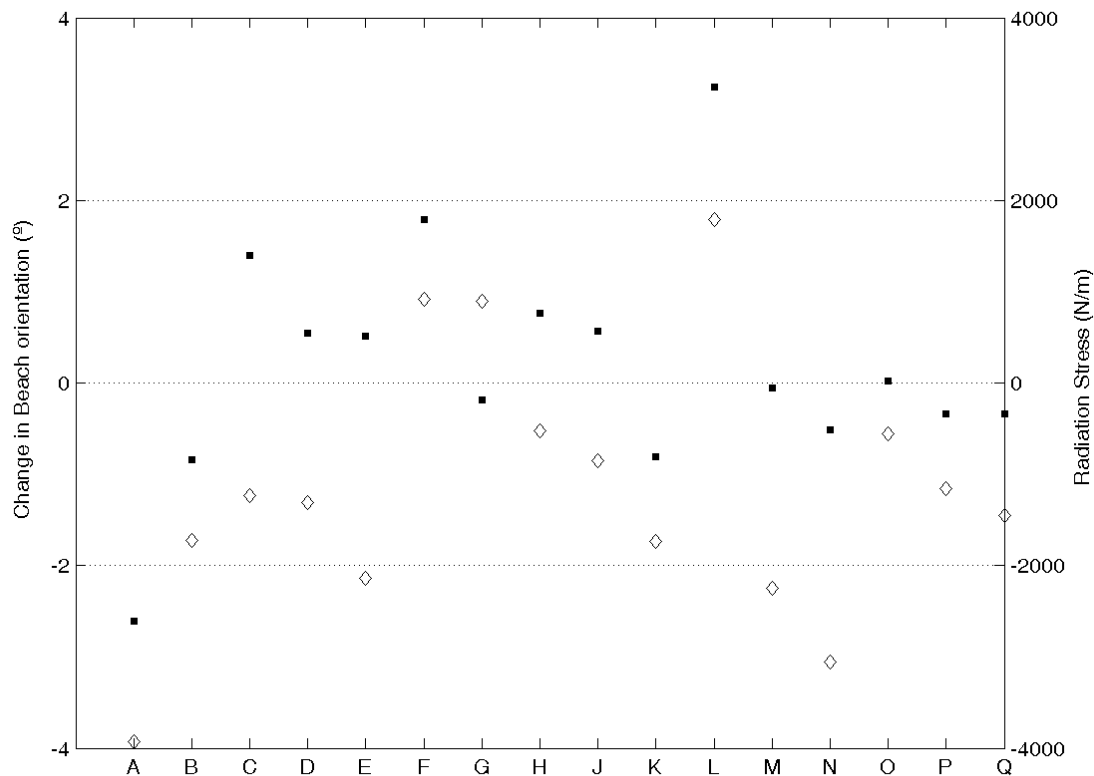


Figure 2.10. Change in beach orientation (squares) and mean S_{xy} (rhombus) for each storm event calculated for Bogatell beach. Mean S_{xy} during the event calculated for waves ≥ 1.5 m. The x-axis relates the name of the events; their dates are given in Table 2.2.

2.5. DISCUSSION

The morphological evolution of artificial embayed beaches is subject to two main constraints: a) these beaches are quite isolated sedimentary cells affected by specific wave conditions, since the perpendicular groins reduce alongshore sediment transport outside the beach boundaries and protect the beach, or certain sections of it, from waves approaching from a range of directions, and b) the beach mobility is limited because the rear section of the beach is normally occupied by promenades, houses or other types of urban structure. These constraints restrict the movement of the shoreline in comparison with open beaches, so embayed beaches have often been designed in order to respond to coastal erosion problems (Short and Masselink, 1999; Hanson *et al.*, 2002). The beach mobility values obtained for Barcelona city beaches are similar to those obtained for other natural embayed beaches (Norcross *et al.*, 2002). In fact, the beach mobility is affected by human interventions in two opposite ways: it is decreased by the wave energy loss caused by protection structures and the limitation of the beach retreat due to promenades, and it is increased by the artificial advance of the shoreline caused by beach nourishment.

Due to the interest in the design of the embayed beach plan form in engineering projects, most of the literature on embayed beaches concerns the equilibrium shape of the beach shoreline, considering a perfect adjustment of the shoreline to the incoming wave direction, in a simplification of the real morphology of the beaches. The study of the artificial embayed beaches of Barcelona provides some insights into this topic.

Changes in the beach orientation are related to differential accretion/erosion patterns alongshore. These changes in the orientation can imply increases or decreases of the total beach area with gains or losses of sediment from the emerged beach area, or no change in the total beach area when the sand is relocated alongshore; this latter case is known as beach rotation. However, differences between both situations are not always evident. For instance, observations from Barcelona beaches indicate that eroding and accreting beach sectors during beach rotation due to storm events can be heterogeneous, i.e., in the retreating sections there are segments that undergo shoreline advance and in the advancing sections there are segments that undergo retreat. A factor for explaining this heterogeneous alongshore behaviour of the shoreline is the formation of sedimentary structures like megacusps that can be related to the submerged morphology of the beaches:

the formation of submerged sandbars and their subsequent transformation into crescentic bars that become attached to the beach. Although similar cusped forms remaining in the same longshore position during storm conditions have been observed on open beaches (Aagaard *et al.*, 2005), such long-lasting megacusps as the ones appearing at La Barceloneta and Bogatell in the second half of the study period, disturbing the configuration of the shoreline for months, have not previously been described on embayed beaches.

Besides the alongshore heterogeneity in the shoreline response, ideal cases of beach rotation caused by storms with no change in the total beach area rarely take place in nature. Here we subjectively consider that beach rotation occurs when there is an opposite behaviour (erosion/accretion) of similar magnitude at the two sections of the beach separated by the pivotal point (Table 2.4). Bogatell beach displays highly significant correlations between changes in the areas at each side of the pivotal point and the change in orientation due to beach rotation, and a very weak relationship between the total change in the emerged beach area and changes in the beach orientation (Table 2.5), i.e. the beach rotates. At this beach, 87.5% of the analyzed storm events produced significant changes in the beach orientation and, of these events, 57% were associated with beach rotation. However, at La Barceloneta beach the correlation between changes in the areas at each side of the beach and beach rotation is significant but lower at the northern side of the beach, and there is a weak relationship between changes in the total emerged beach area and the beach orientation. At this beach, 75% of the analyzed events produced changes in the beach orientation, of which 42% were associated with beach rotation. Finally, Nova Icaria beach showed changes in the beach orientation mainly related to changes in the southern side of the beach that were also responsible for changes in the total beach area, cause the northern side of the beach is a shelter region that experience fewer changes. At this beach, of the 94% events that produced changes in the beach orientation, only 13% produced beach rotation (Table 2.4).

Table 2.5. R-squared values resultant from the comparison between the beach area change (considering the northern and southern sections of each beach independently) and the change in beach orientation due to storm events. Values printed in cursive are those significant at the 95% confidence level; bold are highly significant.

	Northern section	Southern section	Total area change
La Barceloneta	0.27	0.69	0.12
Bogatell	0.84	0.85	0.07
Nova Icaria	0.12	0.88	0.70

Considering the evolution of the beach orientation during the entire study period, Barcelona beaches display a differential behaviour. At Nova Icaria beach the plan form tended towards a characteristic (“equilibrium”) position: comparing the first and last day of the study period, the maximum differences between the two shorelines were 5 m, and beach orientation tended to reach a characteristic (“equilibrium”) value during the study period (Figure 2.11). Similarly, at Bogatell beach time series of beach orientation tended towards a beach orientation of approximately 37° , which was reached and maintained – with some fluctuations – in the second half of the study period. Beach nourishment caused an abrupt change in the beach orientation but the beach rapidly recovered the previous trend (Figure 2.10). However, at La Barceloneta, the temporal evolution of the beach orientation as of late 2002 showed an anticlockwise direction trend with fluctuations caused by storms and nourishments but an absence of a characteristic beach configuration (“disequilibrium”) or at least none was identified during the study period. The differential evolution of the orientation of this beach might be associated with the enlargement of the southern groin carried out in February-March 2002.

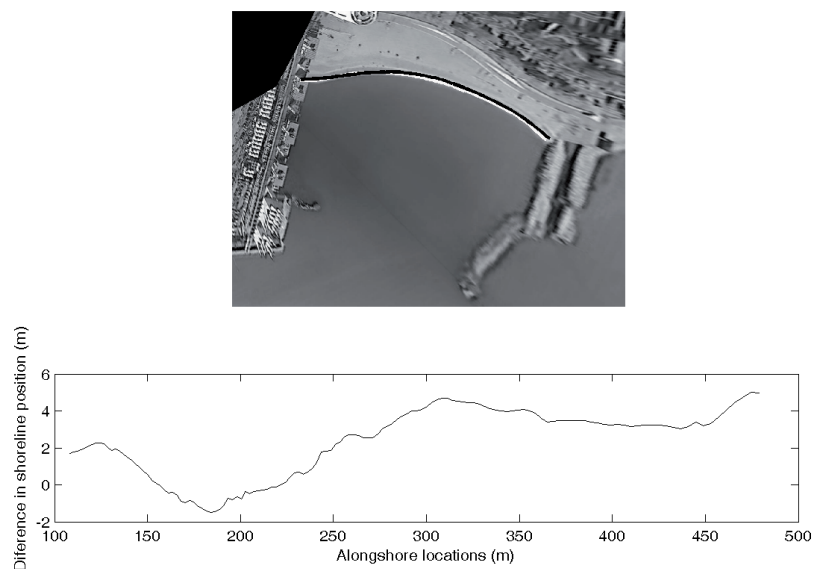


Figure 2.11. Change in the shoreline position of Nova Icaria beach between the first and last day of the study period. The picture shows the last day (1st January 2005) with the first (black line) and the last (white) shorelines superimposed.

2.6. CONCLUSIONS

Over the three-year study period the artificial embayed beaches of Barcelona displayed a beach mobility of similar magnitude to that of natural embayed beaches. The main differences between the behaviour of the artificial embayed beaches under study and that of natural embayed beaches were due to artificial sediment inputs (nourishment), which caused significant advances of the shoreline and temporary changes in the beach orientation. Maximum beach mobility occurs at the ends of the beaches and it is associated to beach rotation.

In addition to artificial nourishment or sand relocations, abrupt changes in the beach orientation were also caused by beach rotation related to storm events and by local erosion or accretion due to storm action. Following these abrupt changes the beaches slowly tended towards certain characteristic orientations at Nova Icaria and Bogatell, while at La Barceloneta no characteristic orientation was reached during the study period.

Storms were responsible for major changes in the configuration of the Barcelona beaches, the greatest were due to beach rotation caused by waves approaching obliquely to the coast. However, beach rotation and wave conditions displayed a complex relationship. Similar storms caused different effects on adjacent beaches depending on the degree of protection, and also on the same beach depending on its previous morphodynamic configuration. Furthermore, the advance and retreat of each beach segment associated with beach rotation were not alongshore-constant due to the influence of the morphodynamics (sediment exchange with the submerged profile and formation of sedimentary structures).

To the authors' knowledge, the high-temporal resolution time series of shoreline position and orientation presented is one of the longest-lasting in the literature on beach rotation of urban beaches. High temporal resolution monitoring of artificial embayed beaches has proven to be a valuable tool for achieving a better understanding of shoreline dynamics, mainly based on the understanding of short-term changes of the beach in response to individual storm events. This monitoring should include the entire beach because of the differential alongshore behaviour of embayed beaches, mostly due to rotation processes and the generation of sedimentary structures. Beach rotation caused the largest shoreline displacements in Barcelona beaches and this behaviour is expected to be representative of the dynamics of other natural and artificial embayed beaches. Finally, this approach

shows embayed beaches as complex and dynamic coastal environments and it complements the more simple description of embayed beaches based on equilibrium plane shape models, which give a good approximation of the configuration that a beach tends to attain under certain constant wave conditions, but where rapid impacts of short-term events are not considered.

3 Dynamics of single-barred embayed beaches

Edited version of E. Ojeda, J. Guillén, and F. Ribas. Dynamic of single-barred embayed beaches.
Submitted to *Marine Geology*.

3.1. INTRODUCTION

Subtidal shore-parallel sandbars are a common feature in a variety of nearshore environments, from high-energy to protected coasts, from microtidal to macrotidal regimes and in swell- or wave-dominated settings (Wijnberg and Kroon, 2002). The number of sandbars can vary between 1 and 4, depending on the site, the conditions and the configuration of the beach, and they can show either an alongshore-uniform shape or a crescentic shape, with undulations at scales of hundreds of metres (van Enckevort and Ruessink, 2003b).

Shore-parallel bars are dynamic morphological features that can migrate along- and across-shore, depending on the wave conditions. Alongshore bar migration, probably driven by the alongshore current, has been described by means of the migration of rips or crescentic shapes in bars, with rates of $O(10 \text{ m/day})$ (see Table 1 in Van Enckevort and Ruessink, 2003b). Cross-shore bar migration has been described at different time scales. At short-term time scales, bars undergo offshore migration during high-energy wave conditions, when the wave height–water depth ratio is large and the undertow current (near-bottom, breaking wave-driven steady flow) is dominant (e.g., Plant *et al.*, 2001). Onshore bar migration occurs as the wave height–water depth ratio decreases, during intermediate wave conditions. In these cases, the undertow is less intense and the cross-shore sediment transport is mainly due to wave non-linearity (wave skewness and wave asymmetry) (e.g., Plant *et al.*, 2001). At larger time scales, multi-barred beaches often show a Net Offshore Migration (NOM) pattern (Shand *et al.*, 1999). This interannual behaviour

involves: 1) the generation of the bar near the shore (at approximately 1 or 2 metre depth); 2) onshore and offshore migrations of the bars according to wave conditions but with a net offshore migration through the surf zone; and 3) bar decay at the seaward margin of the nearshore, prompting the formation of a new bar near the shoreline (starting the process at 1). There is a wide inter-site variation in the duration of this cycle, from 1 year at Hasaki in Japan (Kuriyama, 2002) to more than 10 years in Poland (Rozynski, 2003) or the Netherlands (Ruessink and Kroon, 1994; Wijnberg and Terwindt, 1995).

The changes in the plan-view shape of barred beaches were described in detail by Wright and Short (1984), since they were essential features of their beach state classification. A shore-parallel bar (*Longshore Bar and Trough* state) is developed or enlarged during the peak of a storm, as the bar migrates offshore. Under the subsequent lower energetic conditions, the bar becomes crescentic and migrates slowly onshore (*Rhythmic Bar and Beach* state) until the horns occasionally weld to the shore (*Transverse Bar and Rip* state). If low wave energy continues, the bar attaches completely to the shore (*Low Tide Terrace* state) and the beach finally reaches a non-barred configuration (*Reflective* state). This accretionary sequence can be disturbed by an increase in wave height, which will cause the beach to accommodate to the higher waves by following the opposite sequence, i.e., ending up with a shore-parallel bar. Furthermore, a certain bar morphology can be “arrested” under very low wave conditions, when the wave energy is too low to cause sediment transport (Aagaard, 1998). The parameter used by Wright and Short (1984) to characterize the beach states was the Ω parameter, $\Omega = H_b / (T_p \omega_s)$, where H_b is the breaker wave height, T_p is the peak period of the waves and ω_s is the sediment fall velocity. Coarse beaches subject to low-height, long-period wave conditions will show the lowest possible values of Ω and correspond to the *Reflective* state.

Most studies on bar dynamics have dealt with open beaches and multiple barred beaches. For instance, the long sandy beaches with 1 or 2 sandbars of Duck, USA, and Hasaki, Japan, have been described by Sallenger *et al.* (1985) and Kuriyama (2002). Examples of long sandy beaches with multiple bars are Terschelling, the Netherlands (Ruessink and Kroon, 1994), Wanganui, New Zealand (Shand and Bailey, 1999), the Ebro Delta, Spain (Guillén and Palanques, 1993) and the beach barrier of Thau Lagoon, France (Barousseau *et al.*, 1994). Single-barred embayed beaches, however, have deserved less attention (e.g., studies related to rips such as Short (1985) (Narrabeen beach, Australia) and Holman *et al.* (2006) (Palm Beach,

Australia); short-term studies on bar migration such as Van Maanen *et al.* (2008) (Tairua beach, New Zealand); and studies on beach morphodynamics such as Ranasinghe *et al.* (2004) (Palm Beach, Australia)).

The dynamics of barred beaches in the Mediterranean have been mainly studied at time scales ranging from days to several months (Bowman and Goldsmith, 1983; Guillén and Palanques, 1993). The limited number of long-term morphological series on the Mediterranean does not clearly suggest the occurrence of the NOM pattern. At longer time scales (~10 years), several authors have found off-shore migration of multiple-bar systems on the French Mediterranean coast, but it has been related to the advance of the shoreline (Sabatier and Provansal, 2000) or to the effect of individual storms with long return periods (Certain and Barousseau, 2005).

In this chapter, we analyze the morphological evolution of subtidal sandbars along two of the artificial embayed beaches of the Barcelona city coast (NW Mediterranean). Barcelona beaches (Figure 3.1) are subject to the same climatic conditions but have different characteristics (presence of submerged sandbars, slope, length, orientation, sediment availability and protection against wave action). In the previous chapter the study of the shoreline dynamics of the Barcelona city

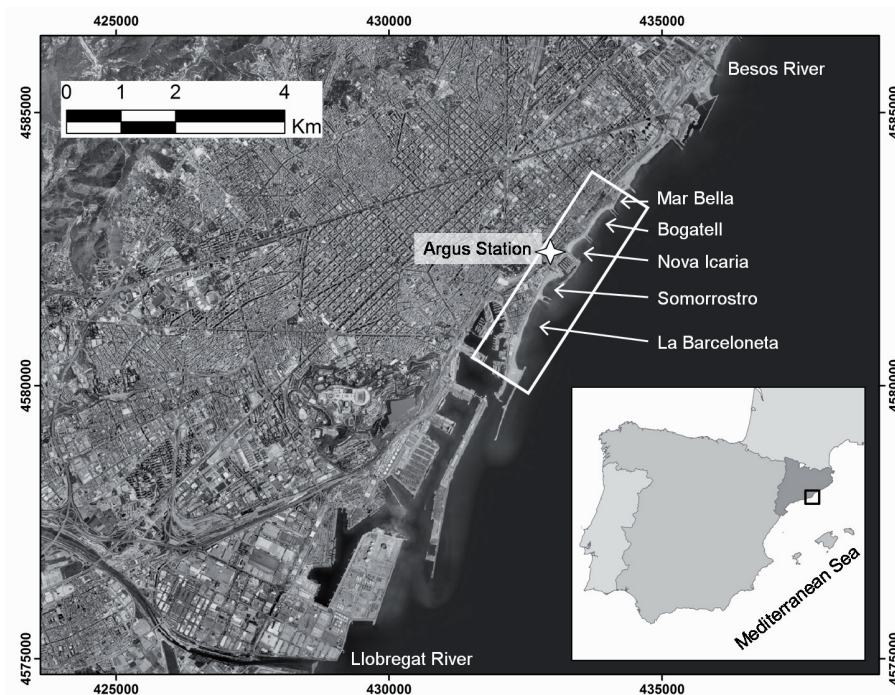


Figure 3.1. Study area with the location of the Argus station. The white rectangle indicates the area visible with the video cameras.

area suggested the existence of a certain coupling between the bar and the shoreline, i.e., an interrelation between the bar and the shoreline behaviours. The aim of the present chapter is to characterize the evolution of the bars of these beaches in order to understand the processes governing their presence and dynamics and their relation to the shoreline evolution. We consider the alongshore uniform and non-uniform behaviour of the beach independently, discuss the differences and similarities found among the artificial embayed beaches studied, and compare them with natural beaches.

3.2. FIELD SITE

Barcelona is located on the north-eastern coast of Spain (NW Mediterranean). In this region the tidal range can be considered negligible, and the waves are the main hydrodynamic force acting on the beaches. Statistical analysis of wave conditions in the region from 1984 to 2004 shows a mean significant wave height value (H_s) of 0.70 m, with H_s maxima of 4.61 m, maximum wave heights of 7.80 m and an averaged mean period of 4.29 s (Gómez *et al.*, 2005). Storms occur mainly from October to April and the most important ones are those coming from the east, due to a combination of the orientation of the beaches and the Mediterranean climate.

The Coastal Monitoring Station of Barcelona focuses on four embayed beaches ranging from 400 to 1100 m length with different orientations and degrees of protection against the wave action (Figure 3.1). An Argus video system (Holman and Stanley, 2007) has been used to study the beaches and the submerged sandbars since October 2001. Five cameras located at a height of 142 m offer a 180° view of the littoral zone. Figure 3.2 is a plan view of the study area obtained by rectifying and merging the 10-minute exposure images of the five cameras.

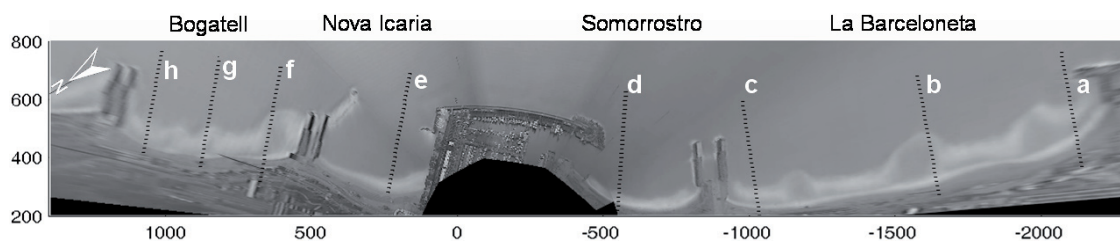


Figure 3.2. Plan view obtained after rectifying and merging the time-exposure images of the five video cameras from 17 April, 2004. The origin of the coordinates is at the video camera's position. The alongshore coordinate, y , increases northwards and the cross-shore coordinate, x , increases seawards. Dotted lines indicate the location of the bathymetric profiles presented in Figure 3.3.

Table 3.1. Morphological characteristics of the four studied beaches.

	La Barceloneta	Somorrostro	Nova Icaria	Bogatell
Length	1100	400	400	600
Beach orientation ⁽¹⁾	20	32	47	38
Slope ⁽²⁾	0.031	0.036	0.049	0.031
D ₅₀ ⁽³⁾	900 μm	450 μm	660 μm	770 μm
no. bars	1	0	0	1

⁽¹⁾ Mean orientation of the shoreline with respect to the north.

⁽²⁾ Mean slopes along the beaches (at the different transects) obtained from 0 to 5 m depth from two bathymetric surveys carried out in October and November 2003.

⁽³⁾ Sediment sampled at the swash zone.

Table 3.1 summarizes the morphological characteristics of the four studied beaches. As can be seen in Figure 3.2, the beaches are separated by double shore-perpendicular dikes, with the exceptions of Nova Icaria and Somorrostro, which are separated by the Olympic Marina, and the southern limit of La Barceloneta, which is an L-shape groin. Furthermore, the northern dike of Nova Icaria continues as a submerged oblique breakwater several tens of metres long (visible in Figure 3.2 due to wave breaking over it). The nearshore sediment of Somorrostro and Mar Bella shows median grain sizes (D_{50}) of 350-400 μm .

Submerged sandbars are present at La Barceloneta and Bogatell but not at Somorrostro and Nova Icaria, the two more sheltered beaches. Three bathymetric surveys of the area during the study period showed the occurrence of a bar at La Barceloneta and a terraced bar at Bogatell (Figure 3.3).

3.3. METHODOLOGY

This chapter comprises 4.3 years of data, from November 2001 to March 2006. During these years only a small number of gaps due to technical problems can be found in the video image data, and these time gaps always lasted less than a week. The year with the greatest number of days without data was 2002 (17 missing days during the whole year).

3.3.1. SHORELINE AND BARLINE EXTRACTION

Chapter 2 examined the shoreline evolution of La Barceloneta and Bogatell beaches from November 2001 to December 2004. In this chapter the extraction of the new shorelines of the years 2005 and 2006 from the time-exposure video images was done following the same procedure. The *reference shorelines* defined for La Barceloneta and Bogatell beaches in the previous study were also used here.

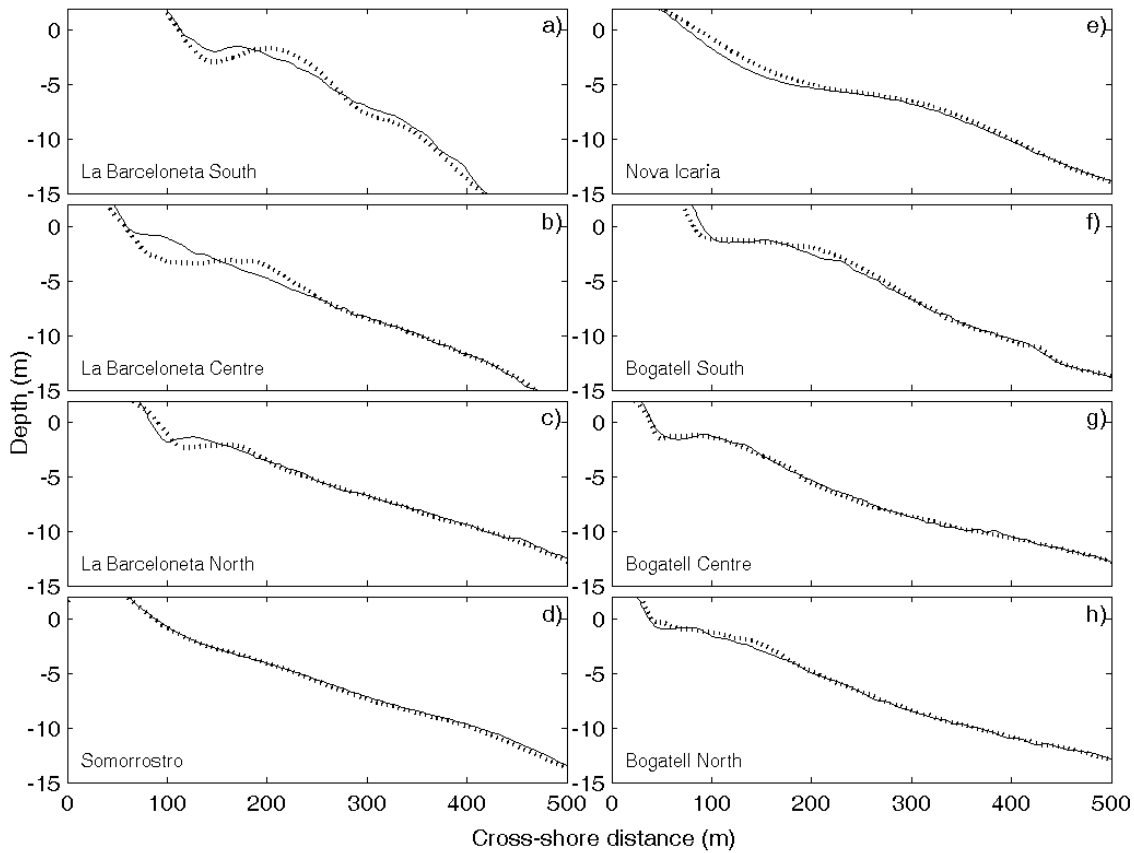


Figure 3.3. Representative bathymetric profiles of the four studied beaches. The solid line corresponds to the bathymetry on 4 October 2003 and the dotted line to that on 5 November 2003. See profile locations in Figure 3.2.

Sandbars were inferred from the rectified time-exposure video images. The rectified video images extended 600 m in the cross-shore direction and 3.7 km in the alongshore direction (Figure 3.2). The accuracy of the photogrammetric transformation from image to ground coordinates is typically one pixel. The worst resolution is found for the alongshore direction at the southern end of La Barceloneta, where one pixel corresponds to less than 20 m alongshore; at the northern limit of Bogatell one pixel corresponds to approximately 10 m.

The mapping of the sandbars requires the occurrence of a certain wave height because it is based on the preferential wave breaking over shallow areas. The minimum H_s which allowed for bar tracking during this study period was 0.90 m at La Barceloneta and 0.70 m at Bogatell. However, this value depends on the depth of the bar crest at each moment. Gaps in the barline dataset were mostly due to low wave energy resulting in the absence of a clear wave-breaking pattern.

The bars are seen in the time-exposure image as a bright line due to the presence of wave foam, contrasting with darker regions where wave breaking does not occur (e.g., Figure 3.2). The bars were extracted from every image showing a clear breakerline through an automated alongshore tracking of the intensity maxima across each beach section (Van Enckevort and Ruessink, 2001). These lines were smoothed alongshore using a Hanning window to remove the noise due to the pixel variability. The half-width of the Hanning window was 30 m at Bogatell, and at La Barceloneta it was changed from 50 m before January 2005 to 25 m thereafter (when the size of the crescentic shapes of the bar became shorter). The location of each bar was stored in a matrix $[X(y,t)]$ that contained the bar crest cross-shore location with respect to the *reference shoreline*, X , at time t and alongshore location y .

3.3.2. MORPHOLOGICAL DESCRIPTORS

The alongshore-averaged bar location $[Xy(t)]$ was calculated by averaging each bar line over the extent of the corresponding beach. Incomplete barlines with less than 80% of the length of the bar visible were eliminated from the alongshore-averaged cross-shore location data set. The lack of a section of bar could be due to an absence of wave breaking over the bar or to the attachment of a bar section to the shoreline (a typical case in the northern section of Bogatell beach).

Time series of alongshore-averaged locations obtained from video images include the apparent migration of the bars produced by changes in the tide level and the wave conditions. Van Enckevort and Ruessink (2001) found that alongshore-averaged cross-shore bar position differed from real bar crest location by a distance of $O(10\text{ m})$. In our case, the apparent migration due to changes in the tide level was negligible. In order to reduce the changes produced by the different wave conditions (H_s), alongshore-averaged locations were calculated only for those data within a 1 m H_s range, i.e., a H_s lower than 1.70 m at La Barceloneta and lower than 1.90 m at Bogatell.

Following Van Enckevort and Ruessink (2003a), the time series of the alongshore-averaged location of the bar at each beach, $Xy(t)$, was decomposed into an interannual $[Xia(t)]$, a seasonal $[Xs(t)]$ and a weekly $[Xw(t)]$ component. First, $Xy(t)$ was yearly-averaged by applying a Hanning filter with a half-window width of 365 days, producing the inter-annual component, $Xia(t)$. The residuals $[Xy(t) - Xia(t)]$ were seasonally-averaged by applying a Hanning filter with a half-

window width of 91 days, isolating the seasonal component, $X_s(t)$. The residuals $[X_y(t) - X_{ia}(t) - X_s(t)]$ give the weekly component, $X_w(t)$. The seasonal component essentially encompasses the response of the sandbars to the seasonal variability in wave height (higher-energy winter months versus lower-energy summer months), while the weekly component contains the bar response to individual storms and to groups of storms, and the measurement noise.

Alongshore non-uniformities in the bars were quantified with the sinuosity, defined as the relationship between the total length of the barline and the distance between its two ends following a straight line. The sinuosity of an alongshore uniform bar will be close to 1 and it will augment when crescentic shapes appear. It is a measurement of the presence of crescentic features along the bar. The best-fit line corresponding to each barline and to each shoreline was used to calculate the bar orientation and the shoreline orientation, respectively. The sinuosity and the orientation of the barlines were also obtained only for the “complete” barlines (i.e., excluding those barlines with less than 80% of the length of the bar visible).

3.3.3. WAVE DATA

Wave data were obtained from two sources: the results of the WANA model data set and the direct measurements from a directional buoy placed in front of Barcelona harbour at 69 m depth. Before March 2004, only the virtual buoy (node WANA2066051) provided directional wave information every three hours. These data are computed by the Spanish National Institute of Meteorology using the HIRLAM and WAM numerical models (Spanish Port Authority). Since March 2004, direct hourly measurements have also been available from a directional buoy (the Cost-Barcelona buoy).

Significant storms affecting the Barcelona coast are those with H_s higher than 2.5 m during the peak of the storm and a minimum duration of 12 h with H_s greater than 1.5 m. If the interval between two consecutive storms is lower than 6 hours, they are considered as a single double-peaked storm.

The time series of the wave energy content (taken as H_s^2) was also decomposed into an interannual $[E_{ia}(t)]$, seasonal $[E_s(t)]$ and weekly $[E_w(t)]$ component following an analogous procedure to that described in subsection 3.3.2. for the alongshore-averaged bar location. This separation was made using the WANA data set for the entire period to avoid changes in the trend due to the difference in the data set.

3.4. WAVE CONDITIONS

The wave conditions during the study period are presented in Figure 3.4. The wave height time series shows a cyclic behaviour, with storm periods (October-April) separated by periods of low storm activity (May-October). The mean significant wave height (H_s) during the study period was 0.71 m and the averaged peak period was 5.7 s. The two most energetic periods affecting the beaches were from October 2001 to May 2002 and from October 2003 to April 2004.

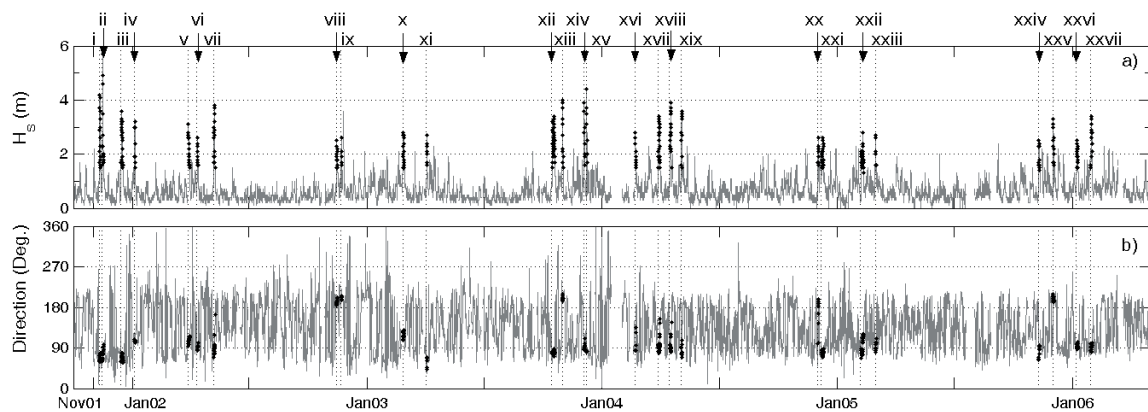


Figure 3.4. a) Significant wave height (H_s), and b) mean wave direction with respect to north. Black dots represent the most significant storm events occurring during the study period (a further explanation can be found in the text), labelled using roman numerals. Given the high H_s values reached during Event ii, this figure and the following figures of this chapter with H_s will show a vertical scale with values ranging between 0 and 6, therefore excluding the 3 values of $H_s > 6$ m occurring during Event ii ($H_s = 6.8, 8.8,$ and 8.7 m).

The most significant storm events affecting the coast of Barcelona during the study period are marked in Figure 3.4 and their characteristics are displayed in Table 3.2. Notice that the nomenclature of these storm events differs from the nomenclature used in Chapter 2. In the previous chapter, the events with incomplete information due to the absence of wave data during some hours of the storm (Events v and xvi) were removed from the data set, because the gaps biased the calculation of the radiation stress. Moreover, Events i and ii were considered as a single event in the previous chapter (Event A), as the shorelines sampled between the two storm events were influenced by the wave conditions. Events i and ii represent the two major storms of the study period: two consecutive intensity peaks from the NE direction separated by a short time lapse.

Table 3.2. Characteristics of the storms with H_s reaching 2.5 m.

Event	Initial date	Mean H_s (m)	Max. H_s (m)	Mean wave direction relative to north	Duration (hours)
i	10-Nov-01	2.6	4.2	68	51
ii	14-Nov-01	3.7	8.8	78	54
iii	14-Dec-01	2.4	3.6	68	69
iv	04-Jan-02	2.3	3.2	105	21
v ⁽¹⁾	28-Mar-02	-	3.1	-	-
vi	11-Apr-02	2.0	2.6	89	33
vii	07-May-02	2.6	3.8	93	48
viii	14-Nov-02	1.9	2.5	193	33
ix	21-Nov-02	2.1	2.6	200	15
x	25-Feb-03	2.0	2.8	118	66
xi	03-Apr-03	2.1	2.7	59	21
xii	15-Oct-03	2.5	3.4	80	90
xiii	31-Oct-03	2.8	4.0	200	33
xiv	04-Dec-03	2.6	3.9	95	21
xv	08-Dec-03	3.0	4.4	83	18
xvi ⁽¹⁾	21-Feb-04	-	2.8	-	-
xvii	28-Mar-04	2.3	3.4	97	75
xviii	15-Apr-04	2.7	3.9	95	48
xix	03-May-04	2.7	3.6	84	30
xx	01-Dec-04	2.0	2.6	162	27
xxi	07-Dec-04	2.0	2.6	78	69
xxii	06-Feb-05	1.9	2.8	92	87
xxiii	01-Mar-05	2.1	2.7	92	27
xxiv	09-Nov-05	1.9	2.5	79	33
xxv	02-Dec-05	2.4	3.3	199	33
xxvi	07-Jan-06	2.0	2.5	94	60
xxvii	29-Jan-06	2.4	3.4	92	54

⁽¹⁾ Incomplete information, lack of data during some hours of the storm.

Figure 3.5 presents the time series of the wave energy content, decomposed into interannual [$Eia(t)$], seasonal [$Es(t)$] and weekly [$EW(t)$] components. The weekly component [$EW(t)$] accounts for rapid changes in the wave height and the seasonal component [$Es(t)$] shows the already mentioned annual variability in the wave data, with a winter season–summer season cycle. The interannual component [$Eia(t)$] shows a trend towards a reduction in the wave energy content from the beginning of the study period. This trend is also visible in the significant wave height time series (Figure 3.4), with a decrease in the number of storms during the last two years of the study period.

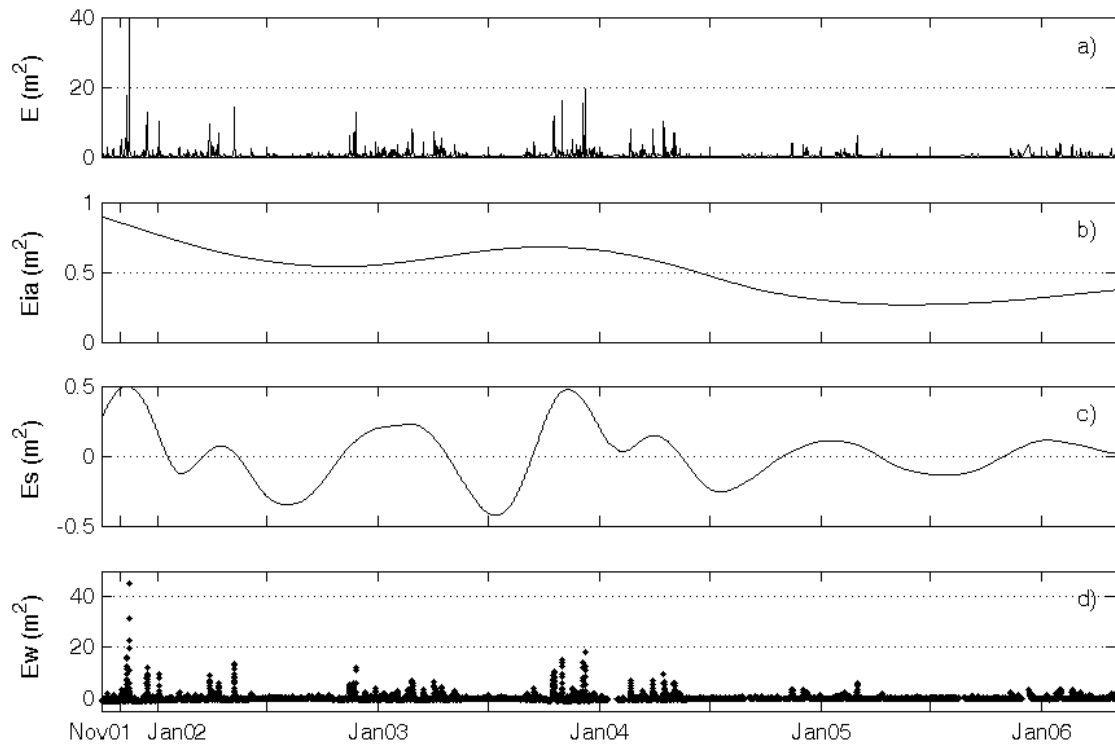


Figure 3.5. a) Wave energy content for the WANA data set, subsequently separated into b) interannual [$E_{ia}(t)$], c) seasonal [$E_s(t)$] and d) weekly [$E_w(t)$] component.

3.5. ALONGSHORE UNIFORM BEHAVIOUR

Alongshore-averaged cross-shore locations of the bars [$Xy(t)$] and the shoreline in relation to the *reference shoreline* are given for both beaches in Figure 3.6. Changes in the location of the bar are significantly greater than those of the shoreline (notice the different scales). The greatest migration of the shoreline was caused by the artificial nourishment of Bogatell beach (June 2002) and the later retreat of the beach, which lasted until the winter of 2003-2004. At La Barceloneta, the shoreline advance caused by the nourishment is less evident because it only affected a small portion of the beach. The subsequent shoreline retreat occurred mostly in February 2003 and in autumn 2003. Another clear migration seen on the La Barceloneta shoreline is the significant retreat during summer 2005.

The short-term behaviours of the alongshore-averaged bar location at Bogatell and La Barceloneta show some similarities, with migrations taking place in the same direction (onshore/off-shore) during the most important stormy periods. The first measurements of the bar at La Barceloneta showed the bar located about 10 m from the *reference shoreline*, and about 30 m at Bogatell. After Events i and ii

both bars had migrated offshore, about 70 m at La Barceloneta and about 50 m at Bogatell, the largest bar migration observed during the study period. The other clear episodes of offshore bar migration observed at both beaches were those in February 2003 (during some minor storms occurring right after the erosion of the nourishment) and two other episodes in the winter of 2003-2004, one during Event xii and another during Events xiv and xv. After these four relatively fast episodes of offshore migration, the barlines showed slower onshore migration. The wave height under which onshore migration occurred depended on the water depth where the bar was located. After the large offshore migration caused by Events i and ii at both beaches, the wave conditions occurring during and after Event v caused onshore bar migrations of about 20 m at La Barceloneta and about 30 m at Bogatell. Between Events x and xi and the stormy conditions occurring on the following days, the bar migrated about 25 m onshore at both beaches. Finally, onshore migration also occurred (to a shorter extent) during Event xiii and its post-storm conditions, and in the stormy period following Event xv. However, there were also some periods when the bars showed different behaviours. For instance,

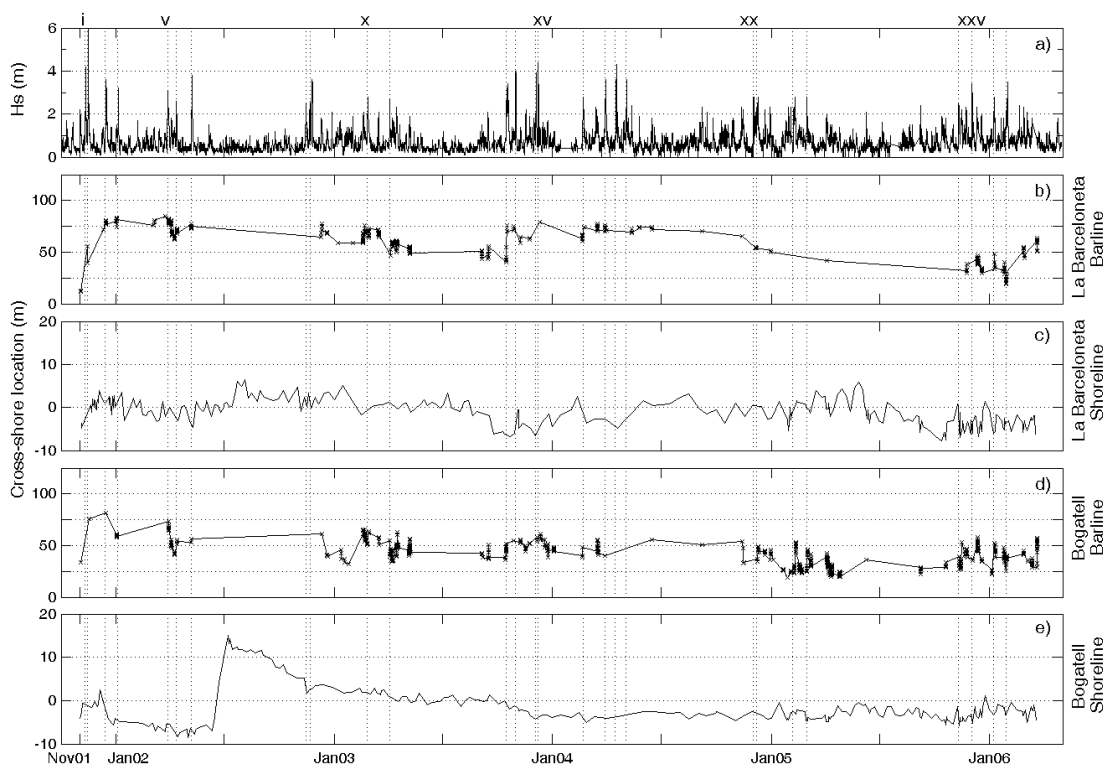


Figure 3.6. Time evolution of significant wave height (a), and alongshore-averaged mean cross-shore location of the bar (b) and the shoreline (c) at La Barceloneta and the bar (d) and the shoreline (e) at Bogatell during the study period. Measurements in (b) and (d) correspond to bar measurements containing more than 80% of the data surveyed when H_s was lower than 1.90 at La Barceloneta and 1.70 in Bogatell.

after Event xxvii the bar at La Barceloneta migrated offshore systematically, while that of Bogatell showed both onshore and offshore migration.

Onshore and offshore migration of the bar and the shoreline did not appear to be systematically correlated either at a medium-term time-scale or at an event time scale. Only certain events produced a discernible effect on both the bar and the shoreline. In these cases, on-offshore bar migration occurred indistinctly with shoreline advance/retreat. For example, offshore bar migration and shoreline retreat took place at both beaches related to Event xii; onshore bar migration and shoreline advance at La Barceloneta related to Event xiii; offshore bar migration and shoreline advance at La Barceloneta related to Events i and ii; and onshore bar migration and shoreline retreat at both beaches related to Event v.

The alongshore uniform behaviour of the bars varied over a range of timescales. Figure 3.7 presents the time series of the cross-shore locations decomposed into interannual [$X_{ia}(t)$], seasonal [$X_s(t)$] and weekly [$X_w(t)$] components. The weekly component [$X_w(t)$] accounts for rapid changes in the bar location and also includes the variability due to the measurement error. The seasonal component [$X_s(t)$] at both beaches shows a certain pattern with offshore migration during

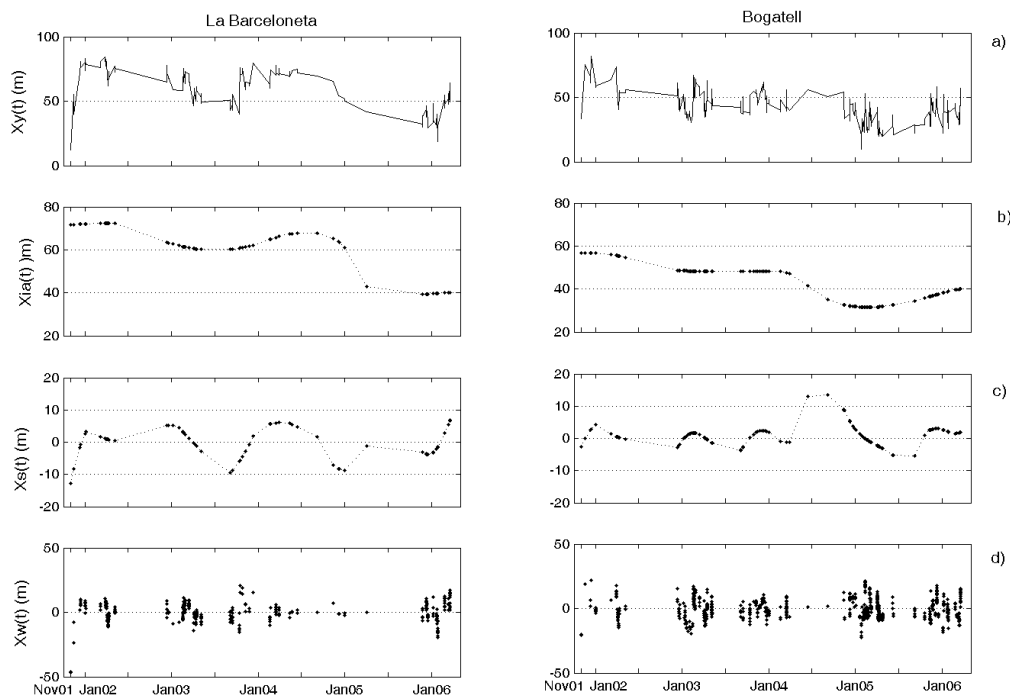


Figure 3.7. a) Alongshore-averaged cross-shore positions [$X_y(t)$] for the bar at La Barceloneta and Bogatell separated into b) yearly [$X_{ia}(t)$], c) seasonal [$X_s(t)$] and d) weekly [$X_w(t)$] components.

the first months of the winter season, followed by some onshore migration. This configuration is visible at both beaches, but with different timings. It is clearly visible at La Barceloneta during the winter seasons of 2001-2002, 2003-2004 and 2005-2006, while at Bogatell it is visible in every winter season except 2004-2005, when only onshore migration occurred during the whole season. The interannual component [$X_{ia}(t)$] shows a net onshore bar migration with an overall change in the bar location of about 30 m at La Barceloneta and about 20 m at Bogatell.

3.6. ALONGSHORE NON-UNIFORM BEHAVIOUR

An analysis of the morphological alongshore variability is required for a complete understanding of the three-dimensional nearshore behaviour. The time-averaged barline during the study period was an approximately rectilinear line that was oblique with respect to the *reference shoreline*, as shown in Figure 3.8. This obliquity was more obvious at Bogatell beach, where the angle was approximately 5.3° , whilst at La Barceloneta beach it was 2.6° . Both of them were closer to the beach on their northern sides.

The morphological descriptor that quantifies the alongshore variability of the bars is their sinuosity (Figure 3.9). Although the two bars showed similar values of the sinuosity on average (~ 1.06), the time series of the bar sinuosity at Bogatell showed

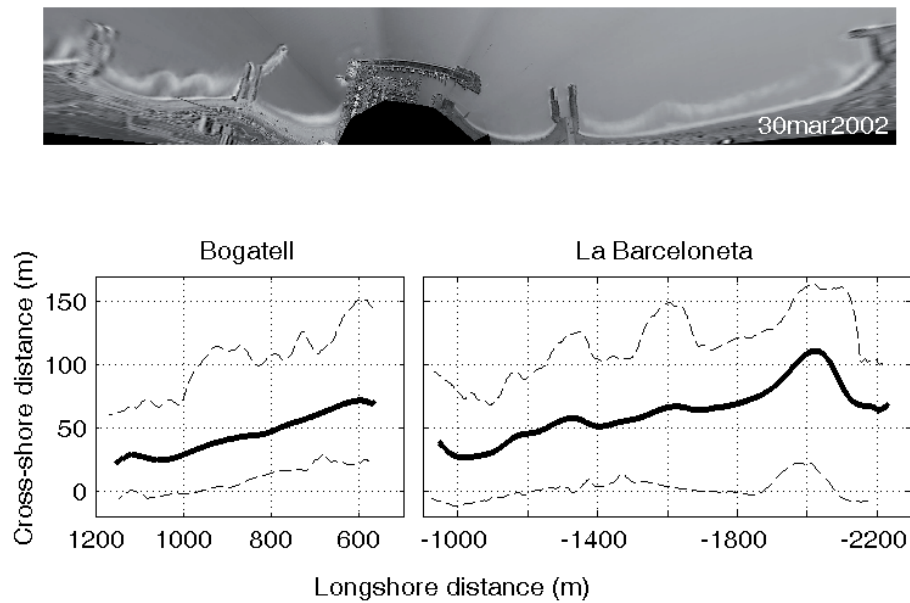


Figure 3.8. Time-averaged barlines during the study period (dark line) and the most remote locations reached by the bars during the study period (lighter lines). Cross-shore distances are relative to the *reference shoreline*.

a larger number of changes. The sinuosity of the bar at La Barceloneta ranged between 1.019 and 1.113. The highest sinuosity values of the bar were reached in February and October 2003 and in the winter of 2005-2006. The sinuosity of the bar at Bogatell ranged between 1.018 and 1.153. The temporal evolution of its sinuosity showed several peaks, with the two maxima in March-May 2002 and in April-June 2004, and other minor peaks in February and October 2003 and in the winter of 2005-2006.

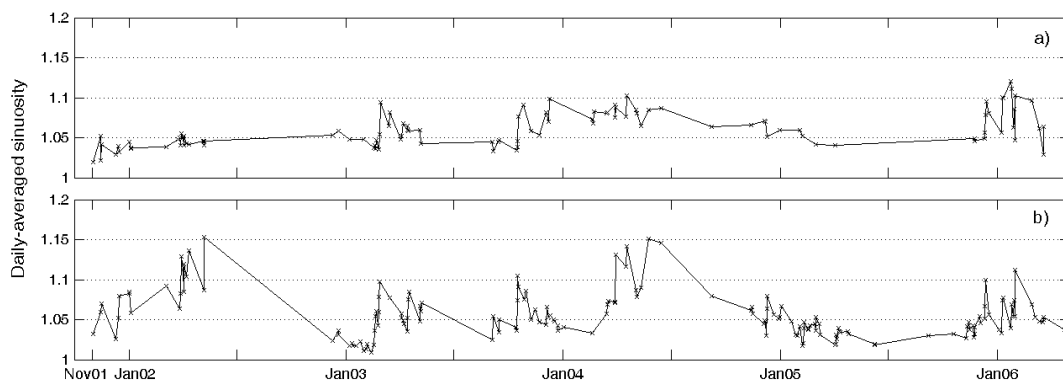


Figure 3.9. Daily-averaged values of the sinuosity of the bar at La Barceloneta (a) and Bogatell (b).

3.6.1. BAR AND SHORELINE EVOLUTION

This subsection presents a more detailed examination of the three-dimensional behaviour of the beaches. Figure 3.10 shows the temporal evolution of the barline $[X(y,t)]$ and shoreline positions at La Barceloneta beach, together with the significant wave height during the study period. The plan views shown in Figure 3.11 are examples of the different beach states that this beach attained during the study period, from the *Longshore Bar and Trough* to the *Low Tide Terrace*. In the same manner, Figures 3.12 and 3.13 show the bar and shoreline evolution at Bogatell beach and examples of the beach states, respectively.

3.6.1.1. La Barceloneta

The shoreline configuration at La Barceloneta beach showed an episode of beach rotation produced by Events i and ii at the beginning of the study period, with an advance of the shoreline in the southern section of the beach and a retreat in the northern section. In summer 2002 the artificial nourishment of the northern section of the emerged beach produced an advance of the shoreline of approximately 14 m. Afterward, the nourished sand in the northern section of the beach was rapidly eroded, leaving a retreated northern section and an accreted southern section. After

Event xiii, two stable megacusps (around the alongshore locations -1300 and -1800 m) formed and remained for more than a year. The northern-located megacusp flattened in early 2005, while the southern one maintained its integrity for almost two years, flattening during the last third of 2005. Notice that the flattening of the southern-located megacusp coincided in time with a certain erosion of the southern limit of the beach. This produced an overall retreat of the shoreline that is also clearly visible in Figure 3.6. From January 2006 to the end of the study period, small megacusps (with a longer wave length in the southern half of the beach than in the northern half) were also observed on the La Barceloneta shoreline.

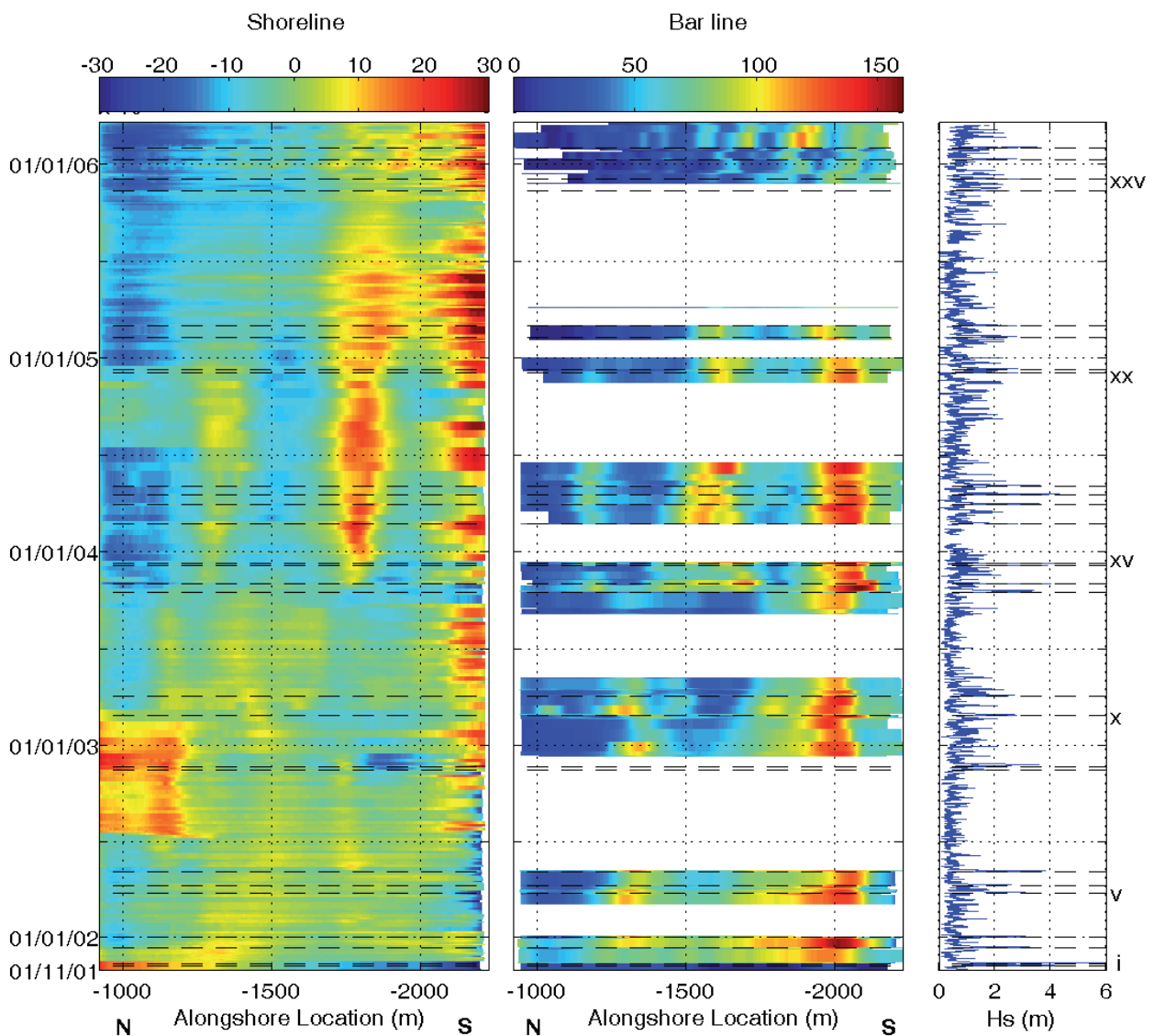


Figure 3.10. Time-space diagrams of the shoreline (left) and barline (centre) positions at La Barceloneta beach. The colour scales are given in metres and represent the distance from the *reference shoreline*. Cold colours represent the most shoreward locations and warm colours the most seaward locations. White horizontal bands in the bar plot represent moments when no data were available. Significant wave height (H_s) is given on the right.

Regarding the bar position at La Barceloneta beach, Events i and ii implied an offshore bar migration and the bar adopted an almost linear configuration, with the exception of a crescentic shape (protuberance) near the southern tip of the beach (see Figure 3.11a). This protuberance was the main long-lasting element of the bar evolution since it remained almost unchanged from late 2001 until early 2005. The most likely reason is that, for several years, there was no other stormy period with the required energy content to be able to change it. By the end of 2001, a second protuberance appeared in the bar, amplified after Event v (there is incomplete information about this event but the H_s reached 3 m), at the same time as an onshore migration that can be seen in Figure 3.6. After a large gap in the bar data, due to the absence of significant wave breaking over the bar for 7 months, the only change produced in the bar was an approach of some bar sections to the shoreline. During this period of fair weather (summer 2002), the onshore bar migration together with the artificially-caused shoreline advance in the northern section gave way to the attachment of the bar to the shoreline. After the erosion of the nourished sand, by the end of February 2003, the bar system became crescentic (see the associated increase in the sinuosity and the plan view of the *Rhythmic Bar and Beach* in Figure 3.11b) and gradually approached the coast (May-September 2003, see also Figure 3.6). Event xii caused significant offshore bar migration and during the onshore migration that occurred subsequently two sections of the bar became attached to the shoreline, attaining a coupled configuration that would last for more than a year (with high sinuosity values, see Figure 3.9). This period of bar and shoreline coupling corresponds to the *Transverse Bar and Rip* beach state (Figure 3.11c) and apparently finished gradually (“apparently” because there were almost seven months without barlines available due to fair weather conditions). In February 2005 the southern attachment was still clear but in the northern bar section the breaking line was almost shore-parallel. By November 2005, after a second large gap in the bar data, the remaining protuberances had already disappeared and the bar was very close to the beach with an almost shore-parallel configuration. After Event xxv, new crescentic shapes appeared on the southern beach and, some weeks later, also on the northern beach, implying again an increase in sinuosity. The new crescentic bar had a significantly smaller wave length than the one previously observed (compare Figures 3.11c and 3.11d). In 2003-2004 the wave length of the crescentic bar was 300 m, while the crescentic bar occurring in late 2005 had an alongshore spacing of 200 m in the southern half of the beach and 100 m in the northern half (see Ribas *et al.* (2007) for a detailed description). At the beginning of 2006, this *Transverse Bar and Rip* beach evolved

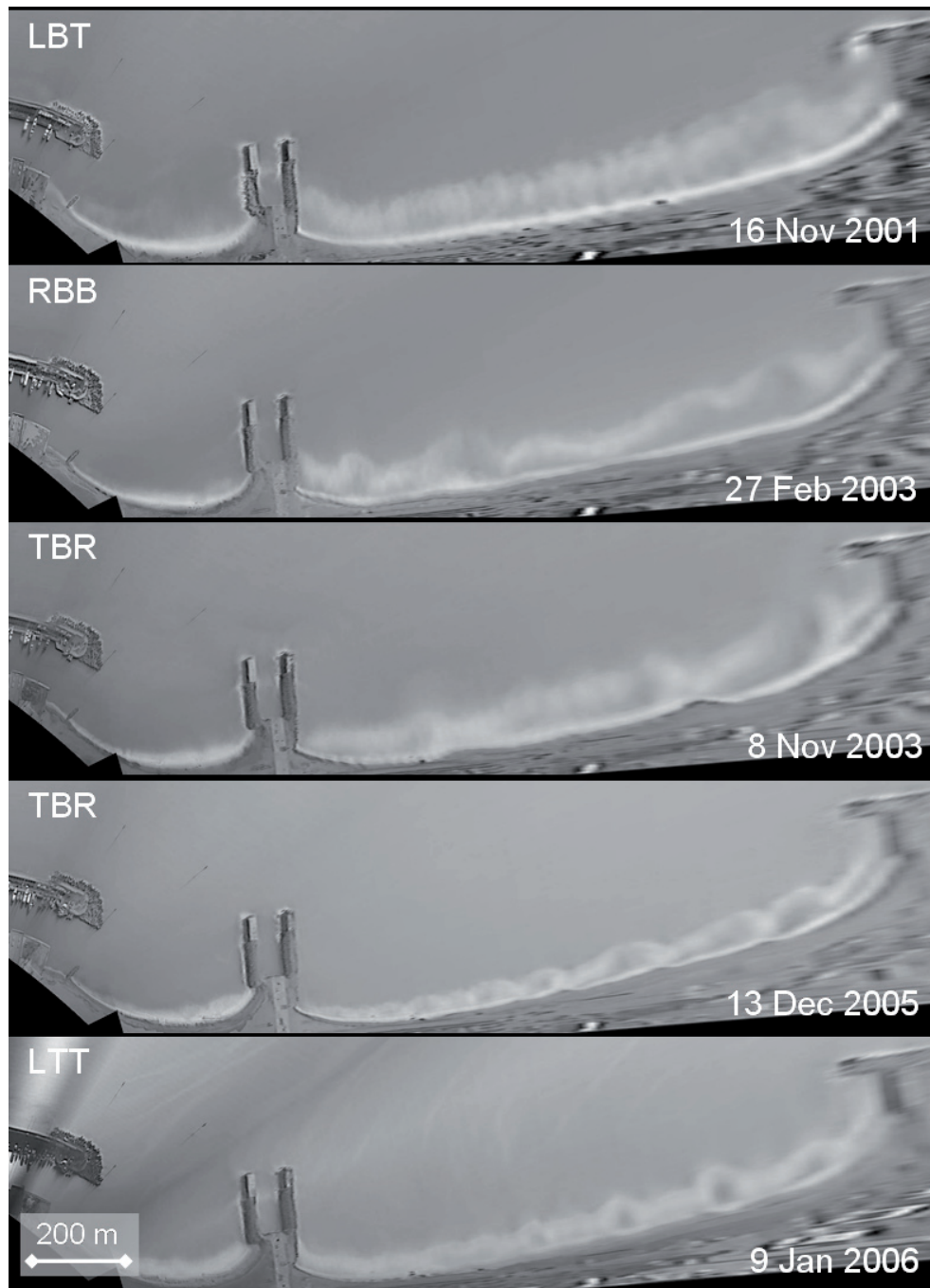


Figure 3.11. Examples of the different beach states attained at La Barceloneta: Longshore Bar and Trough (a), Rhythmic Bar and Beach (b), Transverse Bar and Rip (c and d), and Low Tide Terrace (e).

towards a *Low Tide Terrace*, as can be seen in Figures 3.11d and 3.11e.

3.6.1.2. Bogatell

The November 2001 storms (Events i and ii) also produced beach rotation at Bogatell. The effect of the summer 2002 nourishment was more evident on this beach. It produced an advance of the entire shoreline, with a mean value of approximately 20 m. After the nourishment the sand was partially relocated, producing some retreat in the southern section of the beach and an advance in the northern section. A major erosion of the nourished sand occurred in February

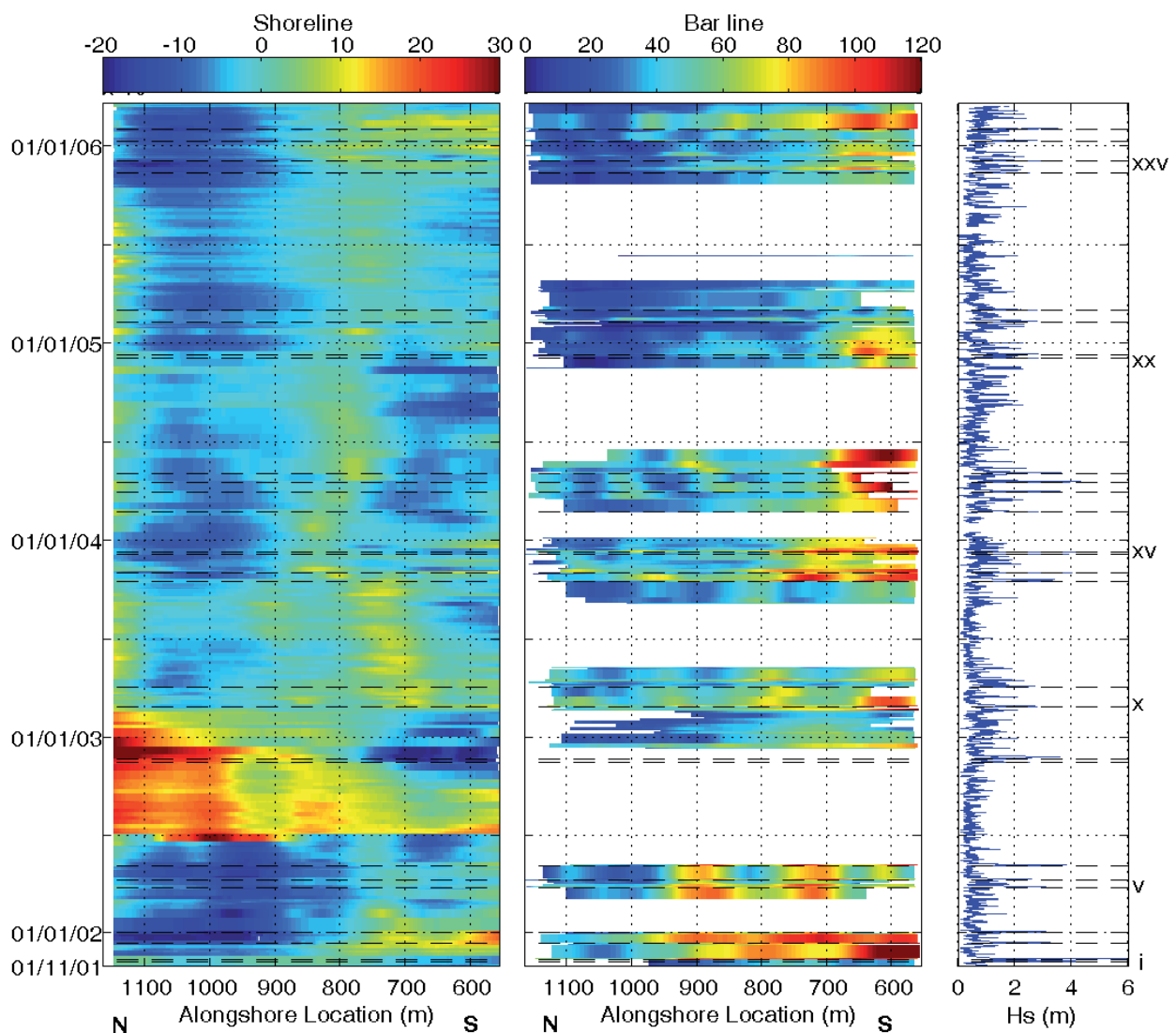


Figure 3.12. Time-space diagrams of the shoreline (left) and barline (centre) positions at Bogatell beach. The colour scales are given in metres and represent the distance from the *reference shoreline*. Cold colours represent the most shoreward locations and warm colours the most seaward locations. White horizontal bands in the bar plot represent moments when no data were available. Significant wave height (H_s) is given on the right.

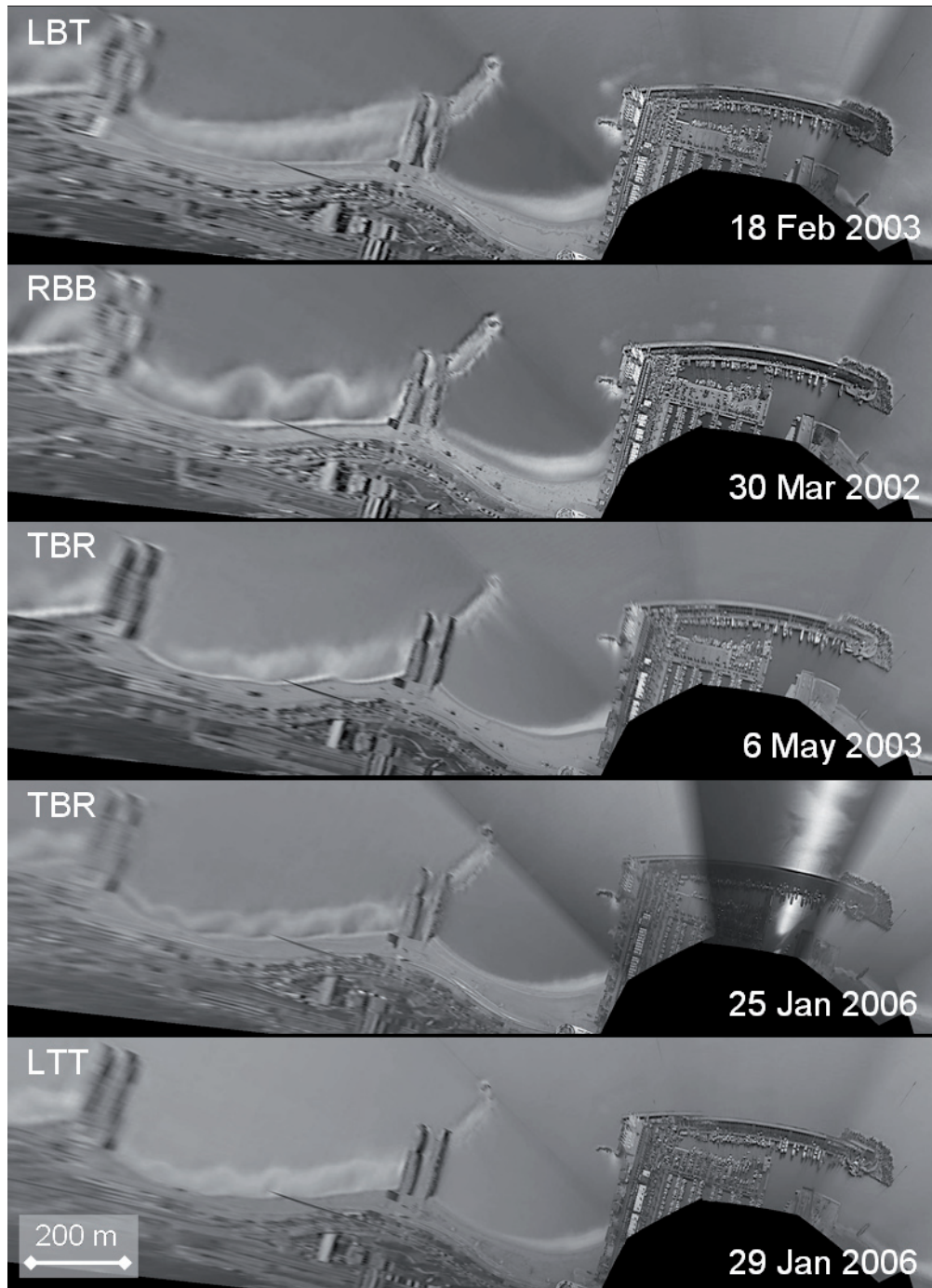


Figure 3.13. Examples of the different beach states attained at Bogatell: a) Longshore Bar and Trough, b) Rhythmic Bar and Beach, c) and d) Transverse Bar and Rip, and e) Low Tide Terrace.

2003, as at La Barceloneta beach. This erosion resulted in the formation of two megacusps (located in the central and central-southern part of the beach) that lasted for almost a year. Another configuration of the shoreline with a more centrally located megacusp was attained after Events xii and xiii, and lasted for two years. The first months of 2006 were characterized by a retreated shoreline in the northern half of the beach and an advanced shoreline in the southern half.

The obliqueness of the Bogatell sandbar, already seen in Figure 3.8, can also be seen in Figure 3.12. Compared to La Barceloneta, this beach shows a more dynamic bar with more frequent changes in the bar morphology from linear to crescentic. For this reason, a detailed description of the different morphologies appearing during the study period is not as obvious as the one presented in the previous subsection. However, several important episodes are discernible. For instance, the erosion of the nourished sand in February 2003 coincided in time with the change from an oblique bar attached to the shore in the northern section of the beach (Figure 3.13a) to a crescentic bar. The change in the typical wavelengths of the crescentic shapes of the bar from around 175 m before mid-2004 to about 100 m after 2005 is also clear (this can be appreciated in the plan views shown in Figure 3.13c and 3.13d). At this beach, the coupling between bar and shoreline is not as evident as at La Barceloneta, although there are some clear examples like the one shown in Figure 3.13c, where the crescentic bar is attached to the shoreline matching the location of the megacusps.

3.6.2. BAR AND SHORELINE ORIENTATIONS

At the previous chapter the occurrence of changes in the shoreline orientation of these beaches was reported. In some cases these changes were related to episodes of beach rotation that occurred abruptly, as a response to storm events, or gradually, as a recuperation of the beach or a trend towards a certain equilibrium orientation. In other cases the changes in beach orientation were due to alongshore differences in the advance or retreat of the shoreline due to storm and post-storm conditions. Figure 3.14 presents the time series of the orientation of the shoreline and the barline at each beach. The magnitude of the changes in orientation of the bar and the shoreline is equivalent for each of the beaches, with a range of angles of approximately 5° at La Barceloneta and 10° at Bogatell. The orientation of the shoreline and the barline at La Barceloneta showed a similar overall trend during the study period, with a gradual anticlockwise change in the angle of orientation (Figure 3.14). However, at Bogatell the shoreline and the barline did not show

long-term changes in their orientation.

At shorter time scales, the changes in the orientation of the bar and the shoreline were in the same direction during most of the study period. However, divergences between the bar and the shoreline changes in the orientation occurred at both beaches during certain periods. The clearest example occurred during the first half of 2003, when the bars at La Barceloneta and Bogatell turned clockwise while the shorelines of both beaches turned anticlockwise. This behaviour was clearly influenced by the preceding artificial nourishment of the beach. In February 2003 the angle of the beach orientation decreased due to the retreat of the northern section of the beach. At the same time, the angle of orientation of the bar increased (while the bar became crescentic) because the southern bar section slightly approached the beach while the northern bar section moved slightly away from the beach.

The response of the beaches to individual storm events does not show an obvious connection. Analogous changes in the orientation of the beach and the bar due to

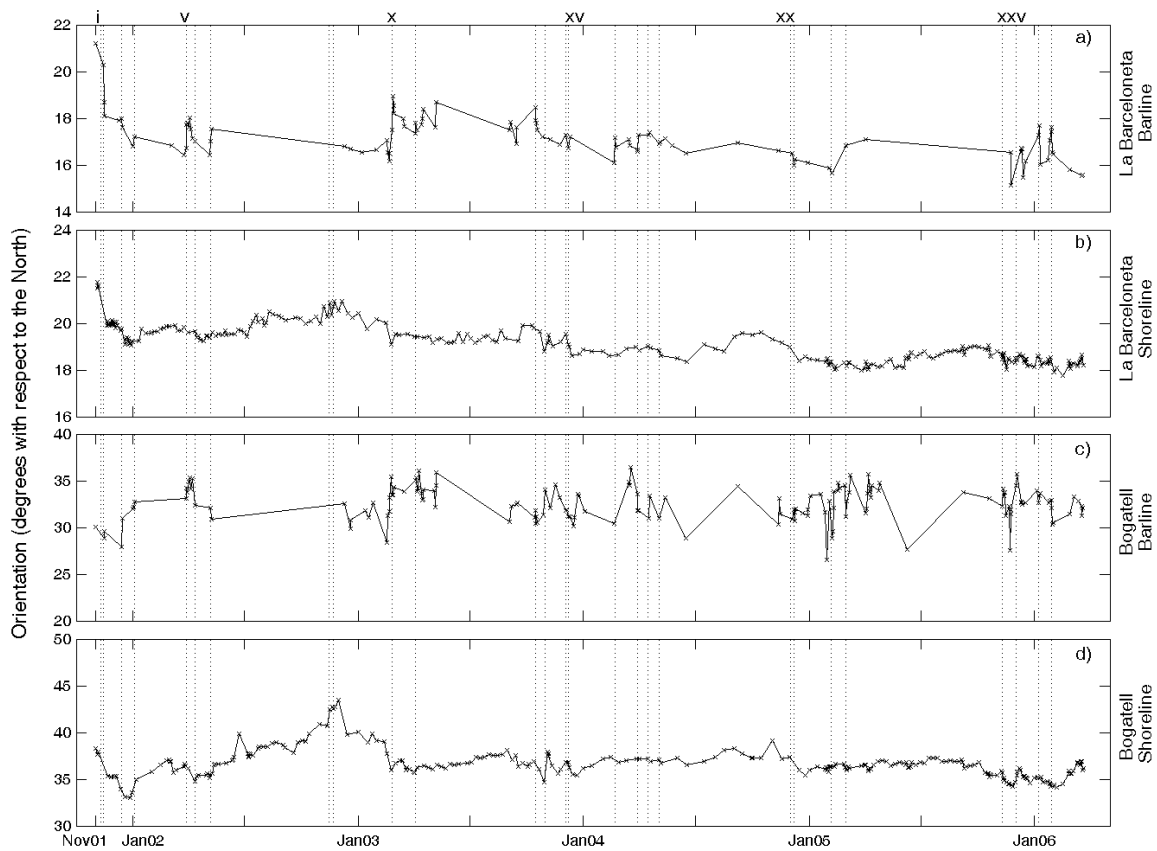


Figure 3.14. Orientation of a) the shoreline at La Barceloneta, b) the barline at La Barceloneta, c) the shoreline at Bogatell and d) the barline at Bogatell, where the angles are measured with respect to north.

specific storm events were clearly visible at both beaches (e.g., Events i, ii or xxvii). However, during other events the shoreline and the barline clearly showed an opposite change (e.g., Event iii at Bogatell).

3.7. DISCUSSION

The video system is used to monitor four artificial embayed beaches along the Barcelona city coast. Two of these beaches, Nova Icaria and Somorrostro, show a high degree of protection against wave action thanks to the presence of the Olympic harbour and the submerged breakwater of Nova Icaria. The morphodynamic state (Wright and Short, 1984) of Nova Icaria and Somorrostro beaches during the study period, based on video images and two bathymetric surveys (see Figure 3.3), was the *Reflective Beach* state, and exceptionally the *Low Tide Terrace* state (see, for instance, the plan views of Somorrostro in Figures 3.11d and 3.11e, and of Nova Icaria in Figure 3.13a). The absence of submerged bars at Nova Icaria and Somorrostro beaches is consistent with the high slopes found in their submerged profiles (gradients of 0.036 at Somorrostro and 0.049 at Nova Icaria), in comparison with the gradients of 0.031 found at La Barceloneta and Bogatell (see Table 3.1). These values are in agreement with the range (0.005-0.03) provided by Wijnberg and Kroon (2002) for subtidal bars in semi-protected and open coasts. The lower wave energy reaching the breaker zone (due to the high degree of protection) is also responsible for the reflective behaviour of these two beaches because the Ω parameter used by Wright and Short (1984) to characterize beach states is proportional to the breaker wave height.

The less steep, longer and more exposed beaches of La Barceloneta and Bogatell often showed barred beach profiles, with a single bar that had a certain obliquity with respect to the *reference shoreline* (the northern section of the bar usually placed in a position closer to the shore or even anchored to it, see Figure 3.8). This orientation would suggest a dominant longshore transport towards the SW in both beaches, according to observations in other Mediterranean areas where bar systems are located progressively seaward in the dominant longshore transport direction (Guillén and Palanques, 1993). These submerged bars followed a general cyclic morphological behaviour, switching among the four intermediate morphodynamic states: *Longshore Bar and Trough* associated with high-energy wave events, and *Rhythmic Bar and Beach*, *Transverse Bar and Rip* and *Low Tide Terrace* associated with low-energy wave periods (see Figure 3.11 and 3.13). This cyclic behaviour is

similar to that observed at Palm Beach, Australia, another single-barred embayed beach (Ranasinghe *et al.*, 2004).

The two single-barred beaches also displayed some differences. The bar at Bogatell, which is small and often terraced (i.e., without a bar trough, see Figure 3.3), underwent numerous changes in its morphodynamic state, generally switching between a linear and a crescentic bar (see Figure 3.12). The different configurations of the larger and better-developed bar at La Barceloneta were more long-lasting. This result is in agreement with the theoretical findings of Calvete *et al.* (2005): smaller bars located closer to the shore develop 3D morphologies more quickly than larger bars located farther away because less sediment is involved in their evolution. For instance, during the study period the bar at Bogatell switched between the four morphodynamic states but the bar at La Barceloneta only underwent the complete “reset” of the nearshore morphology once, associated with high-energy wave events (after Events i and ii). At this beach, the strongest storm events produced the offshore migration of the bar and a certain decrease in the bar sinuosity, but did not generate an alongshore parallel bar. In particular, the protuberance in the southern section endured every storm event after Events i and ii, and it only flattened after several months of fair wave conditions in summer 2005 (see Figure 3.10).

Therefore, in the two artificial single-barred beaches under study the changes from a two-dimensional longshore bar to a three-dimensional longshore bar (as defined by Wijnberg and Kroon, 2002) are related to the morphodynamic cycle and to the wave energy content. In general, low-energy wave action produces the occurrence of down-state transitions (Wright and Short, 1984) from a two-dimensional to a three-dimensional bar. Furthermore, Aagaard (1998) reported that, at some settings where low-energy periods alternate with sporadic high-energy events of short duration, a given bar may be arrested for long periods of time. Then, the morphological evolution of the bar may be out of equilibrium with the prevailing wave climate because the energy level is too low to move the sand and force the bar any further in the accretionary sequence. In these situations, the theoretical morphodynamic state predicted from wave conditions can differ from the real morphology of the beach during long periods of time (this seems to be the case at La Barceloneta during the whole of 2004). In addition, at La Barceloneta and Bogatell beaches, the occurrence of three-dimensional longshore bars is also affected by the sediment availability, which enhances the appearance of crescentic

shapes. For instance, three periods of high barline sinuosity (i.e., crescentic bars) were observed at La Barceloneta (see Figure 3.9) and two of them could be related to an increase in the amount of sediment available in the submerged profile. The first peak in the sinuosity occurred in early 2003, after the erosion of the nourished beach and a few storms at the end of the winter. The second peak was in October 2003, after a major southern storm (Event xiii), when a stable crescentic bar coupled to the beach. The third peak occurred in winter 2005-2006 and followed a retreat of the southern section of the beach together with the flattening of the southern-located megacusp. In this last case the eroded sand did not appear to move alongshore (Figure 3.10, shoreline) and some months later, when the wave conditions allowed the bar tracking, the sandbars were crescentic, with the lowest wavelengths observed during the study period (Figure 3.10, barline).

This increase in the crescentic shape of the bar with new incomes of sediment to the submerged profile is in accordance with observations in nearshore regions of an increase in the bar three-dimensionality after the execution of a shoreface nourishment (Grunnet and Ruessink, 2005). In that case, the authors related the augmentation of the bar 3D morphology to the reduction in the water depth over the bar. According to theoretical studies (Calvete *et al.*, 2005; Klein and Schuttelaars, 2006), when the water depth over a bar decreases the induced increase in the wave dissipation causes an increase in the growth rate of 3D features.

Coupling between the bar and the shoreline morphologies can be clearly seen at La Barceloneta beach. The most evident occurring during the study period started at La Barceloneta beach in mid-October 2003, right after an ESE storm with $H_s > 4\text{m}$ (Event xii). On the beach, two megacusps were formed that coupled with the most approached sections of the submerged bar (*Transverse bar and Rip* state, see Figure 3.11). The wavelength of these crescentic shapes was approximately 400 m and it lasted for more than a year. A second coupling with similar characteristics but a lower wave length was observed in winter 2005-2006, when the bar became crescentic and some undulation of the shoreline could be discerned on the beach (see Figure 3.10).

The coupling of the bar and the shoreline can also be detected in the overall changes in beach orientation during the entire study period and also at shorter time scales. This suggests that longshore sediment transport can play a significant role in the barline orientation, as it does in shoreline orientation. However, the response to

individual storm events was not obvious, as can be seen in Figure 3.14.

The alongshore-averaged cross-shore migration of the bars and the shoreline does not appear to be systematically correlated either at a medium-term time-scale or at an event time scale (see Figure 3.6). At La Barceloneta and Bogatell, when the bar and the shoreline responded to a storm event, onshore or offshore bar migration occurred indistinctly with shoreline advance or retreat. There are no other previous studies certifying the existence of a relationship between the direction of the bar migration and the shoreline change in the field, although a certain relationship seems to emerge in wave flume experiments (Sunamura and Takeda, 1993).

In a longer term perspective (4.5 years), the bar migration described at La Barceloneta and Bogatell followed a net onshore migration pattern. The interannual component of these alongshore-averaged cross-shore positions also shows onshore migration patterns at both beaches (Figure 3.7). This trend coincides with the interannual component of the wave energy content (Figure 3.5), i.e., there is a manifest trend towards wave energy reduction with time. In addition, the November 2001 storms (Events i and ii) prompted an uncommon offshore migration of the bars. Taking into account the wave height–water depth ratio, this large offshore migration increased the water depth and therefore decreased the ratio value, favouring the subsequent onshore migration of the bars with the less energetic wave conditions (e.g., Plant *et al.*, 2001). In any case, the observed overall bar migration trend of Barcelona beaches differs from the long-term Net Offshore Migration (NOM) pattern described in other areas (Ruessink and Kroon, 1994; Shand *et al.*, 1999). Although this could be related to site-specific factors, it should be noted that the NOM process has not been clearly identified in any other Mediterranean beach. Future research should be conducted in order to determine whether this apparent differential behaviour between Mediterranean and other coastal areas is due to the lack of detailed long time series of morphological coastal evolution around the Mediterranean or to some differences in sediment transport processes affecting bar evolution related to the wave climate of the Mediterranean.

3.8. CONCLUSIONS

The four sandy beaches of Barcelona that were under study are protected by shore-perpendicular groins and have medium to coarse sediment and high slopes that permit the presence of, at most, one submerged sandbar. Somorrostro and Nova Icaria, the most protected beaches, are generally in a *Reflective Beach* state. In

contrast, La Barceloneta and Bogatell often show a bar (or a terraced bar) and switch among the different *Intermediate Beach* states. Their morphodynamic behaviour is mainly related to the wave climate affecting the coastal area. However, there are additional morphological changes caused by human interventions (e.g., artificial nourishment, construction of a new structure, or transformation of an existing one), which alter the beach configuration and imply that the beach needs to readjust to a new equilibrium after the intervention.

The data presented in this study support a number of previous observations, laboratory tests and models. Firstly, the morphodynamic state of the two barred beaches does not always relate to the preceding wave conditions, as the natural trend of the beach towards an equilibrium configuration induced by the wave conditions is interrupted by low-energy periods. At Barcelona beaches (as probably at other Mediterranean beaches) the arrest of the beach configuration typically occurs during long periods, mostly associated with the summer season, when the wave energy is too low to cause sediment transport. Secondly, the bar variability increases when the bar dimension decreases (the bar at Bogatell beach is much more variable than the one at La Barceloneta). Thirdly, there is a relationship between the occurrence of crescentic bars and the sediment availability in the submerged profile, related to the erosion of the beach and the erosion of the sand nourished to the beach.

This study also provides some new insights into beach and bar behaviour. Firstly, there is clear evidence of coupling between the bar and the shoreline orientation, with analogous changes in the shoreline and barline orientations at time-scales of seasons to years. This coupling occurs in addition to the coupling of the rhythmic morphologies of the bar and the shoreline related to the *Transverse Bar and Rip* state. Secondly, the interannual component of the net cross-shore migration of the bars at Bogatell and La Barceloneta is observed to be coupled with the interannual wave climate found on these beaches. Thirdly, the overall trend of the net cross-shore migration of the bars during the study period is onshore, in disagreement with the NOM pattern detected in other long-term observations (located in open and higher-energy coasts). This differential behaviour might be due to some differences in sediment transport processes affecting bar evolution or to the duration of the NOM cycle in Barcelona, which may be longer than the study period.

4 Morphodynamic response of embayed beaches to a beach nourishment

Edited version of E. Ojeda and J. Guillén, 2006. Monitoring beach nourishment based on detailed observations with video measurements. *Journal of Coastal Research*, SI (48), 100–106.

4.1. INTRODUCTION

Coastal erosion is a worldwide problem that has been approached in different ways. In recent years, soft engineering projects (such as beach replenishment) are taking the place of hard engineering ones (e.g. construction of shore-protection structures) in some regions because they may represent less environmental and visual impact in the adjacent area and preserve the beach resource. The success of both types of engineering projects needs a previous knowledge of the area where they are going to be implemented and, moreover, subsequent studies (including monitoring of beach performance) are also needed in order to improve the performance of successive interventions (Hanson *et al.* 2002).

Replenishment has been a common practice in the Mediterranean Spanish coast, mainly as an answer to the erosion problems caused by a decline in the sediment inputs to the coastal system and the interruption of the littoral drift produced by the construction of hard structures. During the last 20 years, 600 nourishments have been performed in 400 different sites in Spain with a total sand supply of approximately 110 Mm³ (Hanson *et al.*, 2002).

Due to the fact that some of the nourishment projects were not successful, but mainly as a consequence of the scarcity of sand borrow areas in the Spanish Mediterranean continental shelf and the serious environmental problems related to their exploitation, nourishment projects must be now restricted. This fact generates conflicts with the increasing demand for sand from managers of the tourist coastal areas because wide and sandy beaches are the main tourist attraction.

This controversy implies that nourishment projects should be carefully designed and evaluated in order to obtain optimum results.

Differential GPS, airborne laser mapping, amphibious vehicles and video imaging were specified by Hamm *et al.* (2002) as some of the recently developed techniques that can be taken as the most capable procedures in monitoring nourishment performance. Elko *et al.* (2005) tested the use of video images with traditionally surveyed beach profiles to monitor nourishment performance, finding differences between video-estimated and traditionally surveyed shoreline (MSL) position of 3.0 m on average. They concluded that video images were a worthy complement to traditional beach survey, allowing the identification of morphologic changes that are not evident in survey data.

In most of the Spanish cases the evaluation of the nourishment evolution is based on topographic and/or bathymetric surveys carried out weeks, months or years after the replenishment. However, it is obvious that a number of short-term processes cannot be identified under this sampling strategy. For this reason, the objective of this chapter is to evaluate the beach nourishment carried out along Barcelona city beaches in June-July 2002 using daily images obtained by video cameras. The analyzed period extends from June 2002 (two weeks before the nourishment) to December 2003, when the shape of the shoreline was similar to the pre-nourishment one.

4.2. STUDY AREA

The Catalan coast (Western Mediterranean) is a micro-tidal zone (tidal range < 20 cm) where the mean H_s value (obtained from statistical analysis of the wave conditions from 1984 to 2004) is of 0.70 m, with H_s maxima of 4.61 m, maximum wave heights of 7.80 m and an averaged mean period of 4.29 s (Gómez *et al.*, 2005). Wave height in the region is characterized by a cyclic behaviour, with storm periods (October-April) separated by periods of minor storm activity (May-October). The most important storms are those from the east with a typical duration of few days and often associated with the cyclonic activity in the Western Mediterranean.

The waterfront of Barcelona city (NW Mediterranean) is divided into several sections with the Barcelona Harbour in its southern part followed by La Barceloneta and Somorrostro beach (separated by a double dyke), the Olympic Marina and several smaller beaches in the Northern side: Nova Icaria, Bogatell, Mar Bella and



Figure 4.1. Location of the study area.

Nova Mar Bella. This chapter is focused in two of the beaches – La Barceloneta and Bogatell – and their behaviour in response to the summer 2002 nourishment (Figure 4.1 and Table 4.1).

These beaches were created more than ten years ago from a previous degraded shoreline occupied by small industries, garages and industrial warehouses. As part of the 1992 renewal plan of the city’s waterfront, the distribution of more than 1 Mm³ of sand was undertaken. La Barceloneta beach was filled with 69000 and 139000 m³ of sand during 1991 and 1992, respectively and Bogatell beach was filled with 300000 and 88000 m³ of sand during years 1988 and 1992, respectively (MOPU, 1994). Therefore, the nourishment considered herein follows 10 years with no significant delivery of sand.

Table 4.1. Main features of the study beaches.

Beach	Length	Orientation	Volume of sand nourished in 2002
La Barceloneta	1100 m	N20°E	39539 m ³
Bogatell	600 m	N38°E	71282 m ³

4.3. METHODOLOGY

The morphologic changes produced by the nourishment were monitored using an Argus video system (Holman and Stanley, 2007) located atop a building close to the Olympic Marina at around 142 m high (Figure 4.1). This Argus station is part of the Coastal Monitoring Station of Barcelona and is composed of five cameras pointing at the beaches and offering a 180° view of the coast. In order to obtain quantitative data from the images the distorted 2D screen coordinates were rectified to real-world coordinates. The extraction of the shoreline location from the images will then allow the derivation of shoreline mobility data and emerged beach area time series that will be used to assess the evolution of the beach nourishment.

Given that the number of images and information generated by the system is large, a selection of the images was used in this study with a time lapse between images varying from one to 15 days depending on the wave energy and the proximity in time to the nourishment. Animations of the daily images were also produced to visualize, in a fast way, the important incidents occurring on the beaches, allowing the in-depth study of the relevant episodes.

Errors due to sea level variations and to the analysis process itself (to the way the shorelines were obtained) were minimized by analyzing more than one shoreline per day and using, instead of single shoreline position, the average of the daily values. In total, 173 shorelines of Barceloneta beach and 156 shorelines of Bogatell beach were measured, corresponding to 77 and 84 sample days respectively.

Once all the shoreline positions were obtained, beach mobility information and area variability were derived. Due to the hard structures limiting the back and lateral part of the beaches, the emerged beach area data were easily obtained. A software program was implemented which reduced to a mean the daily values of the shoreline and calculated beach area values. Since the extremities of the beaches were not always clearly visible, the program included the elongation of the beach limits by fitting the last plotted positions to a line and expanding the line to the lateral limit of the beach.

Beach behaviour was analyzed through the evolution of the shoreline position and the beach area. To facilitate the observation of the changes in the shoreline mobility, a series of cross-shore transect -with a distance between consecutive transects of 100 m at La Barceloneta and 50 m at Bogatell- was tracked along each

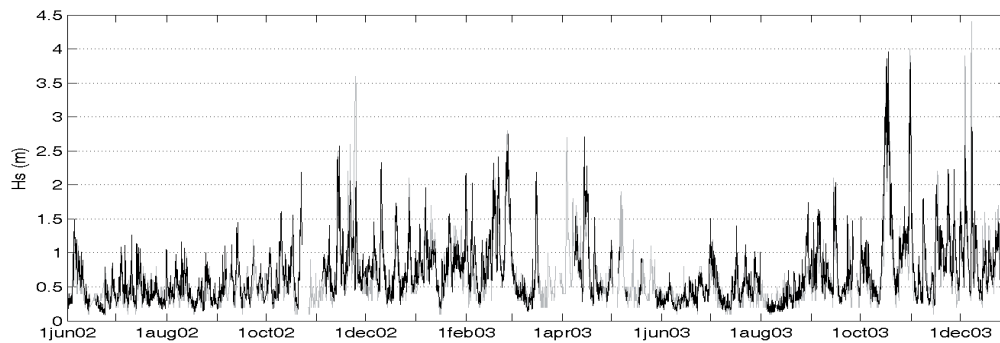


Figure 4.2. Significant wave height measured near Barcelona city during the study period.

of the beaches. The farthest transects in the south part of La Barceloneta beach (<100 m) are not included in the figure due to their high variability.

Wave height data was obtained from the Generalitat de Catalunya scalar buoy located off the Llobregat River (south of the study area). The measurements were taken on an hourly basis with maximum time gaps in the series in March and May 2003. The interruptions of the wave data were solved using data taken from WANA model data set (Spanish Port Authority) and also the Argus images of these days were analyzed in order to check the important events occurring during these periods. The most important storms in terms of H_s were those of mid and late October 2003; the former with ESE direction and H_s almost reaching 4 m and the later with S direction and $H_s > 3.5$ m (Figure 4.2).

4.4. RESULTS

4.4.1. DESCRIPTION OF THE NOURISHMENT

As has been previously seen, from October 2001 to May 2002, a number of storms produced strong erosion in Barcelona city beaches. Since these beaches receive large amounts of users each year, most of them during the summer season (Guillén *et al.*, 2008), different social sectors requested urgent action on the beaches. In response to these demands, approximately 135000 m³ of sand were distributed along three of the city beaches (La Barceloneta, Bogatell and Mar Bella) during June and July 2002. The sand borrow area was located around 20 km northern of Barcelona city (Masnou and Arenys de Mar). The median grain size of the sand ranged between 0.45 and 0.9 mm and it was pumped to the emerged beach from a ship (Figure 4.3). Typically, the ship transported about 1000 m³ of sand from the borrow area to the filling area, carrying out 3-4 sediment discharges per day. The

Bogatell beach received 71282 m³ of sand in 22 days (between 13 June and 5 July 2002) and La Barceloneta beach 39539 m³ between 5 and 17 July 2002. Figure 4.3 shows the characteristic beach configuration immediately before and during the nourishment works.

The nourishment at La Barceloneta beach was only accomplished in the northernmost part of the beach where it caused a mean advance of approximately 13.6 m (Figure 4.4). The mean advance of Bogatell shoreline was 20 m with values ranging between 10 and 30 m along the whole beach (Figure 4.5). Considering that the nourished part of La Barceloneta was approximately 350 m long and that the length of the Bogatell beach is 600 m, the rate of sediment supplied was 113 and 118 m³/m of sand respectively. The increase in the beach area was 5000 m² at La Barceloneta and 12750 m² at Bogatell (Figure 4.6). Therefore, the volume of sand required for increasing the area of the beach 1 m² was 7.9 and 5.6 m³ at La Barceloneta and Bogatell, respectively and the mean sand volumes needed to increase 1 m the beach width along filled areas were of 2768 m³ and 3354 m³, respectively.

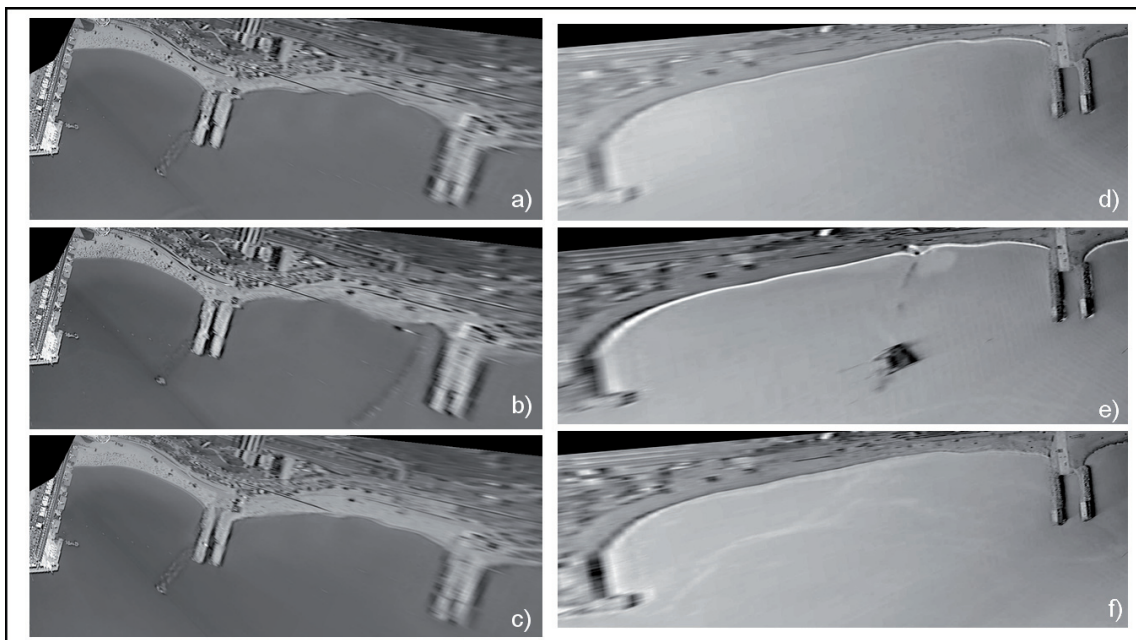


Figure 4.3. Plan views of the beaches in summer 2002. Bogatell beach a) before the initiation of the nourishment works on 12 June; b) during the nourishment, on 22 June, with the ship discharging sand, and c) the beach after the nourishment on 5 July. And La Barceloneta beach d) before the nourishment, on 3 July; e) during the nourishment, on 6 July, with the ship at its northernmost section; and f) the beach after the nourishment on 17 July.

4.4.2. BEACH EVOLUTION AFTER THE NOURISHMENT

4.4.2.1. Emerged beach

During the first weeks after the implementation of the nourishment both beaches readapted their plan shape to the new situations. This redistribution was more evident at Bogatell beach (see Figure 3.12), where the southern beach section retreated and the northern section advanced, but with no effect on the emerged beach area. The effect of individual storms was evident at both beaches, with clear cases of beach rotation, like Event G at La Barceloneta or Event L at Bogatell (refer to Table 2.2 for the characteristics of the storms events). However, the effects of these storm events were superimposed to the continuous area decrease that characterized the evolution of both beaches after the implementation of the nourishment (Figure 4.6).

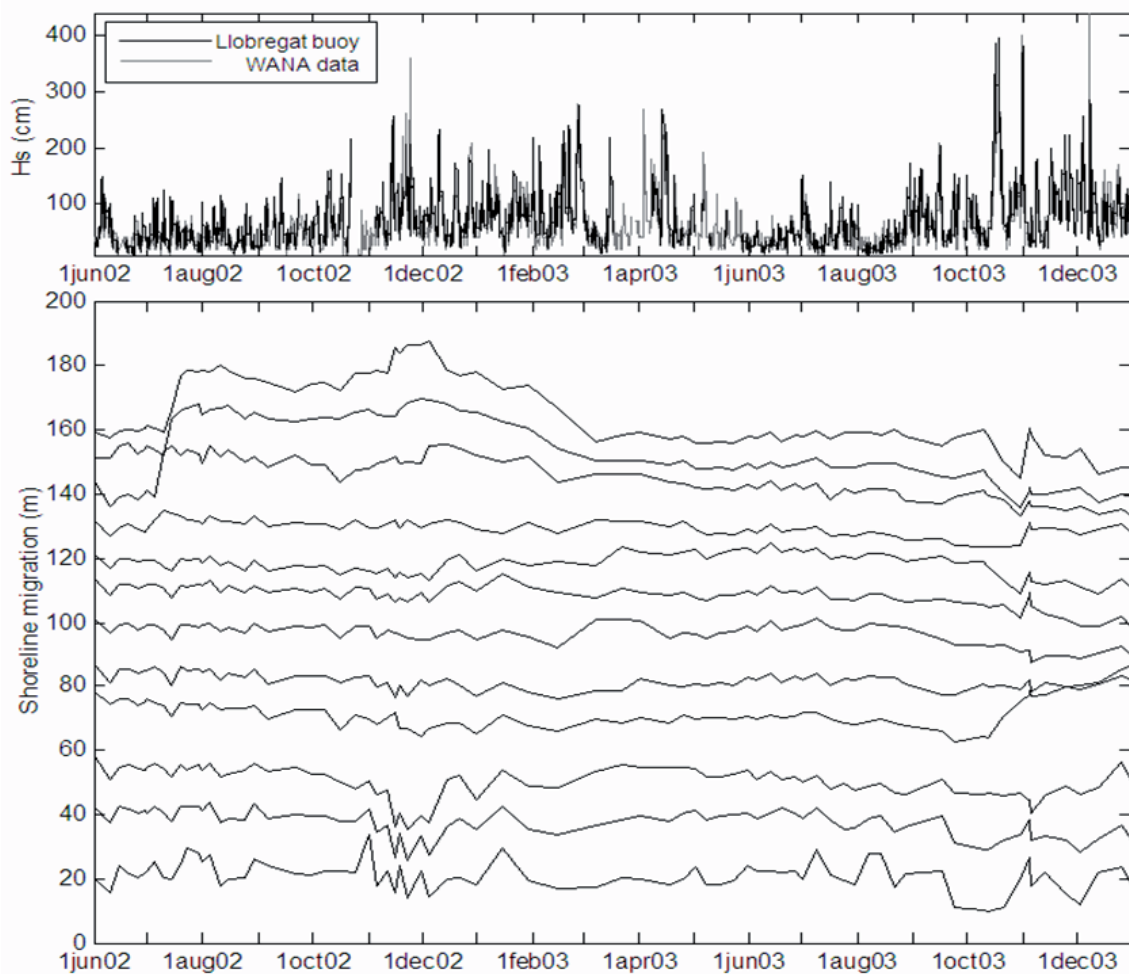


Figure 4.4. Shoreline evolution of La Barceloneta beach. Upper illustration: significant wave height. Lower illustration: time series of shoreline position changes along *control transects* in La Barceloneta (Y axis gives the variation along the transect in meters).

La Barceloneta showed a reduction in emerged beach area of approximately 23 m² per day between 1 August 2002 and 31 December 2003. As can be seen in Figure 3.10, most of the eroded sand from the nourished area did not continue on the emerged beach and was incorporated in the dynamics of the nearshore area. At this beach, approximately a year and a half after the nourishment (October 2003), the emerged beach area reached values lower than the ones before the nourishment was implemented.

The implications of the Bogatell beach nourishment in the beach width and area can be observed in Figures 4.5 and 4.6. The variability of the beach area at Bogatell was not as high as at La Barceloneta. As has been already mentioned, after the nourishment the sand was partially relocated, but with no effect on the beach area as it was only a readjustment of the beach shape. It was at the beginning of September

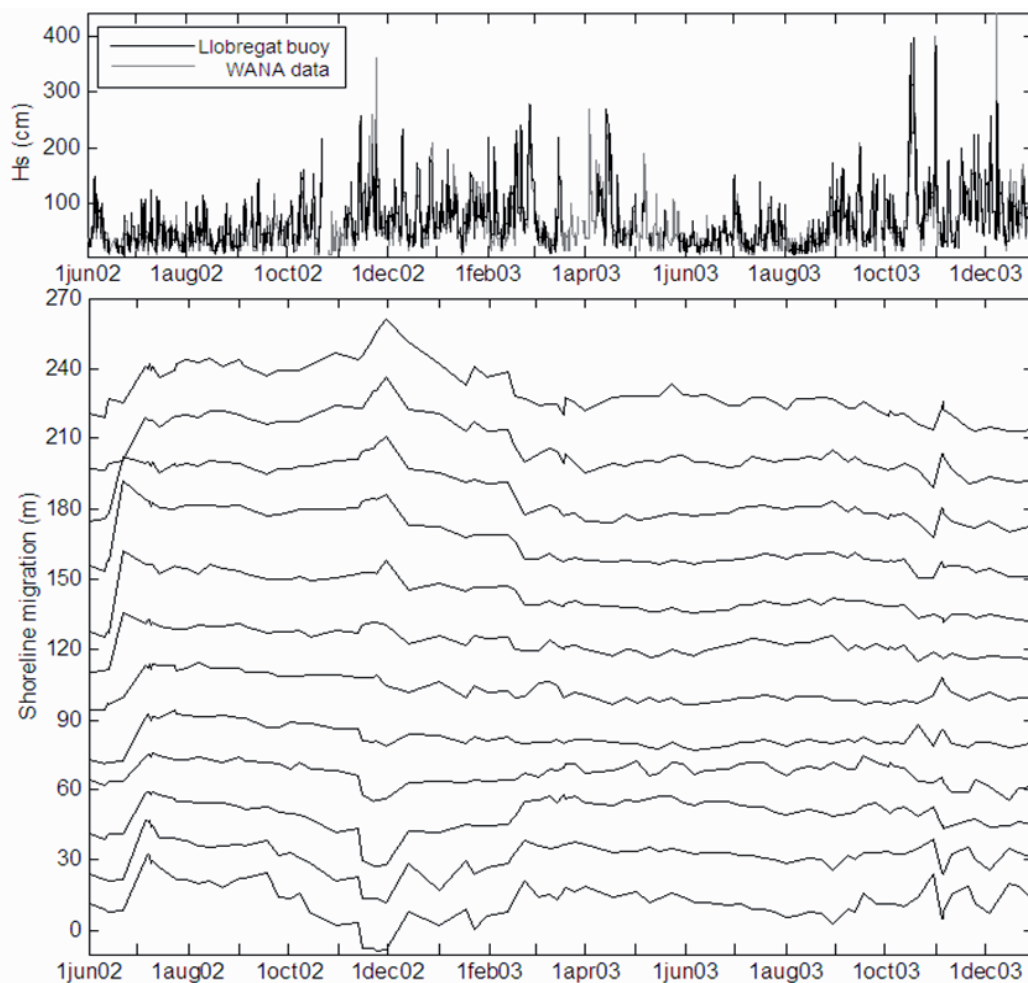


Figure 4.5. Shoreline evolution of Bogatell beach. Upper illustration: significant wave height. Lower illustration: time series of shoreline position changes along *control transects* in Bogatell (Y axis gives the variation along the transect in meters)

2002 when the beach area started to decrease with a rate of beach area loss of 17 m² per day (calculated for the period 1 August 2002 to 31 December 2003). The beach area became more stable from April to September 2003, corresponding with the lower wave energy period, but after this period the beach negative trend resumed. By the end of 2003 the beach area reached stable conditions that maintained in the following years as has been already seen in Chapter 2.

4.4.2.2. Submerged sandbars

The dynamics of the nearshore region after these nourishments changed, mainly, in the emerged beach, but it also affected the submerged sandbars. Before the implementation of the nourishment both sandbars (at La Barceloneta and Bogatell) were tracked on May 2002. At that moment, the sandbar of La Barceloneta had its northern section located close to the beach and, in fact, the nourishment buried that bar section. At Bogatell the bar was closer to the beach in the northern section but it did not seem to be covered by the nourishment.

A slight wave breaking pattern denoted the presence of the bar (excluding the northern section) at La Barceloneta on December 2002. After the erosion of the nourishment, related to the minor storm events occurring on February 2003, the northern bar section was newly formed and, several days later (during Event H,

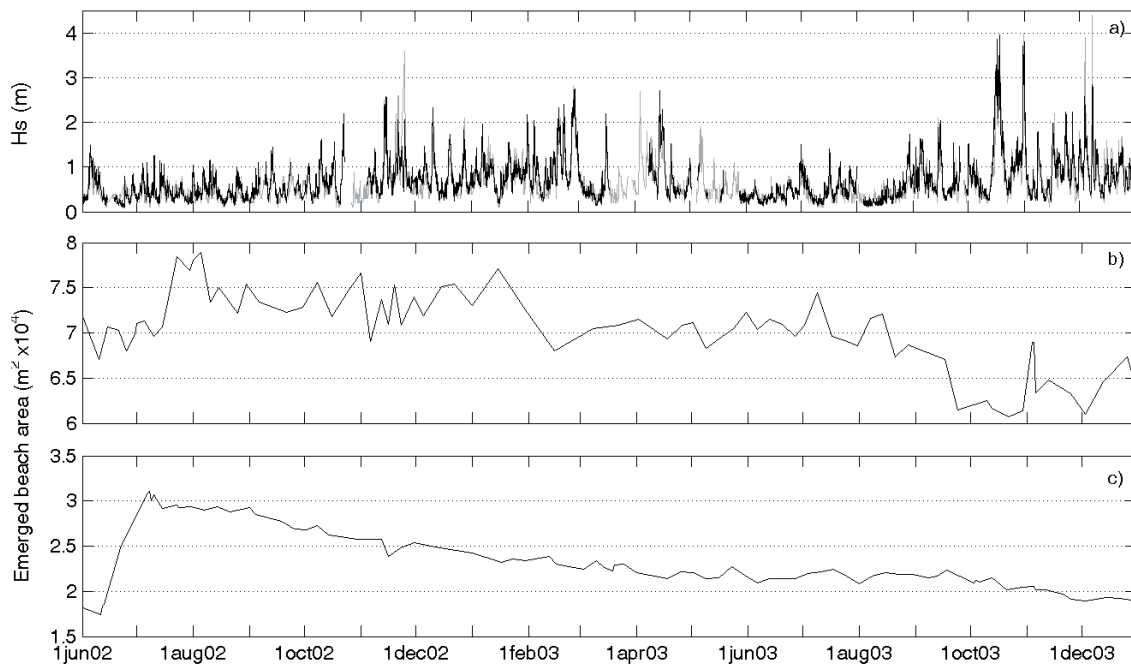


Figure 4.6. Emerged beach area evolution of La Barceloneta and Bogatell beaches. a) significant wave height, b) time series of La Barceloneta emerged beach areas, and c) time series of Bogatell emerged beach areas.

also on February 2003) the bar increased its sinuosity (see Figures 3.9 and 3.10).

At Bogatell, some months before the nourishment (May 2002) the sandbar was a developed crescentic bar located far from the shoreline (Figure 3.12). Due to the low-energy wave conditions, the sandbar was not visible again until several months after the nourishment (December 2002); during some minor storms that had place before December 2002 only the sections of the crescentic bar attached to the shore were visible. Then on December 2002 the bar appeared rectilinear and close to the shoreline and, after the February 2003 storms, the bar became crescentic.

4.5. DISCUSSION

Beach nourishments performed along the Spanish Mediterranean coast are usually designed for combating beach erosion in a medium-term perspective (Lechuga, 2003; Galofre *et al.*, 2004). For instance, Escartin *et al.* (2003) studied the evolution of a sand nourishment of 3.8 Mm³ along the Maresme coast (North of Barcelona). They reported a sediment loss of approximately 47000 m³ on the 10 months following the nourishment and that in 7 years 13% of the initial material had left the system due to alongshore and cross-shore transport, meaning that the volume of sand disappearing of the system was approximately 500 000 m³ (less than 15% of the filled sediment).

However, the nourishment carried out in Barcelona in the summer 2002 had some special characteristics because it was an urgent action undertook to restore the subaerial beach before the tourist season rather than a typical nourishment project. From a tourism-economical perspective, the 2002 nourishment saved the summer tourist season of Barcelona beaches, although from a coastal management point of view their positive effects only were detected for a short period of time. In contrast, the nourishment that was implemented in the city beaches during the period 1988-1992 allowed these beaches to remain useful for ten years. The main difference between those nourishments and the sand filling of 2002 is the amount of sediment supplied, which was one order of magnitude higher in the first one. Consequently, the results suggest that the future design of beach nourishments in Barcelona beaches should include a volume of sand significantly higher than the volume used in the 2002 nourishment in order to achieve convenient beach behaviour in a medium term perspective (several years).

Detle *et al.* (1994) established that expanding the interval between consecutive replenishment implies a rapid increase in the required annual volume of sand; maybe this is also an additional important factor to take into account in the studied case; the possibility of performing minor regular nourishments as an alternative to the ten-year interruption of the beach management response. This idea is in accordance with the Muñoz-Pérez *et al.* (2001) study on reef-protected beaches, where small yearly nourishments similar to the yearly losses are recommended with the intention of attaining economic saving and a better use of the natural resources.

Beach evolution of Barcelona city beaches during the study period shows that the emerged beach area at La Barceloneta on December 2003 was inferior to the pre-nourishment situation, while Bogatell had gain some 2000 m² of beach, suggesting that this beach tends to reach an equilibrium shape. After the nourishment, both beaches experienced almost continuous area reduction for several months, suggesting a strong disequilibrium of the beach that was compensated by the erosion. In fact, the shoreline retreat –represented by losses of subaerial beach surface– was not triggered by a strong storm, but it started almost immediately after the nourishment was accomplished in both beaches and it remained continuous –although with different rates– until the beach reached a configuration similar to the pre-nourishment one. Changes in the shoreline shape associated with storm effects seem to be superimposed on the general trend of subaerial beach losses associated with the beach evolution toward some equilibrium shape. The erosion of the beach nourishment was a fast process, since 100% of the filled sand was lost approximately one year and a half after the nourishment.

Apparently, part of the eroded sediment was transported offshore and stored at a certain depth in the submerged sandbars, as suggested by the increase of the bar sinuosity after February 2003. However, there are evidences that suggest that part of the eroded sediment might have also been transported alongshore bypassing the perpendicular groins. Although, these are supposed to be closed beaches (individual cells), a detailed exam of the time-series of Nova Icaria emerged area (refer to Figure 2.8c) shows a certain relation with the time-series of Bogatell beach area. After the decrease in the beach area generated by Events A and B at Nova Icaria, the beach area remained almost unchanged for almost a year, under different wave conditions. Then, the area of Nova Icaria beach increased with no obvious reason (this beach has not been nourished since its creation). Comparing

the time-series of the emerged area of Bogatell and Nova Icaria (Figure 2.8 b and c), it can be seen that Nova Icaria beach showed an increase in area simultaneously with the decrease of Bogatell beach area, some two months after the nourishment. An increase-decrease trend interrupted by the November 2003 storm. This indicates a probable communication between Nova Icaria and Bogatell beaches, as suggested by previous work done with tracers on these beaches (MOPU, 1994). Other evidences that support this sand by-passing can be appreciated in some of the Argus images corresponding to stormy days when the location of the Bogatell sand bar is oblique to the beach, with the southern end reaching the tip of the dike (for instance, see Figure 4.7). Moreover, in some conditions sediment patches can be observed offshore of the dikes. The sand by-passing between both beaches would imply an active alongshore sediment transport deeper than 7 m.

4.6. CONCLUSIONS

The nourishment of Barcelona beaches carried out in summer 2002 was only effective from a very short-term perspective, given that the shoreline configuration was similar to the pre-nourishment situation approximately one year and a half after it. The limited amount of sand used in the filling and probably the generation of a beach profile strongly in disequilibrium with morphodynamic conditions during the nourishment works were the main reasons for this fast erosive response.

The evolution of the shoreline location after the nourishment corresponds to beach area loss of 23 and 18 m²/day at La Barceloneta and Bogatell beaches, respectively. This implies an approximate volume loss between 103 and 174 m³/day in both beaches until an equilibrium configuration was reached. Bogatell showed an erosive trend after the nourishment during approximately a year and a half, until the beach reached a stable area that maintained almost constant for the following

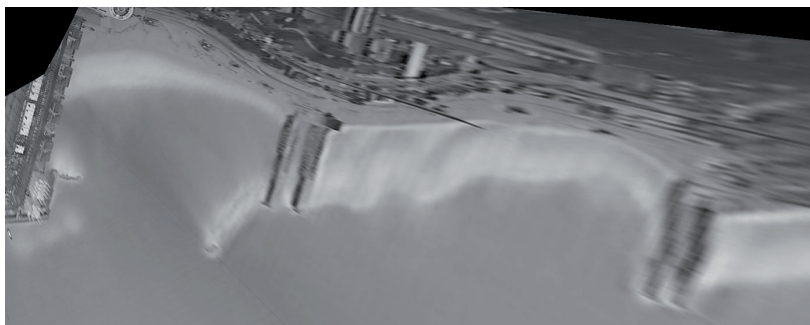


Figure 4.7. Planview of Bogatell beach on 17 October 2003.

years (as has been seen in the previous chapters). Contrastingly, the erosive trend of La Barceloneta did not seem to reach a stable state, not even during the following years that have been analyzed in the previous chapters, so the eroding trend had to be newly alleviated with other human interventions (the sand relocation undertaken in June 2004 and posterior beach nourishments after the study period covered in this thesis).

Maximum erosion of the beaches was not directly related to the strongest storms, but depended on the time elapsed since the nourishment and the wave approach direction. Changes in beach area related to storms were superimposed on the general decreasing trend. The nourishment also affected the submerged sandbars, particularly at La Barceloneta where the northern bar section was buried and the erosion of the new supplied sand induced an increase of the sinuosity of the bar. Moreover, the results suggest that Barcelona's embayed beaches are not isolated sedimentary systems but are affected by headland bypassing.

The example of Barcelona city beaches shows that the beach nourishment evolution can be successfully analyzed using video monitoring techniques, an easy, low-cost technique that allows an increase in sampling frequency, which gives the opportunity of a detailed analysis of the beach behaviour identifying relevant events and their effect on the coast evolution.

5 Morphodynamic response of an open beach to a shoreface nourishment

Edited version of E. Ojeda, B.G. Ruessink, and J. Guillén, 2008. Morphodynamic response of a two-barred beach to a shoreface nourishment. *Coastal Engineering* 55, 1185-1196.

5.1. INTRODUCTION

The use of nourishments in the coastal area has received considerable attention in the last few decades as an alternative to hard engineering solutions (Hamm *et al.*, 2002). The objectives of these so-called soft interventions are diverse and can include beach protection, maintenance of a specific beach area for tourist purposes, or protection of onshore locations against flooding. The location of nourishments ranges from the subaerial (i.e. on the beach or at the dune face) to the subaqueous (i.e. on the shoreface) part of the profile. Along the Dutch coast, for example, shoreface nourishments, introduced in the 1990s through the NOURTEC project (Hoekstra *et al.*, 1994), are common practice nowadays (Hamm *et al.*, 2002), with a yearly volume of nourished sand of about 8 Mm³. Although shoreface nourishments are thus an increasingly interesting option for coastal managers, their design is often highly empirical. The anticipated functioning of shoreface nourishments is based on lee and feeder effects to increase the amount of sand shoreward of the nourishment. The lee effect refers to the ability of the nourishment to increase wave dissipation with a corresponding shoreward reduction in alongshore flow and sediment transport, resulting in deposition shoreward of the nourishment. While the lee effect thus implies the capture of sand from alongshore, the feeder effects refers to the onshore movement of nourished sand itself by wave non-linearity and slow onshore currents inherent to cell-circulation patterns induced by the nourishment (e.g., Van Duin *et al.*, 2004; Grunnet and Ruessink, 2005; Van Leeuwen *et al.*, 2007). Although shoreface nourishments are a large morphological perturbation to a nearshore zone, their effect on natural morphological features, such as sandbars, is not well documented. A better understanding of the way a

shoreface nourishment interacts with autonomous sandbar behaviour may help to reduce the degree of empiricism in nourishment design.

Shoreface nourishments have been carried out at locations in the Netherlands, Belgium, Germany and the USA (see Grunnet, 2004 for an overview and references), but information about the later evolution of these systems is scarce in the literature. Two of the most studied cases are those of Terschelling and Egmond, both in the Netherlands. During the Terschelling-based NOURTEC project, the sand was nourished between two subtidal bars. Grunnet and Ruessink (2005) detail how this nourishment halted the autonomous net offshore migration of the sandbars described in Ruessink and Kroon (1994) for a period of 6 to 7 years. In addition, Grunnet and Ruessink (2005) noted how the nourished sand moved onshore during the first winter season to heighten the shoreward-located sandbar (the feeder effect). Subsequently, the higher-than-usual bar started to interrupt the natural littoral drift (the lee effect), which resulted in a substantial increase in beach width. Also, this bar broke up into several parts. The increased three-dimensionality in the sandbars and the associated offshore-flowing rip currents can be considered as a drawback of shoreface nourishment because they threaten the safety of tourists. Van Duin *et al.* (2004) documented the fate of the Egmond nourishment, implemented as a hump seaward of the outer sandbar. The nourishment maintained its cross-shore position while becoming increasingly subdued. As at Terschelling, it also halted the autonomous net offshore migration of the sandbars, in this case for a 2-year period only. In contrast to the Terschelling nourishment, the Egmond nourishment did not result in an increase in beach width. Neither Van Duin *et al.* (2004) nor Grunnet and Ruessink (2005) specifically analyzed the effects of the nourishment on the location of the sandbars in adjacent coastal stretches. However, such effects are a real possibility. Furthermore, both studies were based on relatively sparse (in time) in-situ surveys, so the timing of specific morphologic changes and their relationship to the offshore wave forcing could not be documented.

In this work we use almost six years of daily video images from the nearshore area of Noordwijk, the Netherlands, following the implementation of a shoreface nourishment seaward of a double sandbar system. The images not only include the nourishment area but also extend another 1.5 km on both sides of the nourishment. With these images and a number of topographic and bathymetric surveys, we analyze the effect of this nourishment on the sandbars and the shoreline location. The sandbar behaviour following the nourishment is contrasted with

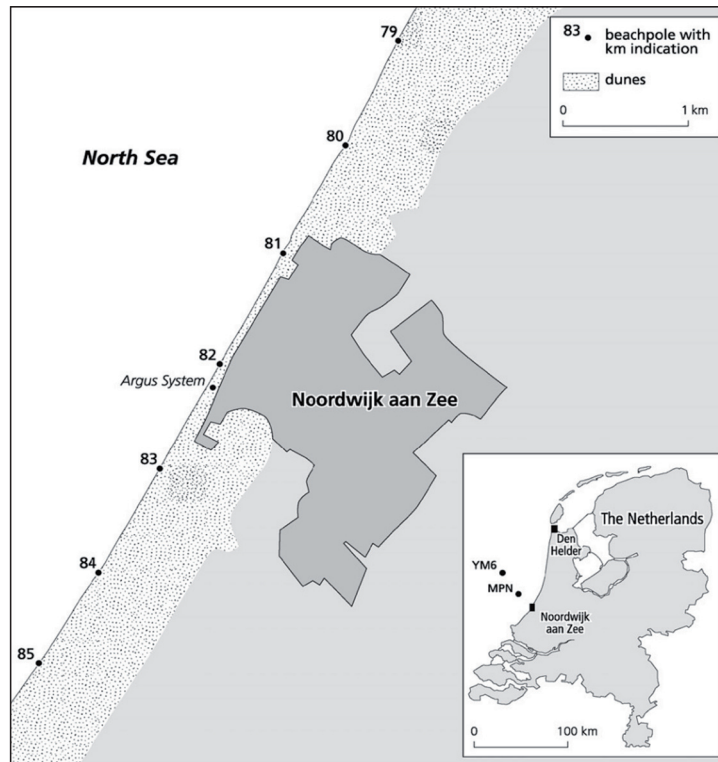


Figure 5.1. Study region with the location of the Argus station. Beach poles indicate distance in kilometres from a regional zero. Beach pole 82 corresponds to $y = 0$.

the autonomous sandbar behaviour, as analyzed earlier for this site from annual surveys (Wijnberg and Terwindt, 1995) and daily video images (Van Enckevort and Ruessink, 2003a,b). In addition, we compare our Noordwijk results with those reported for the other shoreface nourishments at Terschelling and Egmond.

5.2. FIELD SITE DESCRIPTION

Noordwijk is located along the approximately 120 km-long, inlet-free central Dutch coast (Figure 5.1). The overall slope of the nearshore is about 1:150, with a somewhat steeper intertidal beach (typically 1:30). The median grain size of the sediment across the coastal profile shows a seaward fining trend from the beach ($D_{50} = 250 \mu\text{m}$) to a distance of around 600 m (water depth -4 to -5 m, $D_{50} = 150 \mu\text{m}$), then the sediment progressively coarsens up to a distance of 800 m ($D_{50} = 300 \mu\text{m}$) and, finally, it displays a fining trend seaward (Wijnberg, 2002). Thus, the median sediment grain size of the native sediment in the area affected by the shoreface nourishment was about $250 \mu\text{m}$. The nearshore morphology is characterized by two subtidal bars (Van Enckevort and Ruessink, 2003a) extending to about 600 m from the shore, and one intertidal bar (Quartel *et al.*, 2007). While the intertidal bar has a lifetime of several weeks to months (Quartel *et al.*, 2007), the subtidal bars

are multi-annual features whose interannual behaviour prior to the nourishment was similar to that described for many other sandy coasts (Shand *et al.*, 1999): (1) generation near the shore, (2) net offshore migration through the surfzone, and (3) decay. The decay triggers the birth of a new bar (1) and the net offshore migration of the now new outer bar (2). At Noordwijk the time span between successive decays is about 4 years (Wijnberg and Terwindt, 1995). Occasionally, a sandbar may be in different phases alongshore. This causes it to break up, with one part decaying and the other part becoming attached to a landward-located bar (Figure 5.2). This morphological pattern, referred to as bar switching by Shand *et al.* (1999), is not unlike the bifurcations that are often seen in wave ripples.

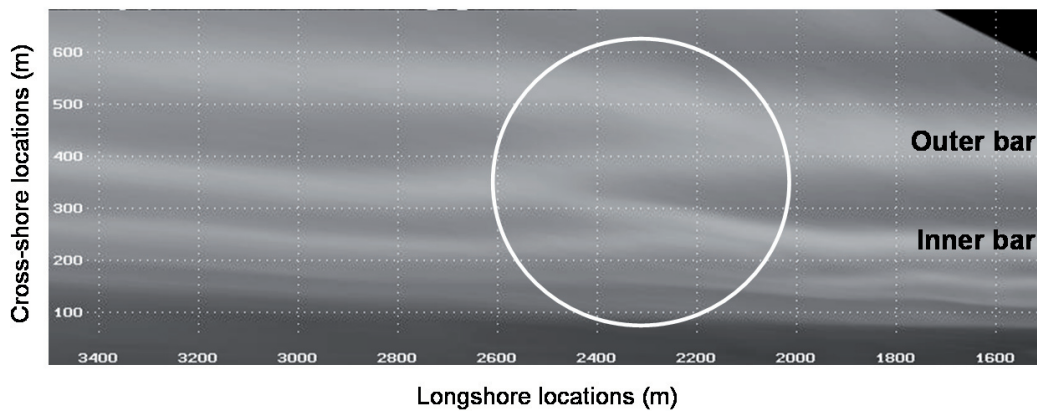


Figure 5.2. Example of bar switch. The image corresponds to the area around beach pole 84 ($y = 2000$ in local coordinates) on 6th November, 1996 (Adapted from Van Enckevort, 2001).

From February to March 1998, a 1.7 Mm^3 nourishment was placed at a depth of 5 to 8 m over an approximately 3 km-wide (alongshore) area (km 80.5 - 83.5 in Figure 5.1), roughly 900 m from the shore (Spanhoff *et al.*, 2005). This corresponds to about $570 \text{ m}^3/\text{m}$ of dumped material. As can be seen in Figure 5.3, the nourishment was implemented as a hump rather than spread out evenly over the seaward side of the outer bar. Figure 5.4 shows a cross-shore profile of the first bathymetric survey where the nourishment can be distinguished (June 2000), with the inner ($x \approx 300 \text{ m}$) and the outer ($x \approx 500 \text{ m}$) bars, and the nourishment located around position $x = 800 \text{ m}$. With a median grain size of $400 \mu\text{m}$, the nourished sediment was substantially coarser than the original sediments.

The yearly averaged offshore ($\sim 18\text{m}$ depth) significant wave height is about 1 m, with a corresponding period ($T_{1/3}$) of 6 s. Predominantly during north-westerly storms the wave height may reach about 5 m, with periods of 8 to 12 s. The tide

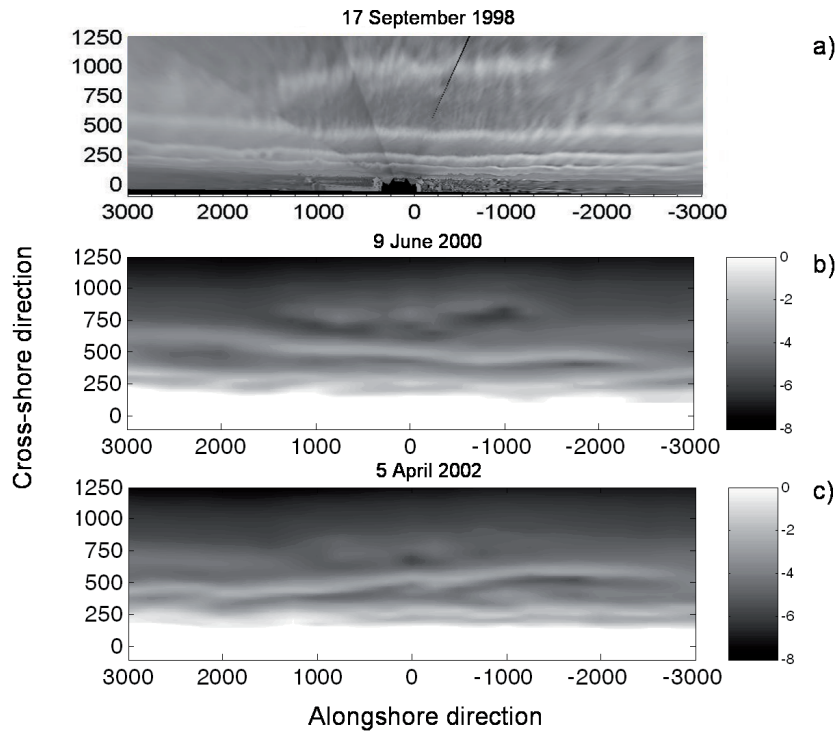


Figure 5.3. a) First Argus image with the bumped region corresponding to the nourishment; b) Noordwijk bathymetry of the study area on 9th June 2000, the first one showing the bumped region formed by the nourishment, and c) 5th April 2002 bathymetry. Notice the differences in the bar configuration between b and c (decrease of bar trough depth). Alongshore distance, in local coordinates, corresponds to beach poles 79 (-3000) to 85 (3000).

is semi-diurnal with a range of about 1.4 m at neap tide and 1.8 m at spring tide. Storm surges typically reach values of up to 1 m.

5.3. METHODOLOGY

The study area was divided into three sections: the 3 km-long central section located just in front of the nourishment ($y = -1500$ to 1500 m, where y is the alongshore coordinate and $y = 0$ corresponds to beach pole 82 in Figure 5.1), and two 1.5 km stretches located south ($y = 1500$ to 3000 m) and north ($y = -1500$ to -3000 m) of the central section.

The data used to characterize the nearshore evolution at Noordwijk following the implementation of the nourishment comprise daily video images collected from mid-September 1998 to mid-July 2004, complemented with bathymetric and topographic surveys. Offshore wave conditions and tidal level fluctuations were obtained from the MPN platform located in front of the study site at 18 m depth (Figure 5.1).

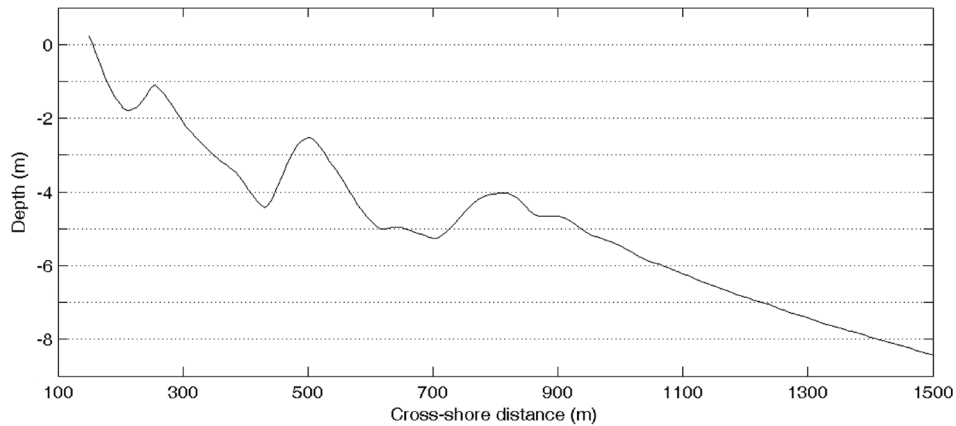


Figure 5.4. Cross-shore profile of the bathymetric survey performed on 9 June 2000. Alongshore location $y = 0$.

5.3.1 VIDEO IMAGERY

Argus video images (Holman and Stanley, 2007) of the nourishment region have been available since mid-September 1998 from an automated video station mounted on the roof of an approximately 60 m-high hotel. The basic premise behind using the video-imaging system to infer sandbar (and nourishment) characteristics, such as sandbar location, is the preferential wave breaking over shallow features. In time-exposure images a sandbar is seen as a breakerline (Lippmann and Holman, 1989; Van Enckevort and Ruessink, 2001), a high-intensity band in clear contrast to darker regions where waves do not break. Our data set consists of daily, low-tide images of five cameras merged and rectified on a 10×5 m grid (alongshore \times cross-shore) following the procedure outlined in Holland *et al.* (1997). Low-tide images were preferred over images at other tidal stages because of the more pronounced wave breaking during low tide. The rectified video images extend 1.35 km in the cross-shore direction to allow the complete observation of the hump formed by the nourishment and, as mentioned above, 6 km in the alongshore direction. The accuracy of the photogrammetric transformation from image to ground coordinates is typically one pixel. The worst resolution is found for the alongshore direction at the northern end of the study area, where one pixel corresponds to about 120 m alongshore; in the region in front of the nourishment the alongshore size of the pixel was lower than 30 m.

From each low-tide plan-view image with at least one alongshore breakerline, the “optical” crest lines of the inner and, if possible, the outer bar and the nourishment were extracted by the automated alongshore tracking of the intensity maxima

across each bar (Van Enckevort and Ruessink, 2001). The resulting lines were smoothed in the alongshore direction using a Hanning window with a 100 m half-width to remove noise due to pixel variability. Inaccurate barlines, for instance due to raindrops on one of the camera lenses, were eliminated from the data. Gaps in the video data are related to the absence of wave breaking over the bars and to technical problems in the data acquisition (predominantly in June-July 2003).

In total, our data set comprised 519 inner-bar, 417 outer-bar and 82 nourishment observations. For each bar and for the nourishment, a matrix $X(y, t)$ was constructed that contained bar crest cross-shore location, X , at times t and alongshore locations y . Each bar line was subsequently averaged over the extent of the entire study section to yield an alongshore-average sandbar or nourishment location $[Xy(t)]$.

Van Enckevort and Ruessink (2001) showed that time series of alongshore-average sandbar location contain artificial variability between the video-observed and the actual sandbar position because of tidal water level variations. Although our dataset was composed of images close to low tide, the tidal level in the different images varied during the study period by more than two metres. Following Pape *et al.* (2007), this artificial variability was reduced by projecting each alongshore-average sandbar position to a fixed water level (here, 0.5 m below mean tidal level), assuming that the artificial sandbar migration between two consecutive observations depends linearly on their water level difference.

The time series of the alongshore-average inner-bar, outer-bar and nourishment location were decomposed into an interannual $[Xia(t)]$, a seasonal $[Xs(t)]$ and a weekly $[Xw(t)]$ component; for computational details see Chapter 3. The seasonal component essentially encompasses the response of the sandbars to the seasonal variability in wave height (higher energy winter months versus lower energy summer months), while the weekly component contains the bar response to individual storms and to groups of storms and measurement noise. The relative importance of each component was quantified by its contribution to the total variance of the bar crest location and compared with the pre-nourishment situation.

Mean migration rates were determined from linear regression to the bar position time series $[Xy(t)]$ and, following van Enckevort and Ruessink (2003a), yearly-averaged migration rates were obtained as the temporal derivative of $Xia(t)$,

seasonal rates as the temporal derivative of $X_{ia}(t)+X_s(t)$, and weekly rates as the temporal derivative of the alongshore-averaged cross-shore position of the bar (i.e., $X_{ia}(t)+X_s(t)+X_w(t)$). Alongshore non-uniformities in the bars were quantified with the sinuosity, defined here as the relationship between the total length of the barline and the distance between its two ends following a straight line. As there are no long-term trends in the offshore wave height, changes in the sinuosity will be nourishment-induced.

5.3.2 IN SITU SURVEYS TO OBTAIN SHORELINE AND BATHYMETRIC DATA

Shorelines were extracted from four different sources with different spatial and temporal resolutions. Firstly, the decadal and centennial shoreline variability at Noordwijk was quantified from a data set of yearly low-water levels sampled with a 1 km resolution from 1843 to 1992, discussed earlier in Verhagen (1989) and Ruessink and Jeuken (2001). Secondly, annual to decadal variability was extracted for the period 1964–2003 using the annual surveys obtained in the framework of the JARKUS scheme (Wijnberg and Terwindt, 1995). The spacing of the cross-shore profiles in the JARKUS data set was 250 m. Thirdly, we used nine bathymetric surveys conducted after the nourishment (2000–2004) to monitor the “efficiency” of the nourishment for coastal safety. For each survey, the available data were interpolated using a quadratic loess filter (Plant *et al.*, 2002) to a regular grid with a cross-shore (alongshore) grid size of 5 (250) m. Finally, shorelines were extracted from dGPS surveys of a 1.5 km area in front of the nourishment from October 2001 to November 2004 on a monthly basis (see Quartel *et al.*, 2008 for details). In the second, third and fourth data source the shoreline was defined to be the low-tide level, around -0.76 m with respect to mean sea level. The alongshore length of the beach section from which the shorelines were quantified amount to 6 km for the first three data series ($y = -3000$ to 3000 m) and 1.5 km for the dGPS data ($y = -750$ to 750 m).

Quartel *et al.* (2008) found the temporal dunefoot (about 3 m above mean sea level) variability to be subordinate to the shoreline variability and to not display any interannual variability. Although dunes are an integral part of the active coastal system, the Noordwijk nourishment did not appear to interact with the dunes and, accordingly, we will not further consider the behaviour of the dunes in our work.

5.4. RESULTS

Firstly, the results focus on the subtidal bar system and describe the behaviour of the nourishment itself and the response of the bars in front of and to the north and south of the nourishment, in terms of both uniform and non-uniform alongshore behaviour. Secondly, they focus on shoreline response to the nourishment.

5.4.1. SANDBARS

5.4.1.1. Nourishment behaviour

The nourishment was implemented seaward of the outer bar between $y = -1500$ and 1500 , approximately 900 m from the shore forming an artificial bar with the crest of the bar at approximately 4 m depth (Figure 5.3a,b). The configuration was slightly tilted alongshore with the northern side in a more shoreward position. The nourishment was tracked in the Argus images for more than 3 years as an alongshore continuous breakerline that was separated from the outer bar by a distinct darker patch of non-breaking waves. Later on, the signal was less clear and less frequent. This suggests that the nourishment retained its bar shape during the first few years, and then became more subdued and finally faded away with time. The bathymetric surveys after the implementation of the nourishment confirm this pattern (Figure 5.3). Intriguingly, the location where the nourishment started to fade away (about 650 m offshore) is about the same as the location where, prior to the nourishment, the outer bar ceased to migrate offshore and started to decay (e.g., Van Enckevort and Ruessink, 2003a; Ruessink *et al.*, 2003).

During the study period, the nourishment migrated landward and approached the outer bar with a total advance of approximately 300 m, corresponding to a mean rate of 0.14 m/day (Figure 5.5). The time series of alongshore-averaged nourishment position shows periods without displacement or low migration rates alternating with periods of higher onshore migration (e.g. late 1998 to early 1999 or late 2001). The alongshore structure of the nourishment did not change notably during the study period either in the oblique orientation of the nourishment or in its alongshore location, as it did not appear to migrate alongshore at all. The onshore migration of the nourishment and its gradual fading highlights the intended feeder effect of the nourishment.

5.4.1.2. Bar section in front of the nourishment

The alongshore-averaged cross-shore positions of both the inner and outer bar in front of the nourishment are also shown in Figure 5.5, together with Van Enckevort and Ruessink (2003a) pre-nourishment data. The net migration of the bars during the 3.4 years prior to the nourishment was offshore, approximately 100 m for the outer bar and 60 m for the inner bar. In the 5.8-year period after the nourishment, the net migration was also offshore but only about 40 m for the outer bar and less than 20 m for the inner bar (Figure 5.5). The migration rates decreased after the implementation of the nourishment, from 0.09 to 0.02 m/day at the outer bar and from 0.05 to 0.01 m/day at the inner bar. In more detail, the overall offshore migration of the outer bar decelerated from mid-2000 and the inner bar, after a period of offshore migration, started to migrate onshore in 2001. It is obvious from Figure 5.5 that even after about 6 years the subtidal bars had not resumed their pre-nourishment, offshore-directed trend.

The role of interannual [$X_{ia}(t)$], seasonal [$X_s(t)$] and monthly [$X_w(t)$] fluctuations on the alongshore-averaged cross-shore position of both bars is presented in Figure 5.6. Although the seasonal fluctuations were greater in the outer bar, in neither of the two cases can a clear seasonal pattern be appreciated; there is only a slight trend (more evident during the first two years) to more offshore locations after winter and more onshore locations after summer. A comparison between

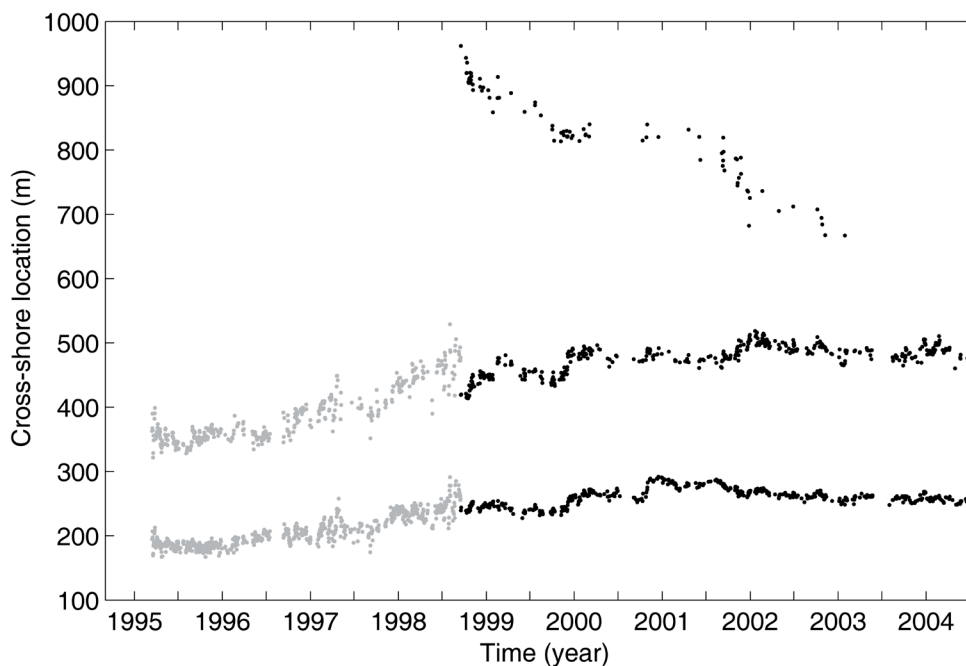


Figure 5.5. Alongshore-averaged cross-shore location for the nourishment and for the inner and outer bar in the central section. Grey: pre-nourishment data.

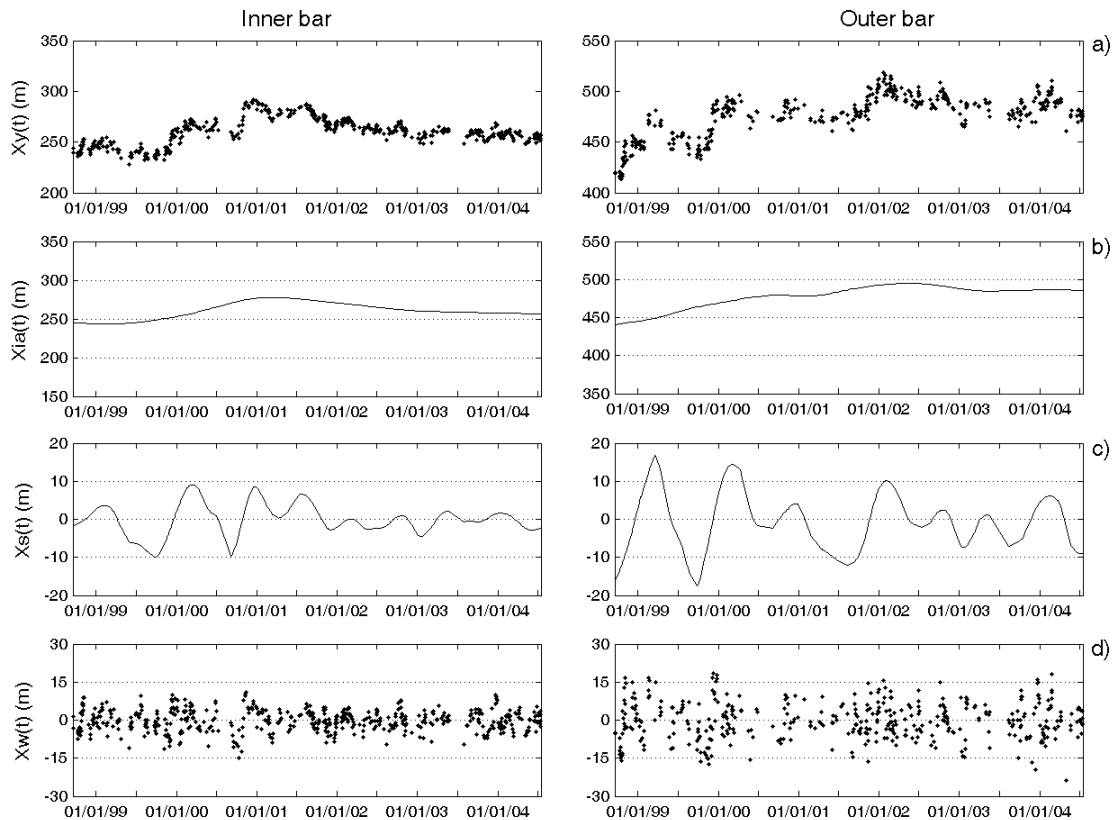


Figure 5.6. a) Inner and outer bar alongshore averaged cross-shore positions [$Xy(t)$] after the nourishment separated into b) yearly [$Xia(t)$], c) seasonal [$Xs(t)$] and d) weekly [$Xw(t)$] component.

yearly-averaged, seasonal, and weekly migration rates of the inner and outer bar for the pre- and the post-nourishment situations is presented in Table 5.1. After the nourishment, interannual migration rates were similar for both bars but, as expected under natural conditions, seasonal migration rates were higher for the outer than for the inner bar, and also higher in the offshore direction than in the onshore direction. In general, post-nourishment migration rates were lower than the equivalent pre-nourishment ones, with two exceptions: a) the inter-annual offshore migration rates of the inner bar, which remained constant, and b) the inter-annual onshore migration of both bars, which increased after the nourishment. On the whole, the nourishment appears to have stabilized the inner and outer bar.

During the pre-nourishment period, the interannual time scales dominated the migration of the bars contributing to 72 and 75% of the total variance of the inner and outer bar time series, respectively. The seasonal and weekly time scales explained 12 and 16% of the total variance at the inner bar and 13 and 12% at the outer bar. The total variance diminished in the post-nourishment period, as

Table 5.1. Cross-shore migration rates for the pre-nourishment (grey background) and post-nourishment situations.

	Offshore migration (m/day)			Onshore migration (m/day)		
	Weekly	Seasonal	Interannual	Weekly	Seasonal	Interannual
<i>Outer bar</i>						
Mean	8.16	0.16	0.08	7.47	0.15	0.00
	5.74	0.12	0.04	4.72	0.10	0.02
St. dev.	10.15	0.10	0.04	8.28	0.13	0.00
	4.74	0.10	0.02	4.14	0.07	0.01
<i>Inner bar</i>						
Mean	5.76	0.10	0.05	5.24	0.04	0.00
	2.79	0.07	0.05	1.98	0.06	0.02
St. dev.	5.58	0.08	0.02	4.80	0.06	0.00
	2.02	0.08	0.02	1.83	0.04	0.01

could be expected because of the arrest of the bars close to their pre-nourishment locations. In addition to the lower values, this arrest of the bars also caused the decrease of the dominance of the interannual component, with contributions of 62% (58%) of the total variance at the inner (outer) bar, and increases mostly in the seasonal component (22 and 23% at the inner and outer bar, respectively). Weekly time scales explained 16% (19%) at the inner (outer) bar.

In every situation the sinuosity values were higher for the inner bar than for the outer bar (Figure 5.7). The sinuosity at both bars slightly increased some years after the implementation of the nourishment (in mid-2000 in the outer bar and during the last third of 2001 in the inner bar).

However, the sinuosity time series at the inner bar flattened some months after the implementation of the nourishment; before the nourishment it was characterized by numerous, irregularly spaced (in time) peaks that disappeared in the post-nourishment situation as the maximum sinuosity values decreased. The slight increase in the sinuosity values in both bars together with the flattening of the sinuosity contour with the disappearance of the peaks at the inner bar do not imply an increase in the bars' three-dimensionality. Furthermore, the post-nourishment alongshore evolution of the inner and outer bar in the study area presented in Figure 5.8 (including the northern and southern flanks) corroborates this result. For instance, the aforementioned increase in the sinuosity of the inner bar in the region in front of the nourishment ($y = -1500$ to 1500 m) during the last third of 2001 can be detected by the appearance of crescentic shapes but does not imply a substantial change from the previous morphology.

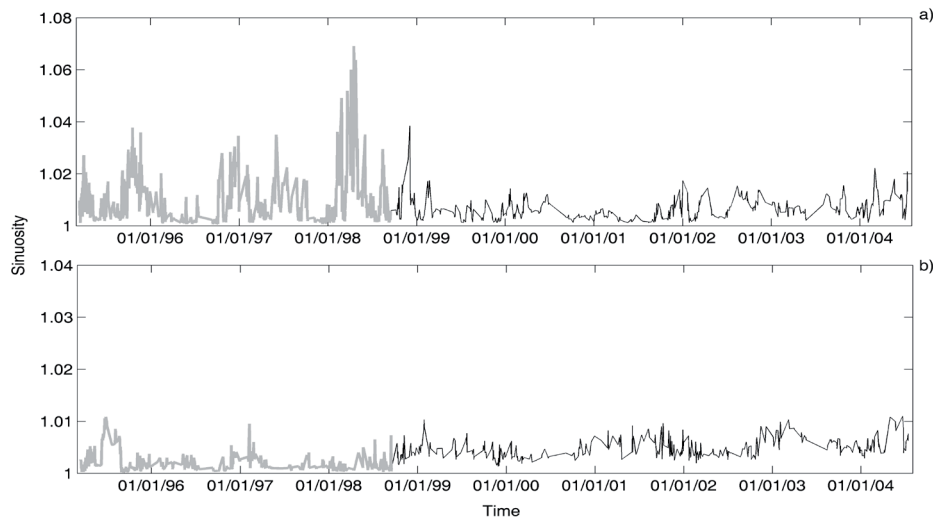


Figure 5.7. Sinuosity of the a) inner and b) outer bar at the 3-km central section for the pre-nourishment (grey line) and the post-nourishment (black line) situations. Note the different scales on the y-axis.

5.4.1.3. Bar sections on both sides of the nourishment

Besides the section in front of the nourishment, the study region also comprised 1.5 km of beach on each side of the nourishment. The analysis of the behaviour of the bar system located on the flanks allowed us to determine whether there was a difference between the section just shoreward of the nourishment and the flanks which could be attributed to the nourishment.

Figure 5.8 presents the barlines for the inner and outer bar stacked vertically with the y axis corresponding to the time. Colours indicate the cross-shore location of each barline and, therefore, different colours along the x axis indicate different cross-shore locations (crescentic shapes can be seen as alternations between warm and cold colours) and vertical changes (y axis) from warm to cold (cold to warm) indicate onshore (offshore) migrations. Both bars show differential alongshore behaviour with the flanks commonly located in more seaward locations than the section in front of the nourishment. On several occasions the seaward-located flanks maintained their locations for several months, as can be seen at the outer bar on the southern flank for two years (2000-2002) preceding an episode of bar switching that will be discussed below.

The net alongshore averaged cross-shore migration of the inner and outer bar was offshore, but of lower magnitude in the central section than on the flanks. The inner bar cross-shore migration varied from low offshore migration rates of 0.01

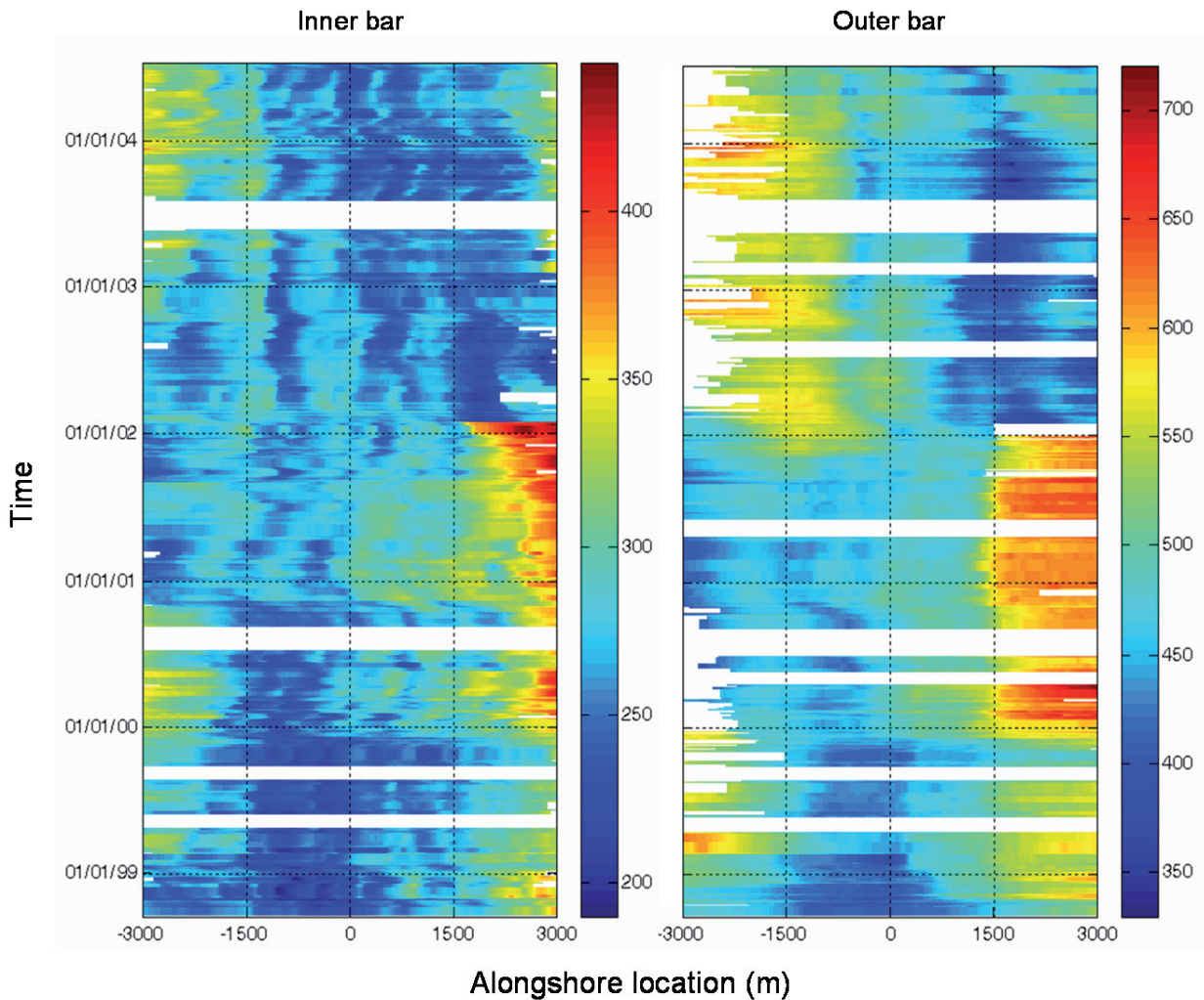


Figure 5.8. Inner and outer bar timestacks. Colours represents the cross-shore location (in metres) of the bar for each alongshore location and time. Blanks represent time gaps equal or longer than 30 days.

and 0.02 m/day in the region in front of the nourishment and on the northern flank, respectively, to higher offshore rates of 0.05 m/day in the southern region, where the offshore migration rates were equivalent to those before the implementation of the nourishment (Figure 5.9). Similarly, the offshore migration rates at the outer bar were lower in front of the nourishment (0.02 m/day) than on the northern side (0.05 m/day) and peaked in the southern region, with rates varying from 0.07 m/day before the switching episode to 0.05 m/day after it (Figure 5.9). In all three sections the offshore migrations occurred episodically related to high-energy wave conditions, when the root-mean-squared wave height (H_{rms}) exceeded 2.5 m, although not all the stormy episodes higher than this threshold showed offshore migration.

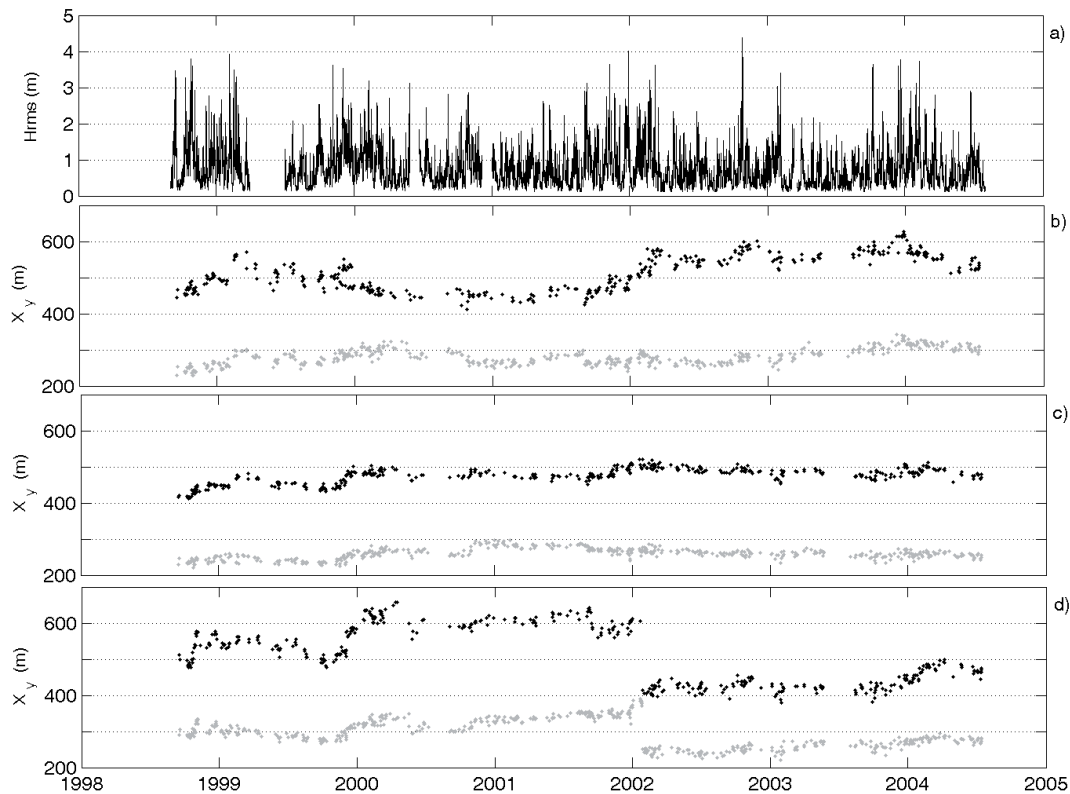


Figure 5.9. Time series of a) H_{rms} (m), and the cross-shore location of the inner (grey) and outer (black) bar on the b) northern, c) central and d) southern sections.

The arrest of the bars sheltered by the artificial nourishment in their pre-nourishment locations while the bar sections located on the flanks migrated offshore caused the bars on both sides of the nourished region to break up and become discontinuous. When this happened, the landward bar on one side of the discontinuity joined the more seaward bar on the other side; this realignment is known as a bar switching (Shand *et al.*, 1999).

Episodes of bar switching were observed on the northern and southern flank in winter 1999-2000 and 2001-2002, respectively. Figure 5.10 illustrates the northern episode, which took place beyond the limit of the study region. The seaward-migrating outer bar (Figure 5.10a; $y = -2075$ to -3725 m) separated around $y = -2300$ m (Figure 5.10b) and kept its offshore migration, while at the inner bar a forked configuration appeared and lasted for several months (Figure 5.10b,c; $y = -2075$ m). The separated section of the outer bar maintained its cross-shore location (Figure 5.10d, $x = 675$ m) and a new forked shape appeared, now joining the inner and outer bar ($y \sim -3175$ m). The southern outer bar realigned with the adjacent northern inner bar, which became discontinuous (Figure 5.10e; $y = -3175$ m). The

forked configuration of the inner bar reappeared at a different location (Figure 5.10f; $y \sim -3725$ m) and the final configuration is shown in Figure 5.10g.

The southern episode of bar switching (Figure 5.11) took place in a more localized region (approximately $y = 1300-1800$ m) and the realignment of the inner and outer bar occurred simultaneously. The southern section of outer bar was at an

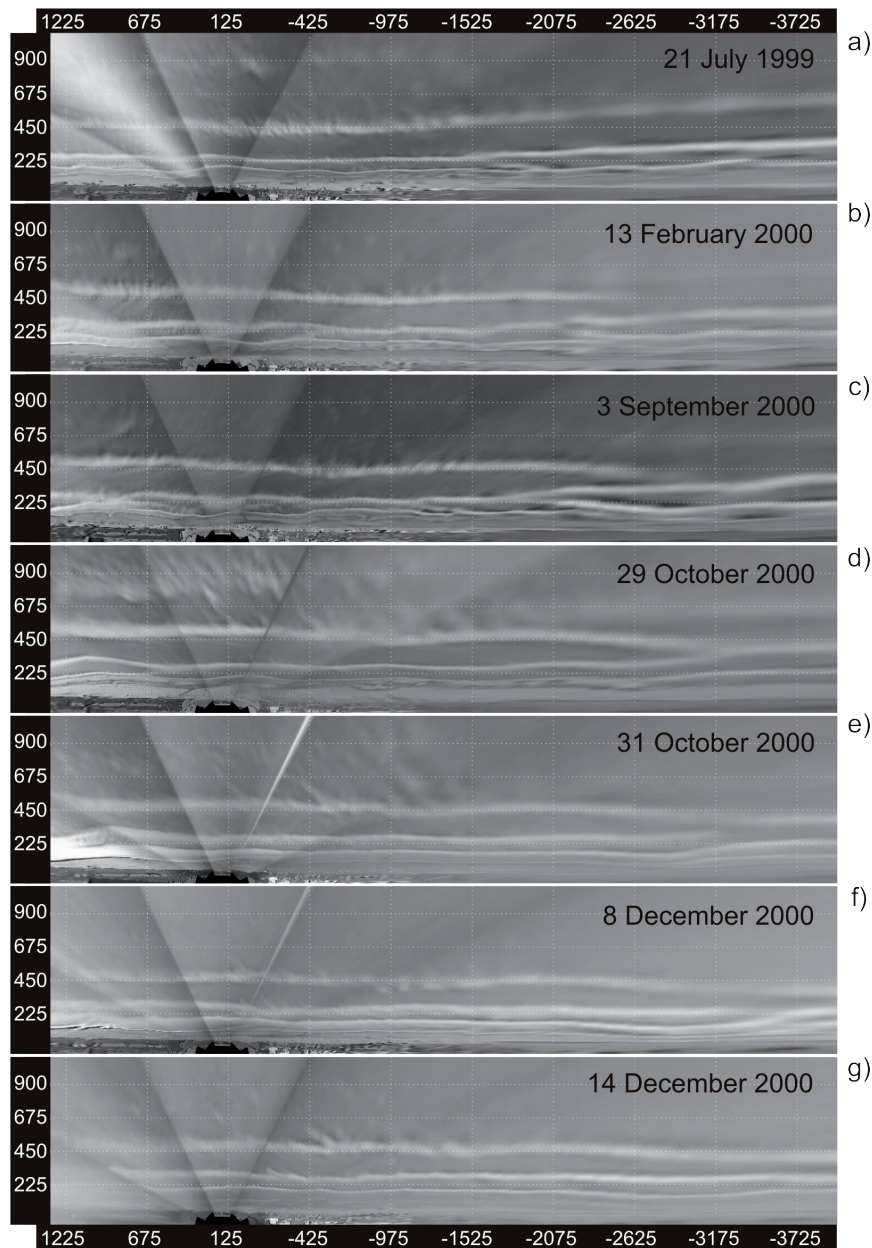


Figure 5.10. Bar switching episode northward of the study region. a) Situation before the bar became discontinuous, b) outer bar separated, c) forked shape formed between the inner and the intertidal bar, d) forked shape formed between the inner and the outer bar, e) outer bar joins the landward section of inner bar and inner bar become discontinuous, f) forked shape formed between the inner and the intertidal bar, g) inner bar switching.

offshore location for approximately 2 years before the switching (Figures 5.8 and 5.9). During this time, on occasions, the bars adopted a forked configuration (similar to the one shown in Figure 5.11d), but the realignment did not take place. Figure 5.11 shows the offshore migration of the outer bar (Figure 5.11b) and the inner bar (Figure 5.11c), the appearance of the forked morphology (Figure 5.11 d) and the new arrangement of the two bars (Figure 5.11e-f).

The northern bar switching took more time to complete than the southern bar switching (Figures 5.10 and 5.11), possibly because of the more energetic wave

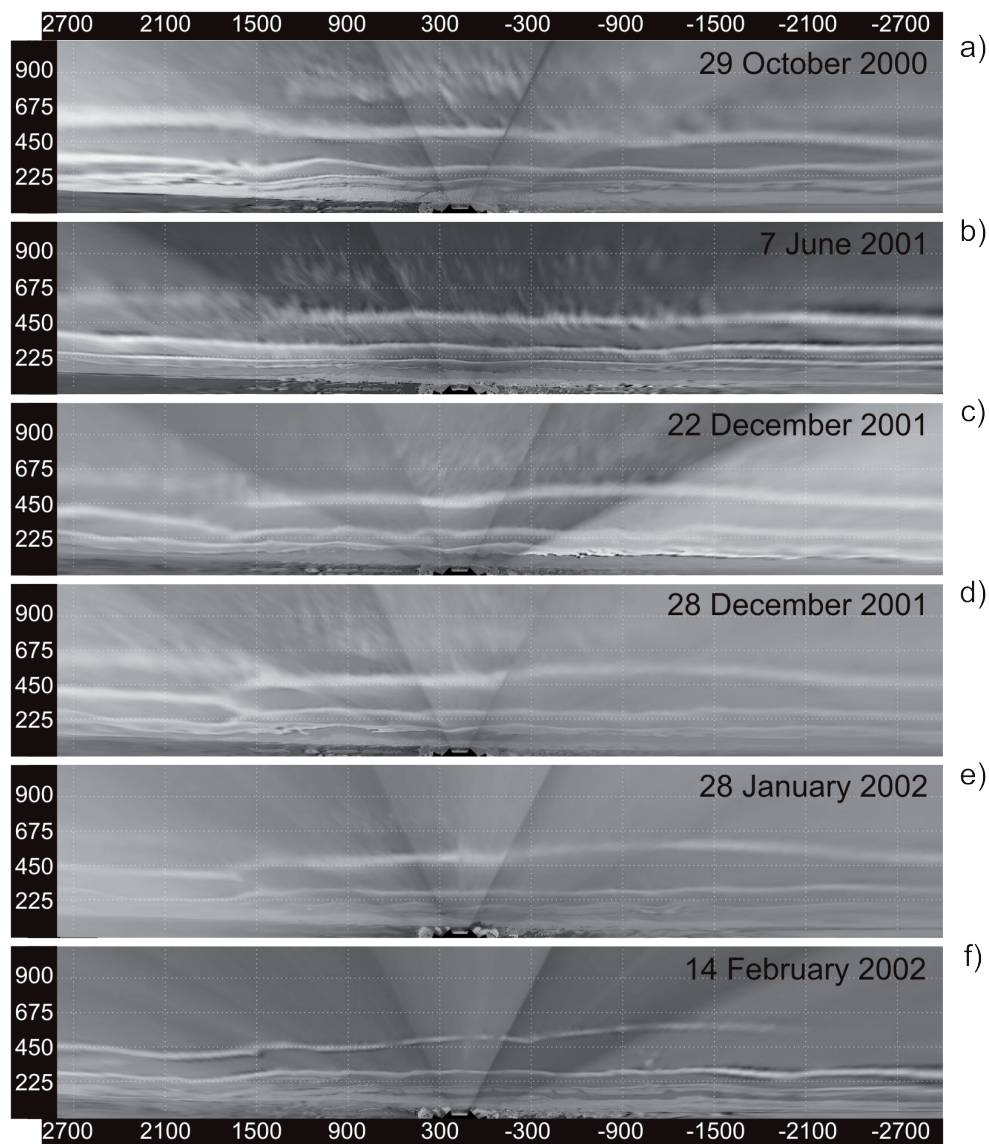


Figure 5.11. Bar switching episode southward of the study region. a) Initial morphology before the formation of the discontinuous outer bar, b) offshore migration of the outer bar, c) offshore migration of the inner bar, d) forked shape and, e) and f) new arrangement of the bar system.

conditions during the southern bar switching in late 2001 (Figure 5.9). Apparently, the end of a switching episode with the realignment of the sections of inner and outer bar requires high-energy wave conditions. The necessity of several high-energy events to attain bar switching has also been reported by Shand *et al.* (2001). The high-energy wave conditions can be confirmed by the behaviour of the other bar sections during the occurrence of the realignment. During the first episode of bar switching (northern flank) in December 1999, in the central and southern sections the inner and outer bars migrated offshore considerably; while during the second episode of bar switching (southern flank) in January 2002, one of the most pronounced offshore migrations took place in the outer bar of the northern section (Figure 5.9).

Bar switches caused the outer bar configuration to rotate around the central section, adopting shore-oblique shapes after each of the switching episodes.

5.4.2. SHORELINE RESPONSE TO THE NOURISHMENT

The time series of the alongshore-averaged shoreline position for the period 1834–2004 is presented in Figure 5.12. Following its advance and retreat before 1880, the shoreline migrated in the seaward direction for more than a century at a rate of

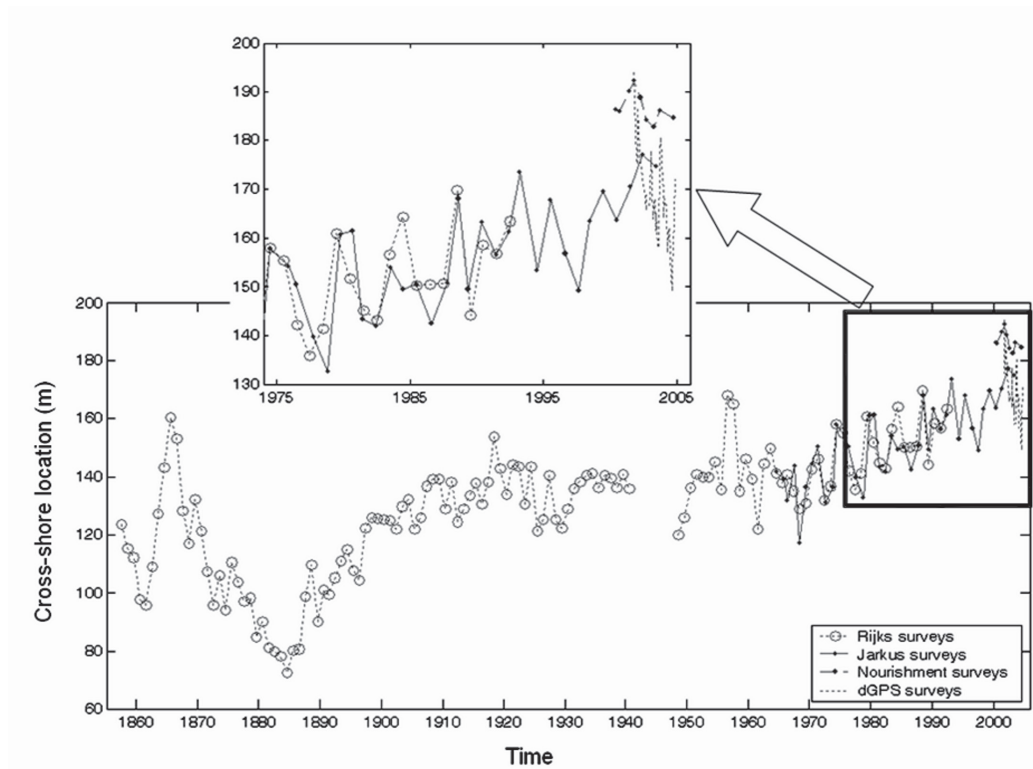


Figure 5.12. Shoreline locations alongshore-averaged for the 6 km study region except for the dGPS surveys, which represent only a 1.5 km section in front of the nourishment area.

0.38 m/year, and the migration rate calculated from 1964 to 2003 was of 0.90 m/year. The detailed dGPS surveys after the nourishment (2001-2004) showed high seasonal variability of the shoreline, although it was of the same magnitude as the yearly variability occurring at the beach in the long-term evolution. On the whole, we see neither a positive influence of the nourishment on the shoreline position, nor a clear break in trend in shoreline position.

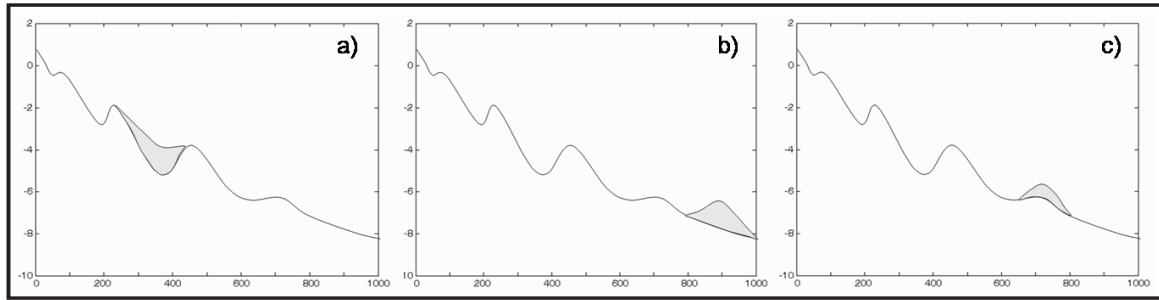


Figure 5.13. Location of the nearshore nourishments in a) Terschelling, b) Noordwijk and, c) Egmond. Notice that this sketch does not represent the real bathymetry at each site.

5.5. INTERSITE COMPARISON

A summary of the characteristics of the Noordwijk, Terschelling and Egmond shoreface nourishments is presented in Table 5.2 and Figure 5.13. In the following we discuss a number of striking differences and similarities between these nourishments.

1) Nourishment migration

Cross-shore migration of the nourishment: While the Egmond nourishment maintained its cross-shore location, at Noordwijk the nourishment migrated approximately 300 m onshore. Apparently, the cross-shore displacement of the nourished sand depends greatly on the location of the nourishment within the active zone. Spanhoff *et al.* (2005) suggested that shoreface nourishments placed on top of the

Table 5.2. Characteristics of the three discussed shoreface nourishments. The D_{50} value refers to the nourished sand.

Location	Year	Length (km)	Total Volume (Mm ³)	Volume (m ³ /m)	D_{50} (μm)
Terschelling	1993	4.6	2.0	435	194 – 207
Noordwijk	1998	3.0	1.7	570	~400
Egmond	1999	2.2	0.9	400	~228

region where bars end their natural cycle (e.g. on top of a degenerating sandbar at Egmond) tend to remain in the same position; while nourishments placed further offshore of this position (e.g. Noordwijk) tend to migrate onshore until they reach this location. Finally, when the sand is placed in the trough between the middle and the outer bar (e.g. Terschelling), the trough is newly formed within months and the sand from the nourishment is incorporated in the bar system, contributing to the formation of a higher onshore bar.

Alongshore migration of the nourished sand: While the Terschelling nourishment migrated alongshore by 400 m/year (Grunnet and Ruessink, 2005), neither the Noordwijk nor the Egmond nourishment experienced a significant alongshore displacement. This is likely to be caused by differences in the wave climate. At Egmond and Noordwijk two main offshore wave directions (from the southwest and the northwest), cause opposite alongshore transport rates, self-cancelling in the long run. Because of its east-west orientation, the wave direction at Terschelling is rather persistent from the west, causing a clear dominance in alongshore transport direction (Grunnet and Hoekstra, 2004).

2) Bar system response

Influence on the autonomous bar cycle: The arrest of the natural offshore migration of bars is a common response of bar systems to shoreface nourishments. However, the intersite difference in the duration of the nourishment effect does not seem to depend on a single factor or a simple combination of several factors. At the Noordwijk site, the arrest of the inner and outer bar at their pre-nourishment cross-shore locations lasted at least 5.8 years, about 1.5 times the original bar cycle duration. In contrast, the Terschelling and Egmond sandbars resumed their offshore migration after about 6 (Grunnet and Ruessink, 2005) and 3 years (Van Duin *et al.*, 2004), respectively, corresponding to about half and one-fifth of the local cycle duration. We ascribe the longevity of the nourishment effect in Noordwijk to (i) the location of the nourishment at the seaward end of the active profile (the Terschelling and Egmond nourishments were located further onshore); (ii) the large grain size of the nourished material (Table 5.2), which may have reduced onshore transport rates relative to those at Terschelling and Egmond; and (iii) the large size of the nourishment relative to the size of the sandbars. At Noordwijk, the sandbars are considerably smaller in maximum height and volume than at Terschelling and Egmond (Ruessink *et al.*, 2003), whereas the volume of nourished material in m^3/m (Table 5.2) was largest at Noordwijk.

Influence on the bar three-dimensionality: One of the requirements for the formation of crescentic shapes in sandbars is the abundance of sediment (Sonu, 1973). In addition, these 3D morphologies have also been related to accretionary systems (Lippmann and Holman, 1990; Short, 1999). In agreement with these previous studies, the nourishment at Terschelling produced an unusual development of 3D morphologies at the middle bar. As a consequence of the redistribution of nourished sediment, the water depth over the middle bar decreased, which may have made the bar more prone to the development of crescentic plan-shapes and rip channels (Grunnet and Ruessink, 2005). It would seem that nourishments positioned seaward of the outer bar do not increase the three-dimensionality of the shoreward located sandbars (e.g., Figure 5.7).

Enhancement of bar switching episodes: Bar switching is also part of the natural, long-term bar behaviour at Noordwijk (at least in the southern section) (Van Enckevort, 2001; Ruessink *et al.*, 2003) so it cannot initially be put forward as one of the effects of the nourishment. However, the location of the bar switching occurring in the southern section before and after the nourishment changed substantially, from $y = 2200 - 2600$ m in 1996 (Figure 5.2) to the limit between the southern and the central sections in 2001 (Figure 5.11, $y = 1300 - 1800$ m), possibly as a result of the nourishment effect. Furthermore, this is the first time that bar switching has been observed in the northern section of the study area and we consider that at least this episode was nourishment-induced. Bar switching is probably due to small alongshore differences in the position and depth of the outer bar (Wijnberg and Wolf, 1994), resulting in alongshore differences in the offshore bar migration rates (Shand, 2003). These conditions are satisfied when the shoreface is nourished since, as stated above, shoreface nourishments result in feeder and lee effects in the region sheltered by the nourishment, creating an alongshore difference with the bars on its flanks. The feeder effect implies an increase in the sand stored in the bars shoreward of the nourishment, and therefore a change in their depths. The lee effect implies both an increase in the amount of sediment (due to a decrease in alongshore currents in the region of shadow of the nourishment) and a decrease in the offshore migration rate due to an increase in the degree of protection of the bars (waves breaking at the nourishment instead of at the bars). In contrast, the sections on the flanks continue their autonomous offshore migration.

3) Shoreline response

Effect on the shoreline location: The shoreline position in the years following the Noordwijk nourishment did not differ greatly from the previous autonomous shoreline behaviour. This is similar to the Egmond case, for which Van Duin *et al.* (2004) argued that the nourished sediment did not feed the beach as the nourishment started to disappear before the sediment could reach the beach. On the other hand, the Terschelling nourishment reversed the shoreline migration from a 3 m/year retreat into a 15 m/year advance (Grunnet and Ruessink, 2005). This difference may be related to the location of the nourishment on the cross-shore profile, as the nourished sand in Egmond and Noordwijk may have diffused before reaching the beach. Also, the pronounced growth of the middle bar at Terschelling may have increased the lee effect relative to that at Egmond and Noordwijk.

5.6. CONCLUSIONS

The 1998 Noordwijk shoreface nourishment delayed the natural development of the two subtidal bars section in front of the nourishment, with a marked decrease in the offshore migration rates for both the inner and the outer bar. This reduced speed occurred first in the outer bar and then in the inner bar, which, in the end, even migrated onshore. Even after almost 6 years, which is about 1.5 times the natural cycle duration of the Noordwijk bars, the subtidal bars had not resumed their autonomous offshore-directed trend. We suspect that this long arrest period compared with other nourished sites (Egmond and Terschelling) is caused by: 1) the grain size of the sediment used to nourish Noordwijk, which was almost twice the grain size at the other sites; 2) the larger size of the nourishment at Noordwijk relative to the sandbar size; and 3) the location of the nourishment, at the distal part of the active nearshore profile. Allaying earlier fears, we did not find any evidence for the growth of three-dimensional shapes after the implementation of the nourishment; in fact, the sinuosity of the sandbars decreased with time. Finally, the nourishment did not affect the temporal evolution of the shoreline.

The arrest of the offshore sandbar migration shoreward of the nourishment and the continuation of this migration elsewhere caused two episodes of bar switching. Both took almost one year to complete, and can therefore not be ascribed to individual wave events. Although bar switching has been briefly mentioned in other papers related to shoreface nourishments (e.g. van Duin and Wiersma, 2002; Spanhoff *et al.*, 2005), it has not been specifically addressed as a nourishment effect. We suggest here that shoreface nourishments enhance the possibilities of bar

switching by creating alongshore gradients in the position and depth of the outer bar and in its cross-shore migration rate and direction.

Finally, irrespective of observed intersite differences, the nourishments in Noordwijk, Terschelling and Egmond show that the nourished sand becomes part of the “natural” bar system – that is, sand losses offshore and/or alongshore appear to be minor relative to the observed onshore effects.

6 Conclusions

The central aim of this thesis is to improve our knowledge on the morphodynamics of anthropogenic impacted beaches at temporal scales of days to years. Two stretches of coast have been monitored using video techniques: the artificial embayed beaches of Barcelona city (NW Mediterranean) and the open beach of Noordwijk at the Dutch central coast (North Sea). The previous scientific knowledge of the morphodynamics of both study sites was quite different. Whereas the nearshore morphodynamics of Noordwijk have been previously studied, the morphodynamics of Barcelona city beaches were poorly understood. For this reason, this work investigates, firstly, the morphodynamics of Barcelona city beaches looking at different parameters like the shoreline mobility and rotation, the changes in the submerged sandbar configuration or the orientation of the shoreline and the sandbars, at different time scales (related to storm events, at seasonal and interannual time scales). And secondly, the response of the nearshore after different types of nourishments at Barcelona and Noordwijk beaches is analyzed. The most relevant findings of this research are organized in three main topics: methodological contributions, morphodynamics of artificial embayed beaches and morphodynamic impacts of artificial nourishments.

6.1. METHODOLOGICAL CONTRIBUTIONS

Video monitoring techniques provided an adequate spatial and temporal resolution to study the nearshore morphodynamics of these stretches of coast at different time scales (from daily to decadal).

The application of video monitoring techniques is site-specific, and automated

algorithms useful for every video monitoring station are still scarce. There are two main singularities of the Barcelona station:

- a) The requirements for the automated shoreline extraction using the Argus software (the Intertidal Beach Mapper code) are not fulfilled at Barcelona city beaches, where the milder wave conditions imply a difficulty in the extraction of the shoreline. This occurs mainly during summer days, when the absence of wave breaking together with the presence of beach users complicates the shoreline detection. In spite of this, the total number of shorelines sampled at Barcelona city beaches for this study adds up to 1500 shorelines between November 2001 and March 2006.
- b) The Argus station of Barcelona monitors a microtidal region with a negligible tidal range of a few tens of centimetres. This absence of a significant tide together with the dominant wave conditions imply a lower number of days when the sandbars can be tracked in comparison with other Argus stations. However, it also implies that the bars tracked in Barcelona are just biased by the variable incident wave height but not by changes in the tide. In addition, this is the first study with video cameras that tackles sandbar dynamics in regions with no tides and low number of days with distinguishable bar breaking patterns.

This thesis provides several methodological contributions; the majority of them are related to the extraction and post-processing of the shoreline. Taking into account the negligible tidal range found in Barcelona city beaches, we have defined a **daily-averaged shoreline** using one or more shorelines of the same day at different moments. This definition is intended to reduce the measurement errors due to the sampling technique and to small sea level variations. In order to avoid the errors induced by the curvature of the beaches, a *reference shoreline* was defined as the result of the average position of more than three years of shoreline mapping fitted to a polynomial curve. The shoreline and the bar dynamics were then studied using lines perpendiculars to the *reference shoreline*. In this manner, both morphological features had the same reference.

A series of morphological descriptors have been used for the different analysis. We have used the **emerged beach area** to quantify changes in the beach and to deepen in the understanding of the beach rotation process. The area of each beach was separated into two sections using a **representative pivotal point** (the point of

the shoreline with minimum variability during the study period) as the division point. The changes occurring at the area of each section were used as a proxy to study beach rotation. The **beach orientation** was firstly defined as a way to clarify the occurrence of beach rotation due to storm events. In this manner, changes in the beach orientation associated to constant beach area, were expected to be due to beach rotation. Additionally, the beach orientation also resulted to be a valuable tool to understand longer-term responses of the beaches (e.g. gradual beach rotation occurring as the beach tended towards a certain equilibrium plane shape), as well as the relationship with the orientation of the sandbars.

Finally, the three-dimensionality of the bars was evaluated using the **sinuosity** ratio, defined as the relationship between the measure of the barline and the distance between its two ends following a straight line. The sinuosity was chosen instead of the standard deviation of the data because, at Noordwijk bars, the standard deviation biased the results as a consequence of the differential migration rates found along the bars, which caused largest offshore migrations in the flanks of the nourishment, and then greater values of the standard deviation.

The methodological contributions and the morphological descriptors defined here can be useful in future studies of Barcelona beaches and other study areas.

6.2. MORPHODYNAMICS OF ARTIFICIAL EMBAYED BEACHES

The three sandy beaches analysed using the Argus station of Barcelona are artificially-created beaches bounded by shore-perpendicular groins; they have high slopes, similar orientations, and are subject to the same wave climate. However, they differ in the dominant morphodynamic state and in the morphological evolution at different time scales (e.g., response to storms or interannual trends).

The morphodynamic state of La Barceloneta and Bogatell beaches switch among the four *Intermediate Beach* states, with Longshore Bar and Trough associated with high-energy wave events, and Rhythmic Bar and Beach, Transverse Bar and Rip and Low Tide Terrace associated with low-energy wave periods. They often show a bar (or a terraced bar) that in plan shape is characterized by its obliquity respect to the shoreline, as the northern bar section is located closer to the shoreline. Nova Icaria is normally in a *Reflective Beach* state with an occasional terraced profile on its southern section. The morphodynamic state of these beaches does not always relate to the preceding wave conditions, as the natural trend of the beach towards

an equilibrium configuration induced by the wave conditions is interrupted by low-energy periods. At Barcelona beaches (as probably at other Mediterranean beaches) the arrest of the beach configuration typically occurs during long periods, mostly associated with the summer season, when the wave energy is too low to cause significant sediment transport.

6.2.1. SEASONAL AND INTERANNUAL BEACH MORPHODYNAMICS

The beach mobility is similar at La Barceloneta and Bogatell beaches and lower at Nova Icaria. Beach mobility is characterized by maximum values at the two ends of each beach although at Nova Icaria the largest beach mobility is only at the southern limit (as the northern section is more protected from the wave action). In general, the beach mobility at the three beaches is of similar magnitude to that of natural embayed beaches (around 5-10 m).

From an interannual perspective, the beach of La Barceloneta shows an erosive trend that is temporary alleviated with human interventions (artificial nourishment and sand relocation). Bogatell beach was nourished in summer 2002 and, after this intervention, it followed an erosive trend during approximately a year and a half; but then the beach reached a stable beach area that has maintained almost constant. Nova Icaria is the most stable of the three beaches. This beach is capable of self-recovery after erosive periods and has not required beach nourishment after its creation. Moreover, the time series of the emerged beach area of Bogatell and Nova Icaria suggest that these beaches are not isolated sedimentary cells, but that alongshore sediment transport can supply sediment bypassing the protection groins.

The shoreline orientation along the study period shows abrupt changes and slow recoveries of a certain characteristic orientation. Abrupt changes are artificially-caused (nourishments, artificial sand relocations) and naturally-caused (beach rotation and local erosion or accretion related to storm events). At Nova Icaria and Bogatell the slow recovery of the beach orientation tended towards a certain characteristic equilibrium (around 43° and 37°N, respectively), while at La Barceloneta the shoreline does not seem to reach a characteristic orientation during the study period and displays an anticlockwise direction trend that might be associated with the enlargement of the southern groin.

La Barceloneta and Bogatell are single-barred beaches. The absence of submerged

bar at Nova Icaria beach is consistent with the high slopes found in their submerged profiles (gradients of 0.049 at Nova Icaria), in comparison with the gradients of 0.031 found at La Barceloneta and Bogatell. The submerged sandbar of Bogatell beach is small and often terraced, and it undergoes frequent changes of its morphology from linear to crescentic. The bar of La Barceloneta is a larger and better-developed bar subject to more long-lasting changes. Therefore, bar dynamics is inversely related to the size of the bar. In the two artificial single-barred beaches under study the changes from a two-dimensional longshore bar to a three-dimensional longshore bar are related to the morphodynamic cycle and to the wave energy content. In general, low-energy wave action produces the occurrence of down-state transitions, from a two-dimensional (associated to the “reset” caused by high-energy events) to a three-dimensional bar. Bogatell beach frequently switched between the four morphodynamic states, but the bar at La Barceloneta only underwent the complete “reset” of the nearshore morphology once, associated with high-energy wave events at the beginning of the study period. At this beach, the strongest storm events produced offshore bar migration and a certain decrease in the bar sinuosity, but did not generate an alongshore parallel bar. The two barred beaches show a clear evidence of coupling between the bar and the shoreline orientation at time-scales of seasons to years.

The cross-shore migration of the bar at La Barceloneta and Bogatell followed a net onshore migration pattern during the study period. The interannual component of this net cross-shore migration is also onshore, with an overall change in the bar location of about 30 m at La Barceloneta and about 20 m at Bogatell. This interannual component coincides with the interannual decrease trend of the wave energy affecting the beaches. The seasonal component of the bar displacement shows a certain pattern that is in agreement with the morphodynamic cycle. This pattern shows offshore migration during the first months of the winter season (when the bar is located closed to the shoreline after the summer months and, therefore, the wave height–water depth ratio is large) followed by some onshore migration as the wave height–water depth ratio decreases.

The observed overall bar migration trend of Barcelona beaches differs from the long-term Net Offshore Migration pattern detected in other long-term observations (located in open and higher-energy coasts). This differential behaviour might be due to some differences in sediment transport processes affecting bar evolution or to the duration of the Net Offshore Migration cycle in Barcelona, which may be

longer than the study period.

6.2.2. BEACH MORPHODYNAMICS RELATED TO STORMS

Storms were responsible for major changes in the configuration of the beaches: shoreline advance or retreat, beach rotation, sandbar migration, formation of megacusps, or changes in the sandbar configuration.

The response of La Barceloneta and Bogatell beaches to storm events was similar, with shoreline displacements varying between -18 and +34 m at La Barceloneta and -20 m and +15 m at Bogatell. However, Nova Icaria shows a different behaviour, only reacting to waves coming from a narrow range of angles (68- 80°) and with the main storms effects occurring in the southern section of the beach (with maximum values of almost 30 m).

Beach rotation and wave conditions displayed a complex relationship. Similar storms caused different effects on adjacent beaches depending on the degree of protection. Also on the same beach, the effect of similar storms depended on the previous morphodynamic configuration of the beach. Furthermore, the advance and retreat of each beach segment associated with beach rotation were not alongshore-constant due to the influence of the morphodynamics (sediment exchange with the submerged profile and formation of sedimentary structures like megacusps). As beach rotation is caused by alongshore sediment transport, it was expected that large values (positive or negatives) of the alongshore component of the radiation stress would be related to beach rotation while low values of S_{xy} during storms would imply predominance of cross-shore sediment transport and therefore no changes in the beach orientation. The results showed that this simple approach gives better results than the use of the wave height or the wave angle alone. There is a highly significant correlation between the change in the beach orientation at La Barceloneta and Bogatell beaches and the S_{xy} value ($r^2=0.71$ and 0.60 , respectively). At Nova Icaria the results were less conclusive.

The alongshore-averaged bar location at Bogatell and La Barceloneta show similar responses to variations in the wave conditions, with migrations taking place in the same direction (onshore/off-shore) during the most important stormy periods. However, the relation between the alongshore-averaged cross-shore migration of the bars and the shoreline in response to storms was complex as they do not appear to be systematically correlated (when the bar and the shoreline responded

to a storm event, onshore or offshore bar migration occurred indistinctly with shoreline advance or retreat).

Megacusps were formed at La Barceloneta and Bogatell beaches when the submerged sandbars became crescentic and attached to the beach. They do not occur at Nova Icaria due to the absence of submerged sandbars. The processes of megacusps development and migration remain unclarified in this study. For instance, a relationship between wave direction and formation of megacusps was not evident at the beaches. Finally, there is a clear change in the megacusps wave length during the study period, with shorter wave lengths occurring at the end of the study period (winter of 2005-2006). This is in agreement with model results.

6.3. MORPHODYNAMIC IMPACTS OF ARTIFICIAL NOURISHMENTS

Human interventions in the nearshore alter the morphodynamic configuration of the beach and imply a morphological readjustment after the intervention. In general, nourishments cause a disruption of the natural beach trend and have a limited effect on the beaches. The duration of this effect depends on different factors such as the type of nourishment, its location, the type of sand used to fill in, the volume of sand, or the way the plan shape of the beach is distorted.

6.3.1. BEACH NOURISHMENT

The nourishment of Barcelona beaches carried out in summer 2002 had a temporary effect on the dynamics of the beaches given that the shoreline configuration was similar to the pre-nourishment situation approximately one year and a half after it. The limited amount of sand used in the filling and probably the generation of a beach profile strongly in disequilibrium with morphodynamic conditions during the nourishment works were the main reasons for this fast erosive response.

At La Barceloneta the beach nourishment had a limited effect in the total beach area, but it achieved its objective that was to protect the northern section of the beach and supply some extra room for the visitors during the summer season. The beach nourishment accomplished at Bogatell beach almost doubled the emerged beach area. In spite of the differences, both beaches showed similar rates of emerged beach area losses with values of 22 and 18 m²/day at La Barceloneta and Bogatell beaches, respectively. Maximum erosion after the nourishment was not directly related to the strongest storms, but depended on the time elapsed since the nourishment and the wave approach direction.

The dynamics of the nearshore after these nourishments changed, mainly, in the emerged beach with an increase in the erosive trend, but it also affected the submerged sandbars. At La Barceloneta the erosion of the nourished sand induced an increase of the sinuosity of the bar. At Bogatell some months before the implementation of the nourishment the tracked bar was a crescentic bar located in an offshore position, and when it was visible again some months after the nourishment it was an alongshore-parallel bar close to the shoreline. In this case, the increase in the sinuosity of the bar was related to a change in the beach configuration with the erosion of the northern section of the beach.

6.3.2. SHOREFACE NOURISHMENT

The shoreface nourishment accomplished at Noordwijk on early 1998 changed the nearshore morphodynamics, producing an alteration at the submerged sandbars, but not affecting the temporal evolution of the shoreline. The effect of the nourishment in the natural migration cycle of the bars was still appreciated after the 5.8 years of the study period, more than the duration of the effect observed at other nourished sites. This difference is probably due to: 1) the larger grain size of the sediment used to nourish Noordwijk; 2) the larger size of the nourishment at Noordwijk relative to the sandbar size; and 3) the location of the nourishment, at the distal part of the active nearshore profile.

The nourishment altered the natural NOM cycle of the bars in the region in front of the nourishment in such a way that the offshore migration rates of both bars decreased and even inverted towards on-shore migration at the inner bar. Allaying earlier fears, there is no evidence for the growth of three dimensional shapes after the implementation of the nourishment; in fact, the sinuosity of the sandbars decreased with time.

The change of the bar dynamics in the region in front of the nourishment also had an alongshore effect due to the differences among the bar behaviour at that stretch of coast and at the sections located in the flanks of the nourishment. In this manner, we found that the shoreface nourishments enhance the possibilities of bar switching by creating alongshore gradients in the position and depth of the outer bar and in its cross-shore migration rate and direction.

6.4. FUTURE RESEARCH

The data analyzed in this thesis provides a primary source of information to verify models related to coastal morphodynamics. For instance, a first attempt to model the formation of crescentic bars in La Barceloneta beach through a nonlinear morphodynamic model was able to reproduce the spacing of the crescentic bar at different conditions (Ribas *et al.*, 2007). Further research is needed in order to adapt the model to the morphology of embayed beaches (lateral boundaries, curvilinear shoreline, alongshore variability in the initial bathymetry), particularly given that in the literature there are no comparison of models and observations of crescentic bars at artificial embayed beaches.

Another topic related to morphodynamic models is to use the resultant data of the plan shape of the beaches to develop a model that can reproduce rotation of the embayed beaches due to storm events, as well as the long-term trends of the beaches orientation. We will also attain a deeper understanding of the beach rotation process by analyzing topographic dGPS data to evaluate the relative importance of the longshore and cross-shore sediment transport in the beach changes.

Further work also implies to improve the methodology followed on the extraction of data from the video images. Although the effect of the H_s in the video-mapped sandbars has been minimized by using a 1-m range of H_s , a following step should be to develop a methodology to minimize the errors on the video-mapped sandbars induced by the variation of the wave height. This is a work already in progress and we expect the main differences to be related to the alongshore-averaged cross-shore position of the bars.

In addition to the scientific contributions that this study adds to the general knowledge of the coastal system, results can also provide a valuable tool for coastal management applications. For instance, it is possible to make use of the continuous monitoring of the beaches to evaluate the performance of human interventions like the efficiency of artificial nourishments, the degree of protection attained by the construction of groins, or the results of beach cleanings. Furthermore, there is the possibility of using the results to extract Coastal State Indicators (CSI) that will facilitate management decisions.

Bibliography

- Aagaard, T., 1998. Nearshore bar morphology on the low-energy coast of northern Zealand. *Geografisk Tidsskrift* 58, 27–31.
- Aagaard, T., Kroon, A., Andersen, S., Sørensen, R.M., Quartel, S., and Vinther, N., 2005. Intertidal beach change during storm conditions; Egmond, The Netherlands. *Marine Geology* 218, 65–80.
- Aarninkhof, S.G.J., 2003. Nearshore Bathymetry derived from Video Imagery. PhD thesis, Delft University of Technology.
- Aarninkhof, S.G.J., Turner, I.L., Dronkers, T.D.T., Caljouw, M., and Nipius, L., 2003. A video-based technique for mapping intertidal beach bathymetry. *Coastal Engineering* 49, 275–289.
- Almar, R., Coco, G., Bryan, K.R., Huntley, D.A., Short, A.D., and Senechal, N., 2008. Video observations of beach cusp morphodynamics, *Marine Geology* 254, 216–223.
- Anthony, E.J., Gardel, A., Dolique, F., and Guiral, D., 2002. Short-term changes in the plan shape of a sandy beach in response to sheltering by a nearshore mud bank, Cayenne, French Guiana. *Earth Surface Processes and Landforms* 27, 857–866.
- Barusseau, J.P., Radulescu, M., Descamps, C., Akouango, E., and Gerbe, A., 1994. Morphosedimentary multiyear changes on a barred coast (Gulf of Lions, Mediterranean Sea, France). *Marine Geology* 122, 47–62.
- Becker, J.M., Firing, Y.L., Aucan, J., Holman, R.A., Merrifield, M., and Pawlak, G., 2007. Video-based observations of nearshore sand ripples and ripple migration, *Journal of Geophysical Research* 112, C01007. doi: 10.1029/2005JC003451.
- Birkemeier, W., and Holland, K.T., 2001. The Corps of Engineers' Field Research Facility: more than two decades of coastal research. *Shore and Beach* 69, 3–12.
- Bowman, D., and Goldsmith, V., 1983. Bar morphology of dissipative beaches: an empirical model. *Marine Geology* 51, 15–33.

- Browder, A.E., and Dean, R.G., 2000. Monitoring and comparison to predictive models of the Perdido Key beach nourishment project, Florida, USA. *Coastal Engineering* 39, 173–191.
- Calvete, D., Dodd, N., Falqués, F., and van Leeuwen, S.M., 2005. Morphological development of rip channel systems: normal to near-normal wave incidence. *Journal of Geophysical Research* 110, C10006. doi: 10.1029/2004JC002803.
- Certain, R., and Barousseau, J.P., 2006. Sediment availability and conceptual models of sand bars morphodynamics for a microtidal beach (Sète, France). In: *Proceedings of the 5th International Conference on Coastal Dynamics '05, Barcelona, Spain, (on CD)*.
- Chickadel, C.C., 2007. *Remote Measurements of Waves and Currents over Complex Bathymetry*. PhD thesis, Oregon State University.
- Chickadel, C.C., Holman, R.A., and Freilich, M.F., 2003. An optical technique for the measurement of longshore currents. *Journal of Geophysical Research* 108, 3364. doi: 10.1029/2003JC001774.
- Dette, H.H., Führböter, A., and Raudkivi, A.J., 1994. Interdependence of beach fill volumes and repetition intervals. *Journal of Waterway, Port, Coastal, and Ocean Engineering* 120(6), 580–593.
- Dolan, R., Hayden, B.P., and Heywood, J., 1978. Analysis of coastal erosion and storm surge hazards. *Coastal Engineering* 2, 41–53.
- Elgar, S., Gallagher, E., and Guza, R. T., 2001. Nearshore sand bar migration, *Journal of Geophysical Research* 106(C6), 11623–11627.
- Elko, N.A., Holman, R.A., and Gelfenbaum, G., 2005. Quantifying the rapid erosion of a nourishment project with video imagery. *Journal of Coastal Research* 21, 633–645.
- Escartin, F.J., Campos, C., Castañeda, A.M. and Novoa, M., 2003. Resultado de la Segunda campaña de seguimiento de la evolución de las playas del Maresme. Tramo Arenys de Mar- Port Balís (Barcelona). In: *VI Jornadas Españolas de Ingeniería de Costas y Puertos Almería, Spain, Chapter 10*.
- Farris, A.S., and List, J.H., 2007. Shoreline change as a proxy for subaerial beach volume change. *Journal of Coastal Research* 23, 740–748.
- Galofré, J., Montoya, F.J., and Villanueva, T., 2004. Beach nourishment and litoral longshore transport interrupted by marina: l'Hospitalet case study. In: *Proceedings of the 29th International Conference on Coastal Engineering, Lisbon, Portugal, 3365–3377*.
- Gómez J., Espino, M., Puigdefabregas, J., and Jerez, F., 2005. Xarxa d'Instrumentació Oceanogràfica i Meteorològica de la Generalitat de Catalunya (XIOM). Boies d'onatge dades obtingudes l'any 2004. Informe Técnico.
- González, M., and Medina, R., 2001. On the application of static equilibrium bay formulations to natural and man-made beaches. *Coastal Engineering* 43, 209–225.
- Grunnet, N.M., 2004. *Morphodynamics of a shoreface nourishment in a barred nearshore zone*. Ph.D. Thesis, Utrecht University.
- Grunnet, N.M., and Hoekstra, P., 2004. Alongshore variability of the multiple barred coast

- of Terschelling, The Netherlands. *Marine Geology* 203, 23–41.
- Grunnet, N.M., and Ruessink, B.G., 2005. Morphodynamic response of nearshore bars to a shoreface nourishment. *Coastal Engineering* 52, 119–137.
- Guillén, J., and Palanques, A., 1993. Longshore bar and trough systems in a microtidal, storm-wave dominated coast: the Ebro Delta (NW Mediterranean). *Marine Geology* 1115, 239–252.
- Guillén, J., García-Olivares, A., Ojeda, E., Osorio, A., Chic, O., and González, R., 2008. Long-term quantification of beach users using video monitoring. *Journal of Coastal Research* (DOI: 10.2112/07-0886.1).
- Guillén, J., Stive, M.J.F., and Capobianco, M., 1999. Shoreline evolution of the Holland coast on a decadal scale. *Earth Surface Processes and Landforms* 24, 517–536.
- Hamm, L., Capobianco, M., Dette, H.H., Lechuga, A., Spanhoff, R., and Stive, M.J.F., 2002. A summary of European experience with shore nourishment. *Coastal Engineering* 47, 237–264.
- Hanson, H., Brampton, A., Capobianco, M., Dette, H.H., Hamm, L., Laustrup, C., Lechuga, A., and Spanhoff, R., 2002. Beach nourishment projects, practises, and objectives - a European overview. *Coastal Engineering* 47, 81–111.
- Hoekstra, P., Houwman, K.T., Kroon, A., Van Vessem, P., and Ruessink, B.G., 1994. The NOURTEC experiment of Terschelling: process-oriented monitoring of a shoreface nourishment (1993-1996). In: *Proceedings of the 1st Conference on Coastal Dynamics 94*, ASCE, New York, USA, 402–416.
- Holland, K.T., 1995. *Foreshore dynamics: Swash motions and topographic interactions on natural beaches*. PhD thesis, Oregon State University.
- Holland, K.T., 1998. Beach cusps formation and spacings at Duck, USA. *Continental Shelf Research* 18, 1081–1098.
- Holland, K.T., and Holman, R.A., 1993. The statistical distribution of swash maxima on natural beaches. *Journal of Geophysical Research* 98, 10271–10278.
- Holland, K.T., and Holman, R.A., 1996. Field observations of beach cusps and swash motions. *Marine Geology* 134, 77–93.
- Holland, K.T., Holman, R.A., Lippmann, T.C., Stanley, J., and Plant, N., 1997. Practical use of video imagery in nearshore oceanographic field studies, *IEEE Journal of Oceanic Engineering* 22, 81–92.
- Holman, R.A., and Guza, R.T., 1984. Measuring run-up on a natural beach. *Coastal Engineering* 8, 129–140.
- Holman, R.A., and Stanley, J., 2007. The history and technical capabilities of Argus. *Coastal Engineering* 54, 477–491.
- Holman, R.A., Lippmann, T.C., O'Neill, P.V., and Hathaway, K., 1991. Video estimation of subaerial beach profiles. *Marine Geology* 97, 225–231.
- Holman R.A., Sallenger Jr.A.H., Lipmann, T.C., and Haines, J.W., 1993. The application

- of video image processing to the study of nearshore processes. *Oceanography* 6, 78–85.
- Holman, R.A., Symonds, G., Thornton, E.B., and Ranasinghe R., 2006. Rip spacing and persistence on an embayed beach. *Journal of Geophysical Research* 111, C01006, DOI: 10.1029/2005JC002965.
- Hsu, J.R.C., Silvester, R., and Xia, Y.M., 1989. Generalities on static equilibrium bays. *Coastal Engineering* 12, 353–369.
- Kingston, K., 2003. Applications of complex adaptive systems approaches to coastal systems. PhD thesis, University of Plymouth.
- Kingston, K.S., Ruessink, B.G., Van Enckevort, I.M.J., and Davidson, M.A., 2000. Artificial neural network correction of remotely sensed sandbar location. *Marine Geology* 169, 137–160.
- Klein, M.D., and Schuttelaars, H.M., 2006. Morphodynamic evolution of double-barred beaches. *Journal of Geophysical Research* 111, C06017. DOI: 10.1029/2005JC003155.
- Klein, A.H.F., Filho, A.B., and Schumacher, D.H., 2002. Short-Term Beach Rotation Processes in Distinct Headland Bay Beach Systems. *Journal of Coastal Research* 18, 442–458.
- Klein, A.H.F., Vargas, A., Raabe, A.L.A., and Hsu, J.R.C., 2003. Visual Assessment of Bayed Beach Stability using Computer Software. *Computers & Geosciences* 29, 1249–1257.
- Komar, P.D. 1998. Beach processes and sedimentation, 2nd edition. Upper Saddle River (N.J.) Prentice Hall, 544 pp.
- Konicki, K.M., and Holman, R.A., 2000. The statistics and kinematics of transverse sand bars on an open coast. *Marine Geology* 169, 69–101.
- Kroon, A., Davidson, M.A., Aarninkhof, S.G.J., Archetti, R., Armaroli, C., Gonzalez M., Medri, S., Osorio, A., Aagaard, T., Holman, R.A., and Spanhoff R., 2007. Application of remote sensing video systems to coastline management problems. *Coastal Engineering* 54, 493–505.
- Kuriyama, Y., and Yamada, T., 2002. Influence of low-frequency standing waves on longshore bar development, In: *Proceedings of the 28th International Conference on Coastal Engineering*, Cardiff, Wales, ASCE, 2926–2935.
- Lechuga, A., 2003. Assessment of nourishment project at the Maresme coast, Barcelona, Spain. *Shore and Beach* 71, 3–7.
- Lippmann, T.C., 1992. Edge wave response to a modulating incident wave field. PhD thesis, Oregon State University.
- Lippmann, T.C., and Holman, R.A., 1989. Quantification of sand bar morphology: A video technique based on wave dissipation. *Journal of Geophysical Research* 94, 995–1011.
- Lippmann, T.C., and Holman, R.A., 1990. The spatial and temporal variability of sand bar

- morphology. *Journal of Geophysical Research* 95, 11575–11590.
- Lippmann, T.C., Holman, R.A., and Hathaway, K., 1993. Episodic, non-stationary behaviour of a two sand bar system at Duck, NC, USA. *Journal of Coastal Research*, (SI) 15, 49–75.
- Madsen, A.J., and Plant, N.G., 2001. Intertidal beach slope predictions compared to field data. *Marine Geology* 173, 121–139.
- Martino, E., Moreno, L. and Kraus, N.C., 2006. Uncertainties in design guidance for headland-bay beaches. In: *Proceedings of the 5th International Conference on Coastal Dynamics '05*, Barcelona, Spain, (on CD).
- Masselink, G., Kroon A., and Davidson-Arnott, R.G.D., 2006. Intertidal bar morphodynamics in wave-dominated coastal settings: a review. *Geomorphology* 73, 33–49.
- Medina, R., Marino-Tapia, I., Osorio, A., Davidson, M., and Martin, F.L., 2007. Management of dynamic navigational channels using video techniques. *Coastal Engineering* 54, 523–537.
- MOPU (Ministerio de Obras Públicas, Transportes y Medio Ambiente). Dirección General de Costas, 1994. *Control y Evolución de las playas Olímpicas* (Barcelona). Tomo I.
- Moreno, L., and Kraus, N., 1999. Equilibrium shape of headland-bay beaches for engineering design. In: *Proceedings of Coastal Sediments'99*, Long Island, New York, ASCE, 860–875.
- Morichon, D., Dailloux, D., Aarninkhof, S.G.J., and Abadie, S., 2008. Using a shore based video system to hourly monitor storm water plumes (Adour River, Bay of Biscay). *Journal of Coastal Research* 24, 133–140.
- Morris, B.D., Davidson, M.A., and Huntley, D.A., 2001. Measurement of the response of a coastal inlet using video monitoring techniques, *Marine Geology* 175, 251–272.
- Muller, J., Wüst, R.A.J., and Hearty, P.J., 2006. Sediment transport along an artificial shoreline: 'The Strand', Townsville, NE-Queensland, Australia. *Estuarine, Coastal and Shelf Science* 66, 204–210.
- Muñoz-Pérez, J.J., Lopez de San Roman-Blanco, B., Gutierrez-Mas, J.M., Moreno, L., and Cuena, G.J., 2001. Cost of beach maintenance in the Gulf of Cadiz (SW Spain). *Coastal engineering* 42, 143–153.
- Norcross, Z.M., Fletcher, C.H., and Merrifield, M., 2002. Annual and interannual changes on a reef-fringed pocket beach: Kailua Bay, Hawaii. *Marine Geology* 190, 553–580.
- Osorio, A., 2005. *Desarrollo de técnica y metodologías basadas en sistemas de video para la gestión de la costa*. PhD thesis, Universidad de Cantabria.
- Pape, L., Ruessink, B.G., Wiering, M.A., and Turner, I.L., 2007. Recurrent neural network modelling of nearshore sandbar behaviour. *Neural Networks* 20, 509–518.
- Plant, N.G., 1998. *The role of morphodynamic feedback in surf zone sand bar response*, PhD thesis, Oregon State University.

- Plant, N.G., and Holman, R.A., 1997. Intertidal beach profile estimation using video images. *Marine Geology* 140, 1-24.
- Plant, N.G., Freilich, M.H., and Holman, R.A., 2001. Role of morphologic feedback in surf zone sandbar response. *Journal of Geophysical Research* 106, 973-989.
- Plant, N.G., Holland, K.T., and Puleo, J.A., 2002. Analysis of the scale of errors in nearshore bathymetric data. *Marine Geology* 191, 71-86.
- Quartel, S., 2007. Beachwatch. The effect of daily morphodynamics on seasonal beach evolution. PhD thesis, University of Utrecht.
- Quartel, S., Kroon, A., and Ruessink, B.G., 2008. Seasonal accretion and erosion of a microtidal sandy beach. *Marine Geology* 250, 19-33.
- Quartel, S., Ruessink, B.G., and Kroon, A., 2007. Daily to seasonal cross-shore behaviour of quasi-persistent intertidal beach morphology. *Earth Surface Processes and Landforms* 32, 1293-1307.
- Ranasinghe, R., McLoughlin, R., Short, A., and Symonds, G., 2004. The Southern Oscillation Index, wave climate, and beach rotation. *Marine Geology* 204, 273-287.
- Ranasinghe, R., Symonds, G., Black, K., Holman, R.A., 2004. Morphodynamics of intermediate beaches: a video imaging and numerical modeling study. *Coastal Engineering* 51, 629-655.
- Ribas, F., Garnier, R., Ojeda, E., Falqués, A., Guillén, J., and Calvete, D., 2007. Observation and modeling of crescentic bars in Barcelona embayed beaches. In: *Proceedings in the sixth international symposium of coastal sediments, Louisiana, New Orleans, 3, 2111-2123.* (ISBN: 978-0-7844-0926-8).
- Rozynski, G., 2003. Data-driven modeling of multiple longshore bars and their interactions. *Coastal Engineering* 48, 151-170.
- Ruessink, B.G., and Kroon, A., 1994. The behaviour of a multiple bar system in the nearshore zone of Terschelling, the Netherlands: 1965-1993. *Marine Geology* 121, 187-197.
- Ruessink, B.G., and Jeuken, C.J.L., 2001. Dunefoot dynamics along the Dutch coast. *Earth Surface Processes and Landforms* 27, 1043-1056.
- Ruessink, B.G., Wijnberg, K.M., Holman, R.A., Kuriyama, Y., and van Enckevort, I.M.J., 2003. Intersite comparison of interannual nearshore bar behaviour. *Journal of Geophysical Research* 108, 3249-3261.
- Sabatier, F., and Provansal, M., 2000. Sandbar morphology of the Espiguette spit, Mediterranean Sea, France. In: *Proceedings of the International Workshop on Marine Sandwave Dynamics, Lille, France, 179-187.*
- Sallenger, A.H., Holman, R.A., and Birkemeier, W.A., 1985. Storm induced response of a nearshore-bar system. *Marine Geology* 64, 237-257.
- Sánchez, R., 2006. Anàlisi de l'estabilitat del litoral de Barcelona: Platges Olímpiques. MSc. Thesis, Universitat de Barcelona.

- Shand, R.D., 2003. Relationships between episodes of bar switching, cross-shore bar migration and outer bar degeneration at Wanganui, New Zealand. *Journal of Coastal Research* 19, 157-170.
- Shand, R.D., Bailey, D.G., and Shepherd, M.J., 1999. An inter-site comparison of net offshore bar migration characteristics and environmental conditions. *Journal of Coastal Research* 15, 750-765.
- Shand, R.D., Bailey, D.G., Shepherd, M.J., 2001. Longshore realignment of shore-parallel sand-bars at Wanganui, New Zealand. *Marine Geology* 179, 147-161.
- Shepard, F.P., 1950. Beach cycles in southern California. U.S. Army Corps of Engineers, Beach Erosion Board, Technical Memo number 20.
- Short, A.D., 1985. Rip-current type, spacing and persistence, Narrabeen Beach, Australia. *Marine Geology* 65, 47-71.
- Short, A.D., 1999. Wave dominated beaches. In: Short, A.D. (ed.), *Handbook of Beach and Shoreface Morphodynamics*. Chichester, United Kingdom: John Wiley & Sons, 71-203.
- Short, A.D., 2002. Large scale behaviour of topographically-bound beaches. In: *Proceedings of the 28th International Conference on Coastal Engineering, Cardiff, Wales, ASCE*, 3778-3785.
- Short, A.D., and Masselink, G., 1999. Embayed and structurally controlled beaches. In: Short, A.D. (ed), *Handbook of beach and shoreface morphodynamics*. John Wiley & Son, Chichester, 230-250.
- Short, A.D., Trembanis, A.C., and Turner, I.L., 2000. Beach oscillation, rotation and the Southern Oscillation, Narraben Beach, Australia. *Proceedings of the 27th International Conference on Coastal Engineering, Sydney Australia*. 2439-2452.
- Siegle, E., 2003. Sediment transport and morphodynamics at an estuary mouth: a study using coupled remote sensing and numerical modelling. PhD thesis, University of Plymouth.
- Silvester, R., 1960. Stabilization of sedimentary coastlines. *Nature* 188, 467-469.
- Sonu, C.J., 1973. Three-dimensional beach changes. *Journal of Geology* 81, 42-64.
- Spanhoff, R., Kroon, A., and De Keijzer, S., 2006. Shoreface nourishment as a natural laboratory with emphasis on the Egmond case. In: *Proceedings of the 5th International Conference on Coastal Dynamics '05, Barcelona, Spain, (on CD)*.
- Stewart, C.J., and Davidson-Arnott, R.G.D., 1988. Morphology, formation and migration of longshore sandwaves; Long Point, Lake Erie, Canada. *Marine Geology*, 81, 63-77.
- Stockdon, H.F., and Holman, R.A., 2000. Estimation of wave phase speed and nearshore bathymetry from video imagery, *Journal of Geophysical Research* 105, 22015-22033.
- Sunamura, T., and Takeda, I., 1993. Bar movement and shoreline change: predictive

- relations. *Journal of Coastal Research*, (SI) 15, 125–140.
- Trenhaile, A.S., 1987. *The geomorphology of rock coasts*. Oxford University Press, Oxford, UK, 393 pp.
- Turner, I.L., Whyte, D., Ruessink, B.G., and Ranasinghe, R., 2007. Observations of rip spacing, persistence and mobility at a long, straight coastline. *Marine Geology* 236, 209–221.
- Van Duin, M.J.P., and Wiersma, N.R., 2002. Evaluation of the Egmond shoreface nourishment. Part I: Data analysis. MSc Thesis, WL | Delft Hydraulics.
- Van Duin, M.J.P., Wiersma, N.R., Walstra, D.J.R., van Rijn, L.C. and Stive, M.J.F., 2004. Nourishing the shoreface: observations and hindcasting of the Egmond case, The Netherlands. *Coastal Engineering* 51, 813–837.
- Van Enckevort, I.M.J., 2001. Daily to yearly nearshore bar behaviour. Ph.D. Thesis, Utrecht University.
- Van Enckevort, I.M.J., and Ruessink, B.G., 2001. Effect of hydrodynamics and bathymetry on video estimates of nearshore sandbar position. *Journal of Geophysical Research* 106, 16969–16979.
- Van Enckevort, I.M.J., and Ruessink, B.G., 2003a. Video observations of nearshore bar behaviour. Part 1: alongshore uniform variability. *Continental Shelf Research* 23, 501–512.
- Van Enckevort, I.M.J., and Ruessink, B.G., 2003b. Video observations of nearshore bar behaviour. Part 2: alongshore non-uniform variability. *Continental Shelf Research* 23, 513–532.
- Van Leeuwen, S., Dodd, N., Calvete, D., and Falqués, A., 2007. Linear evolution of a shoreface nourishment. *Coastal Engineering* 54, 417–431.
- Van Maanen, B., de Ruiter, P.J., Coco, G., Bryan K.R., and Ruessink, B.G., 2008. Onshore sandbar migration at Tairua Beach (New Zealand): Numerical simulations and field measurements. *Marine Geology* 253, 99–106.
- Verhagen, H.J., 1989. Sand waves along the Dutch coast. *Coastal Engineering* 13, 129–147.
- Voigt, B. 1998. *Glossary of Coastal Terminology*. Washington State Department of Ecology, Coastal Monitoring & Analysis Program, Publication No. 98–105.
- Wijnberg, K.M., 2002. Environmental controls on decadal morphologic behaviour of the Holland coast. *Marine Geology* 189, 227–247.
- Wijnberg, K.M., and Wolf, F.C.J., 1994. Three-dimensional behaviour of a multiple bar system. In: *Proceedings of the 1st Conference on Coastal Dynamics 94*, ASCE, New York, USA, 59–73.
- Wijnberg, K.M., and Terwindt, J.H.J., 1995. Extracting decadal morphological behaviour from high-resolution, long-term bathymetric surveys along the Holland coast using eigenfunction analysis. *Marine Geology* 126, 301–330.

Bibliography

Wijnberg, K.M., and Kroon, A., 2002. Barred beaches. *Geomorphology* 48, 103–120.

Wright, L.D., and Short, A.D., 1984. Morphodynamic variability of surf zones and beaches: a synthesis. *Marine Geology* 56, 93–118.